

Deutsches Institut für Ernährungsforschung (DIfE) Potsdam – Rehbrücke
Abteilung Biochemie und Physiologie der Ernährung
Arbeitsgruppe Energiestoffwechsel

**Comparative study of gene expression during the differentiation
of white and brown preadipocytes**

Dissertation

zur

Erlangung des Doktorgrades (Dr. rer. Nat.)

an der Mathematisch-Naturwissenschaftlichen Fakultät
der Universität Potsdam

vorgelegt von

Dipl. Ing. Stéphane Bœuf

Potsdam, März 2002

Teile dieser Dissertation sind veröffentlicht:

Boeuf, S., Klingenspor, M., van Hal, N. L. W., Schneider, T., Keijer, J., Klaus, S. Differential gene expression in white and brown preadipocytes. *Physiol. Genomics* 7: 15-25 (2001).

ABSTRACT

Introduction

Mammals have two types of adipose tissue: the lipid storing white adipose tissue and the brown adipose tissue characterised by its capacity for non-shivering thermogenesis. White and brown adipocytes have the same origin in mesodermal stem cells. Yet nothing is known so far about the commitment of precursor cells to the white and brown adipose lineage. Several experimental approaches indicate that they originate from the differentiation of two distinct types of precursor cells, white and brown preadipocytes. Based on this hypothesis, the aim of this study was to analyse the gene expression of white and brown preadipocytes in a systematic approach.

Experimental approach

The white and brown preadipocytes to compare were obtained from primary cell cultures of preadipocytes from the Djungarian dwarf hamster. Representational difference analysis was used to isolate genes potentially differentially expressed between the two cell types. The thus obtained cDNA libraries were spotted on microarrays for a large scale gene expression analysis in cultured preadipocytes and adipocytes and in tissue samples.

Results

4 genes with higher expression in white preadipocytes (3 members of the complement system and a fatty acid desaturase) and 8 with higher expression in brown preadipocytes were identified. From the latter 3 coded for structural proteins (fibronectin, metargidin and a actinin 4), 3 for proteins involved in transcriptional regulation (necdin, vigilin and the small nuclear ribonucleoprotein polypeptide A) and 2 are of unknown function. Cluster analysis was applied to the gene expression data in order to characterise them and led to the identification of four major typical expression profiles: genes up-regulated during differentiation, genes down-regulated during differentiation, genes higher expressed in white preadipocytes and genes higher expressed in brown preadipocytes.

Conclusion

This study shows that white and brown preadipocytes can be distinguished by different expression levels of several genes. These results draw attention to interesting candidate genes for the determination of white and brown preadipocytes (necdin, vigilin and others) and furthermore indicate that potential importance of several functional groups in the differentiation of white and brown preadipocytes, mainly the complement system and extracellular matrix.

ABSTRACT

Einleitung

Säugetiere haben zwei verschiedene Arten von Fettgewebe: das weiße Fettgewebe, welches vorwiegend zur Lipidspeicherung dient, und das braune Fettgewebe, welches sich durch seine Fähigkeit zur zitterfreien Thermogenese auszeichnet. Weiße und braune Adipozyten sind beide mesodermalen Ursprungs. Die Mechanismen, die zur Entwicklung von Vorläuferzellen in den weißen oder braunen Fettzellphenotyp führen, sind jedoch unbekannt. Durch verschiedene experimentelle Ansätze konnte gezeigt werden, daß diese Adipozyten vermutlich durch die Differenzierung zweier Typen unterschiedlicher Vorläuferzellen entstehen: weiße und braune Preadipozyten. Von dieser Hypothese ausgehend, war das Ziel dieser Studie, die Genexpression weißer und brauner Preadipozyten auf Unterschiede systematisch zu analysieren.

Methoden

Die zu vergleichenden Zellen wurden aus primären Zellkulturen weißer und brauner Preadipozyten des dsungarischen Zwerghamsters gewonnen. „Representational Difference Analysis“ wurde angewandt, um potentiell unterschiedlich exprimierte Gene zu isolieren. Die daraus resultierenden cDNA Fragmente von Kandidatengenen wurden mit Hilfe der Microarraytechnik untersucht. Die Expression dieser Gene wurde in braunen und weißen Fettzellen in verschiedenen Differenzierungsstadien und in braunem und weißem Fettgewebe verglichen.

Ergebnisse

12 Gene, die in braunen und weißen Preadipozyten unterschiedlich exprimiert werden, konnten identifiziert werden. Drei Komplement Faktoren und eine Fettsäuren Desaturase werden in weißen Preadipozyten höher exprimiert; drei Struktur Gene (Fibronectin, Metargidin und α Actinin 4), drei Gene verbunden mit transkriptioneller Regulation (Necdin, Vigilin und das „small nuclear ribonucleoprotein polypeptide A“) sowie zwei Gene unbekannter Funktion werden in braunen Preadipozyten höher exprimiert. Mittels Clusteranalyse (oder Gruppenanalyse) wurden die gesamten Genexpressionsdaten charakterisiert. Dabei konnten die Gene in 4 typischen Expressionsmuster aufgeteilt werden: in weißen Preadipozyten höher exprimierte Gene, in braunen Preadipozyten höher exprimierte Gene, während der Differenzierung herunter regulierte Gene und während der Differenzierung hoch regulierte Gene.

Schlußfolgerungen

In dieser Studie konnte gezeigt werden, daß weiße und braune Preadipozyten aufgrund der Expression verschiedener Gene unterschieden werden können. Es wurden mehrere Kandidatengene zur Bestimmung weißer und brauner Preadipozyten identifiziert. Außerdem geht aus den Genexpressionsdaten hervor, daß funktionell unterschiedliche Gruppen von Genen eine wichtige Rolle bei der Differenzierung von weißen und braunen Preadipozyten spielen könnten, wie z.B. Gene des Komplementsystems und der extrazellulären Matrix.

1 INTRODUCTION	1
1.1 Plasticity of the adipose organ	1
1.2 White and brown adipocytes	2
1.3 Differentiation of brown preadipocytes.....	5
1.4 Relevance in human obesity.....	6
1.5 Experimental approach.....	7
1.5.1 Representational difference analysis	7
1.5.2 Microarrays.....	8
1.6 Hypothesis and aims	9
2 MATERIALS AND METHODS	10
2.1 Materials.....	10
2.1.1 Chemicals	10
2.1.2 Media and solutions.....	10
2.1.2.1 Water	10
2.1.2.2 Buffers and solutions	10
2.1.2.3 Medium and solutions for cell culture	10
2.1.2.4 Media for bacterial cultures	11
2.1.3 E.coli strain and plasmid.....	11
2.1.4 Oligonucleotides.....	11
2.1.4.1 Gene specific PCR primers.....	11
2.1.4.2 Other oligonucleotides.....	12
2.1.5 Animals.....	12
2.1.5.1 Breeding colony of Djungarian dwarf hamster.....	12
2.1.5.2 Mouse strain.....	12
2.2 Isolation of cells and primary cell culture of preadipocytes	12
2.2.1 Primary cell culture of preadipocytes	12
2.2.2 Isolation of adipocytes and of stromal-vascular fraction.....	14

2.3 Basic molecular biology methods	14
2.3.1 Phenol/chloroform extraction and precipitation	14
2.3.2 Measurement of DNA and RNA concentrations	14
2.3.3 Agarose gel electrophoresis	15
2.3.4 Southern blotting	15
2.3.5 RNA isolation from tissue or cells	15
2.3.6 Northern blotting	15
2.3.7 PCR	16
2.3.7.1 RT-PCR	16
2.3.7.2 3' RACE PCR	16
2.3.7.3 Amplification of cloned DNA fragments	17
2.3.7.4 Purification of PCR products	17
2.3.8 Gel purification of DNA fragments	17
2.3.9 DNA cloning	17
2.3.10 Isolation of plasmid DNA	17
2.3.11 Preparation and labelling of probes	18
2.3.12 Northern blot hybridisation	18
2.3.13 DNA sequencing	18
2.4 cDNA representational difference analysis	18
2.4.1 Preparation of the RNA probes	19
2.4.2 mRNA isolation and reverse transcription	21
2.4.3 Generation of the amplicon	21
2.4.4 The cycles of subtractive hybridisation and selective amplification	22
2.4.4.1 Preparation of the drivers	22
2.4.4.2 Preparation of the testers	22
2.4.4.3 Subtractive hybridisation	23
2.4.4.4 Selective amplification	23
2.4.4.5 Generation of DP2	24
2.4.4.6 Generation of DP3	24
2.4.5 Cloning of the difference products	24
2.5 Microarrays	25
2.5.1 Experimental design	25
2.5.2 Choice and preparation of clones for the screening on microarrays	26
2.5.3 Microarray manufacturing	28
2.5.4 Sample preparation and labelling	29

2.5.5 Microarray hybridisation	29
2.5.6 Microarray scanning	30
2.5.7 Data analysis and normalisation	31
2.5.7.1 Comparison of multiple hybridisations.....	31
2.5.7.2 Statistical model for the data normalisation.....	31
2.5.7.3 Correction for the background.....	32
2.5.7.4 Local normalisation	34
2.5.7.5 Global normalisation	37
2.6 Cluster analysis and statistics	40
3 RESULTS	41
3.1 Primary cell cultures of preadipocytes	41
3.2 Representational Difference Analysis	41
3.3 Differential gene expression in white and brown preadipocytes	44
3.3.1 Microarray data.....	44
3.3.2 Confirmation on Northern blots.....	47
3.4 Cluster analysis of gene expression	48
3.4.1 Characterisation of the clusters.....	48
3.4.2 Distribution of genes in the clusters	51
3.4.3 Characterisation of the difference products	55
3.5 Gene expression in cell culture	56
3.5.1 Expression of the genes differentially expressed in preadipocytes	56
3.5.2 Gene expression during differentiation.....	58
3.5.3 Gene expression after β -agonist treatment.....	61
3.6 Gene expression in vivo	63
3.6.1 Inter individual variability of gene expression	63
3.6.2 Differential gene expression in WAT and BAT	66
3.6.3 Exposure to cold	68
3.7 Expression of RAMP2 in adipose cells.....	69

4 DISCUSSION	73
4.1 Methodological aspects.....	73
4.1.1 Representational difference analysis	73
4.1.2 Microarray hybridisations.....	74
4.2 Biological aspects	76
4.2.1 Biological controls.....	76
4.2.1.1 Mitochondrial proteins.....	76
4.2.1.2 Structure-related genes	77
4.2.1.3 Cell cycle genes	78
4.2.1.4 Other differentiation markers.....	78
4.2.1.5 Conclusions	79
4.2.2 General description of the expression data	79
4.2.2.1 Typology of the expression data.....	80
4.2.2.2 A comparison of cell culture and tissue.....	81
4.2.2.3 Inter individual variability of gene expression in adipose tissues	82
4.2.3 Functions involved in adipocyte differentiation	83
4.2.3.1 Complement and fatty acid metabolism	83
4.2.3.2 Structure and extra cellular matrix (ECM)	85
4.2.3.3 Regulation of gene expression.....	87
4.2.3.4 Signal transduction and cell trafficking.....	89
4.3 Summary and conclusions	91
5 REFERENCES	93

ABBREVIATIONS

ADM	adrenomedullin
ASP	acylation-stimulating protein
BAT	brown adipose tissue
cDNA	complementary deoxyribonucleic acid
C/EBP	CAAT/enhancer binding protein
CGRP	calcitonin gene related peptide
COX	cytochrome c oxidase
CRLR	calcitonin receptor like receptor
CV	coefficient of variation
DD	differential display
DNA	deoxyribonucleic acid
DP	difference product
ECM	extracellular matrix
EST	expressed sequence tag
factB	complement factor B
FADS	fatty acid desaturase
FCS	foetal calf serum
GAPDH	glyceraldehyde-3-phosphate-dehydrogenase
HCAP	hepatocellular carcinoma associated protein
HDL	high density lipoprotein
IAA	isoamyl alcohol
mRNA	messenger ribonucleic acid
NE	norepinephrine
NEFA	non-esterified fatty acid
NRF	nuclear respiratory factor
OB-Rb	leptin (ob) receptor
PAI-1	plasminogen activator inhibitor 1
PCR	polymerase chain reaction
PGC1	PPAR gamma coactivator 1
PPAR	peroxysome proliferator activated receptor
RACE	rapid amplification of cDNA ends
RAMP	receptor activity modifying protein
RCP	receptor component protein
RDA	representational difference analysis
RNA	ribonucleic acid
RT-PCR	reverse transcription PCR
SD	standard deviation
snrpA	small nuclear ribonucleoprotein peptide A
T3	triiodothyronine
TIMP	tissue inhibitor of metalloproteinase
TGF	transforming growth factor
TNF	tumor necrosis factor
TZD	thiazolidinediones
UCP	uncoupling protein
WAT	white adipose tissue

1 INTRODUCTION

1.1 Plasticity of the adipose organ

In the last decades, researchers have come to the view that adipose tissues are much more than simple fat stores. The adipose tissues revealed to play an active role in energy homeostasis and it is now generally recognised that they are a central integrator of the metabolic program (Rosen et al., 2000). Symptomatic for this evolution is the lack of description of the adipose tissues as an organ until recently (Cinti, 1999). Yet, an adipose organ can be defined. It is constituted of two tissues, the white and the brown adipose tissue (WAT and BAT), collaborating in lipid metabolism.

WAT is the major place for lipid storage in the body and an important endocrine tissue. BAT is also a lipid storing and endocrine active tissue which additionally has the capacity to produce heat by non-shivering thermogenesis. The uncoupling protein 1 (UCP1) located in the inner mitochondrial membrane of brown adipocytes uncouples respiration from ATP synthesis by dissipating the proton gradient formed during respiration and thus producing heat. Brown adipocytes are characterised by the expression of UCP1, a high respiratory capacity and mitochondrial content, and multilocular fat storage, in contrast to the unilocular fat stores in white adipocytes. Despite the opposed functions of these two cell types in energy storage and energy dissipation and the morphological differences between them, white and brown adipocytes are very similar from a molecular point of view. They both contain the whole machinery for lipolysis and lipogenesis and so far there is only one molecular marker distinguishing them, UCP1, which is expressed exclusively in brown adipocytes. Indeed, UCP1 expression defines a brown adipocyte.

From a very strict point of view, the denomination of WAT and BAT as tissues could be misleading. Several evidences show that the view of WAT and BAT as two anatomically distinct tissues is not acceptable. UCP1 expression is detectable in rat typical WAT depots, it is found in sparse multilocular cells with high mitochondrial content (Cousin et al., 1992). It is now recognised that both white and brown adipocytes are found in all visceral and subcutaneous fat depots (Cinti, 2001), so that a new classification of adipose tissues could be conducted in analogy to muscle. A continuum exists between typical WAT consisting in majority of white adipocytes and typical BAT (Cousin et al., 1992).

The proportion and amount of white and brown adipocytes in different depots is greatly dependant on age and physiological or pathological conditions. Here are a few examples of such situations:

- Most mammals are born with active BAT depots. Small rodents and hibernators keep active BAT depots throughout life (Klaus, 2001a), but in other mammals perinatal BAT disappears with age. In ruminants, for example, the loss of BAT is very rapid and no UCP1 can be detected anymore one week after birth (Casteilla et al., 1989).

- Cold acclimation induces tremendous changes in adipose tissues. It leads to hyperplasia of BAT in rodents (Bukowiecki et al., 1982; Klaus, 2001a). Cold acclimation induces the appearance of brown adipocytes in typical WAT depots of rodents and even in species devoid of any BAT depots in adult life, such as dogs (Cousin et al., 1996; Young et al., 1984; Cambon et al., 1998; Champigny et al., 1991). This induction of brown adipocytes is a highly variable genetic trait (Guerra et al., 1998).
- The treatment of rats with a β_3 -agonist, mimicking partly the effects of cold exposure, induces the appearance of brown adipocytes in WAT depots but no BAT hyperplasia (Himms-Hagen et al., 1994; Ghorbani et al., 1997). Treatment of animals with thiazolidinediones (TZDs), a class of peroxisome proliferator-activated receptor γ (PPAR γ) agonists, induces an augmentation of BAT mass (Tai et al., 1996) and was recently found to trigger as well the appearance of UCP1 expressing brown adipocytes in inguinal and retroperitoneal WAT of mice (Sell et al., 2001).
- Obesity, a multifactorial disorder, is the most obvious and apparent pathology of the adipose organ in western societies (Palou et al., 2000). Besides hypertrophied WAT, most rodent models of obesity display atrophied BAT depots (Himms-Hagen et al., 1998).

These examples show that the composition and the size of adipose tissue depots can change dramatically in short time periods. The adipose organ is doubtless the most plastic organ in adult organisms. What are the mechanisms underlying this plasticity ?

Besides mature adipocytes, adipose tissues contain also precursor cells: adipoblasts and preadipocytes (Ailhaud, 2001). In different physiological situations the proliferation and differentiation of these preadipocytes can be triggered. High caloric diets induce de novo production of white adipocytes (Miller et al., 1984) and cold acclimation the production of brown adipocytes (Bukowiecki et al., 1982). Preadipocytes are present in adipose tissues throughout life and differentiation of new white or brown adipocytes can still be detected in old animals (Kirkland et al., 1990; Morroni et al., 1995). Recruitment of new adipocytes is certainly an important process in the regulation of fat mass. Hyperplasia and hypertrophy both contribute to the pathogenesis of obesity.

To summarise, the mechanisms involved in the regulation of fat mass include the regulation of adipocyte size through lipolysis and lipogenesis and the regulation of adipocyte number through recruitment and dedifferentiation or apoptosis (Prins et al., 1997).

1.2 White and brown adipocytes

Regarding the plasticity of the adipose organ as the ability of heterogeneous adipose tissue depots to modify their composition and size in response to a given situation, the question of the mechanism underlying this plasticity becomes more complex. How can brown adipocytes appear in typical WAT

depots ? What mechanism explains the rapid loss of perinatal brown adipose tissue in some species ? Is a conversion possible from a white adipocyte to a brown adipocyte ? Or vice versa ? Are white and brown adipocytes two distinct cell types ?

Considering brown and white adipocytes as distinct cell types leads to the following hypothesis: two distinct types of precursor cells exist, the white and the brown preadipocytes, and recruitment of new adipocytes is the fundamental mechanism of adipose tissue plasticity. The establishment of white and brown preadipocytes primary cell cultures from rodents gave support to this hypothesis. As a matter of fact, precursor cells isolated from BAT depots grown in cell culture differentiate to UCP1-expressing brown adipocytes, while the precursor cells isolated from typical WAT depots differentiate in majority to white adipocytes with no UCP1 expression and more triglyceride accumulation. Only in majority, because a low level of UCP1 expression is found in differentiated cultures of white preadipocytes as well. Yet, it has been shown that this expression is due to about 10-15 % of the adipocytes expressing UCP1, thus being brown adipocytes (Klaus et al., 1995). β -adrenergic stimulation of cells induces an increase in UCP1 expression in WAT cultures, but does not increase the number of UCP1 expressing adipocytes (Klaus et al., 2001b). These observations exclude the hypothesis of the white adipocytes differentiated in cell culture being 'dormant' brown adipocytes and points to the presence of brown preadipocytes in typical WAT depots. In parallel, white adipocytes are found in BAT cultures. Coming back to our hypothesis, this shows that the preadipocyte pools located in different depots are heterogeneous and thus provides us with an explanation for the possible appearance of brown adipocytes in WAT depots and vice versa.

The observation of transgenic lipodystrophic mice corroborates this hypothesis as well. Two strains of WAT-free mice were established by inhibiting the differentiation of preadipocytes through two distinct mechanisms. One of these strains was absolutely WAT-free, but the animals had small amounts of BAT; in the other strain WAT was severely atrophied, but their brown fat was hypertrophied (Moitra et al., 1998; Shimomura et al., 1998). The genetic modification of both mouse strains affected the development of their adipose tissues. The presence of BAT in both strains, even if inactive, indicates that the precursor cells from WAT and BAT reacted differently to this altered gene expression. Brown preadipocytes were not impeded in their differentiation.

Yet, our hypothesis of the existence of two distinct precursor cell types should be confronted to other possible explanations of adipose tissue plasticity. One could think of white and brown adipocytes as representing two different stages of differentiation of one cell type. This hypothesis is intuitively suggested by the observation of the postnatal loss of brown adipocytes in some species. A recent work definitively demonstrates that this cannot be the case, at least in mice. Strains of transgenic mice were established in a way that it became possible to trace cells having expressed UCP1 at any time point of their development. It could be shown that the majority of white adipocytes found in adult mice were cells which had never expressed UCP1 and thus, that they do not derive from brown adipocytes. No

transient brown adipocyte stage occurs during the emergence of white adipocytes (Moulin et al., 2001a).

D. Lončar proposed the existence of a convertible adipose tissue (Lončar, 1991). Supporting this hypothesis, it has been demonstrated that multilocular UCP1-expressing adipocytes emerging in WAT after β_3 -agonist treatment are produced without undergoing any mitosis (Himms-Hagen et al., 2000). The authors of this study conclude that these adipocytes derive directly from white adipocytes. The multilocular cells found in WAT with lower UCP1 expression and atypical mitochondria were not typical brown adipocytes. Are they convertible adipocytes? As a matter of fact, this study does not demonstrate directly that the multilocular cells derive from white adipocytes. It cannot be excluded that they originate from preadipocytes having undergone differentiation without mitosis. While it is generally accepted that cultured preadipocytes have to undergo postconfluent mitosis before differentiation, Entenman et al. (1996) have shown that in human primary cell cultures of preadipocytes, mitosis is not necessary for differentiation. Recently it has also been demonstrated that mitosis is not a required step in the differentiation of preadipocytes from the 3T3-L1 cell line (Qiu et al., 2001). As β_3 -agonists are known not to stimulate proliferation of preadipocytes (Klaus et al., 2001c), a direct differentiation of brown preadipocytes in WAT during β_3 -agonist treatment is plausible. The atypical phenotype of these multilocular cells could be linked to the different endocrine and paracrine environment in WAT and BAT. An alternate explanation of these data is the possibility of brown adipocytes to enter a dormant state. Dormant brown adipocytes might be reactivated by an adequate stimulus (Himms-Hagen et al., 1998).

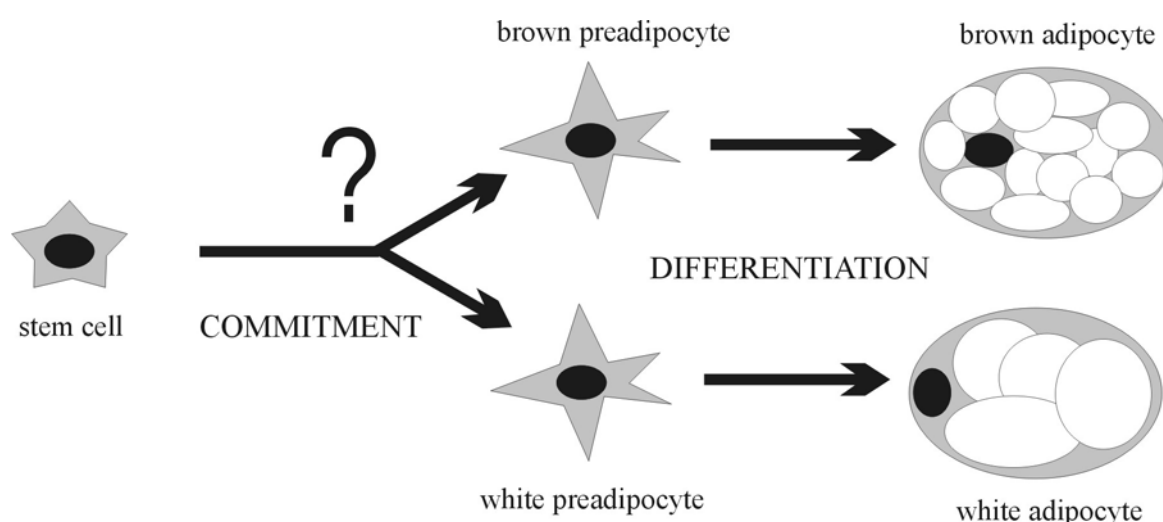


Figure 1. Schematic representation of the differentiation of white and brown preadipocytes. White and brown adipocytes have a common origin in mesodermic stem cells. The time point and the mechanism of the commitment of precursor cells to the white or brown adipose lineage is unknown.

To conclude, the delimitation between the white and the brown adipose cell type is still unclear and discussed. Even if a conversion of mature adipose cells cannot be excluded completely, it seems that recruitment of new adipocytes is the major mechanism underlying the great plasticity of adipose tissues. The working hypothesis from which this study emanates is that white and brown adipocytes represent two distinct cell types and that they have distinct precursors, white and brown preadipocytes (figure 1). As elucidated above, several independent experimental approaches corroborate this hypothesis.

1.3 Differentiation of brown preadipocytes

The differentiation of white preadipocytes has been studied extensively in cell lines and primary cell cultures. Preadipocytes originate from mesodermal stem cells. In cell culture, they proliferate until they reach confluence. More important for the onset of differentiation than confluence itself is the growth arrest of preadipocytes in G1/S phase. Adipogenic and mitogenic factors can then induce differentiation. Early markers of differentiation are expressed, the cells eventually undergo postconfluent mitosis and change their morphology from a fibroblast-like to a rounded shape. Finally, they undergo functional differentiation, i.e. adipogenesis. The two major transcription factors involved in this differentiation program are PPAR γ and C/EBP α (CAAT/enhancer binding protein α) (Ailhaud, 2001; Rosen et al., 2000).

Much less is known about the differentiation of brown preadipocytes. They have the same origin as white preadipocytes, and it is absolutely unclear when their commitment to the brown adipose lineage occurs. Brown preadipocytes are morphologically identical to white preadipocytes. Only recently, a marker for brown preadipocytes has been isolated. Till now it is in fact only a RNA fragment from which no full-length sequence could be determined (Moulin et al., 2001b).

The functional differentiation of brown preadipocytes consists in the acquisition of the ability for two distinct functions: lipid storage and thermogenesis. These two differentiation processes can be dissociated. Whereas adipogenesis in brown adipocytes is regulated similarly to white adipocytes, the acquisition of thermogenic capacity has its own mechanisms of regulation (Klaus et al., 1995). β -adrenergic stimulation is certainly the most important regulator of brown preadipocytes differentiation. Norepinephrine (NE) stimulates activation of brown adipocytes as well as the proliferation of brown preadipocytes. This effect of NE on recruitment is part of the adaptive response to cold exposure (Nedergaard et al., 1995). Additionally, the thyroid hormone triiodothyronine (T3) and PPAR γ ligands are also known to stimulate brown preadipocytes differentiation (Klaus et al., 1995; Rabelo et al., 1997).

Trying to answer the question of the determination of brown preadipocytes and of the mechanisms specific to brown adipocytes differentiation, one approach is to analyse the promoter regions of genes

related to the brown adipocyte phenotype, and first of all UCP1. Several important regions have been isolated in the UCP1 promoter. An upstream enhancer controlling BAT specific expression has been identified. Nevertheless, this enhancer requires the BAT phenotype to be active (Kozak et al., 1994a; Cassard-Doulcier et al., 1998). The mechanism underlying the specificity of expression is still unknown. The other characteristic of brown adipocytes is their high respiratory capacity. The mechanisms of control of mitochondria biogenesis in adipocytes are still very unclear. Nuclear respiratory factor 2 (NRF2) is involved in the acquisition of the BAT phenotype (Villena et al., 1998). An important step in understanding brown preadipocytes differentiation has been done with the discovery of the PPAR γ coactivator PGC1. Cold exposure induces an increase in PGC1 levels, inducing in turn the expression of UCP1 and of nuclear respiratory factors. Thus, PGC1 appears as a master regulator of the thermogenic function of brown adipocytes (Wu et al., 1999). But how is the expression of PGC1 regulated ?

The studies evoked here have provided important clues for the understanding of the regulation of the thermogenic function in brown adipocytes. But they do not answer the question of the primary determinants of these cells. In order to better understand the determination of white and brown adipose cells, the aim of this project was to identify differences in gene expression between white and brown preadipocytes during their differentiation. To do so, it has been chosen to use a systematic approach to screen for such differences.

1.4 Relevance in human obesity

In humans, BAT is important postnatally, but disappears within the first year of life. Nevertheless, clusters of brown multilocular adipocytes can be found in former BAT depots in adults. More brown adipocytes are found in younger individuals or in individuals exposed to cold. The contribution of these to body temperature regulation is controversial, but in any case would not exceed 1 to 2 % of energy expenditure (Himms-Hagen et al., 1998).

In primary cell cultures of human preadipocytes from any depot, β -adrenergic stimulation or TZD treatment can induce UCP1 expression (Champigny et al., 1996; Digby et al., 1998). This inducibility is subject to high inter-individual variability (Klaus, 2001a). These results suggest the presence of brown preadipocytes in human adipose tissue. Adaptive thermogenesis is an attractive target for antiobesity drugs (Lowell et al., 2000). The understanding of the determination process of white and brown preadipocytes could contribute to the establishment of new therapeutical strategies for the treatment of obesity. Brown preadipocytes or adipocytes in human could represent an important target for physiological or pharmacological interventions (Rosen et al., 2000).

1.5 Experimental approach

The identification of genes expressed differentially between cell types, tissues, healthy and pathological individuals etc. is an important biological question in many research areas. In the last decade, the techniques available developed tremendously and the possibility of large-scale gene expression analysis has been opened. Several approaches are available for differential gene expression studies: differential display (DD, Liang and Pardee, 1992), subtractive hybridisation, representational difference analysis (RDA), RNA arbitrarily primed PCR (RAP-PCR, Welsh et al., 1992), serial analysis of gene expression (SAGE, Lash et al., 2000) and expression microarrays.

For the study of differentially expressed genes in white and brown preadipocytes a combination of RDA and microarray hybridisations has been chosen.

1.5.1 Representational difference analysis

The two populations of DNA to compare will be termed as tester and driver: the tester contains “target” sequences not present in the driver (or present at a lower level).

For a long time, detection of differences between DNA populations was a technically very difficult task. In 1993, Lisitsyn published the description of a new method for “finding small differences between the sequences of two DNA populations”: the representational difference analysis (Lisitsyn et al., 1993; Lisitsyn, 1995). It is based on subtractive hybridisation, a method first described by Bautz and Reilly in 1966, but which, though different attempts of optimisation, could achieve only low rates of enrichment in target sequences (Wieland et al., 1990), and thus low sensitivity. Subtractive hybridisation is based on the reassociation kinetics of single strand DNA fragments from the tester mixed to a large excess of driver. Target sequences, not present in the driver, will preferentially reanneal with themselves, whereas other sequences from the tester, present also in the excess of driver, will rather reanneal with driver sequences. Thus, in the population of the tester:tester hybrids, a high enrichment in target sequences will be achieved. Different methods can then be used to isolate the tester:tester hybrids. Lisitsyn combined subtractive hybridisation with selective PCR amplification: the tester DNA is ligated to an adapter at its 5' ends. After an elongation step to fill in the oligonucleotide cohesive ends, only tester:tester hybrids can be PCR amplified when using the adapter oligonucleotide as a primer. Several cycles of subtractive hybridisation and selective amplification are successively applied, comparing the respective difference product to the original driver again (figure 2). The method profits from the second order kinetics of reassociations and is able to achieve very high enrichments in target sequences.

Lisitsyn applied RDA to compare genomic DNA simplified by synthesizing so called representations. RDA was adapted to the comparison of cDNAs by Hubank and Schatz (1994). In this case, there is no need to reduce the complexity of the samples. The cDNAs are digested with a 4-cutter restriction

enzyme (DpnII) to produce representations, which are the cDNA fragments populations that will be compared. The mean cutting length is 256bp, so that a vast majority of mRNAs is represented. Moreover, a lower stringency is used than in the genomic DNA protocol, allowing to detect low differences in gene expression, and not only on/off effects. 2 fold differences in expression may be detected by this method.

RDA has a number of advantages over the other techniques available for the study of differential gene expression (Pastorian et al., 2000). It results in an exponential enrichment in target sequences, simultaneously removing the uninteresting fragments. On average, the fragments are relatively long and located in the coding sequence, unlike for DD. Furthermore, it is possible to detect genes with relatively low differences in gene expression and not only on/off effects. This was particularly suitable for this project. The cells compared being morphologically and functionally identical, it was not possible to foresee how large the differences in gene expression between them would be.

RDA has recently been employed to identify genes specifically expressed in visceral adipose tissue of obese, diabetic rats in contrast to diabetes-resistant rats (Hida et al., 2000). We applied it to mRNAs from brown and white semi-confluent preadipocytes, in both directions. 3 cycles subtractive hybridisation and selective amplification were performed and the difference products 2 and 3 (DP2 and 3) obtained after 2 or 3 cycles RDA respectively were cloned and screened.

1.5.2 Microarrays

Microarrays result from the automation and miniaturisation of the dot blot technique, opening the doors for large-scale gene expression studies (Lennon et al., 1991). In 1995, Schena et al. described the use of a two-colour labelling protocol for the analysis of differences in gene expression between different plant tissues. This method was applied to human gene expression analysis (Schena et al., 1996) and is now broadly used for any kinds of application (Duggan et al., 1999).

PCR amplified cDNA fragments are fixed on a solid support, a glass slide. The use of a micro-dispensing robot permits the deposition of minimal amounts of DNA solution on the slide, down to 50 pl, allowing concentrations of more than 2500 spots/cm² (Van Hal et al., 2000). For the comparison of the expression of the spotted genes in two different mRNAs, the arrays are hybridised to a mixture of cDNAs corresponding to these mRNAs and labelled with two distinct fluorescent dyes. After hybridisation, the slide is scanned at the wavelengths corresponding to the two dyes, producing two images of the array, one for each mRNA. These images can be compared, and thus differences in expression can be quantified.

Microarrays have been used in three studies for the analysis of gene expression in WAT: to compare wild-type mice to ob/ob mice (Soukas et al., 2000) and to assess the effect of obesity and diabetes mellitus on gene expression in epididymal fat (Nadler et al., 2000). They have also been used to detect abundant mRNAs in human adipose tissue (Gabrielsson et al., 2000). Furthermore, in three studies

gene expression has been analysed in adipose cells during adipogenesis. One study compared preadipocytes to adipocytes from human primary cell cultures (Zhou et al., 1999). In the two other studies 3T3-L1 preadipocytes cultures were used. Guo et al. (2000) made a simple comparison of preadipocytes to adipocytes, whereas Soukas et al. (2001) used a cluster analysis to characterise gene expression profiles during differentiation *in vitro* and *in vivo*.

In these studies commercially available arrays spotted with several thousands of cDNA fragments were used. We chose another approach. The difference products obtained through RDA were spotted on microarrays which were hybridised to probes of brown and white preadipocytes as well as other cell types and tissues. Thus, the microarray hybridisations served as a screening of the difference products. Furthermore they provided information about the expression of the isolated genes at various states of cell differentiation. The combination of RDA with microarray analysis has been applied several times (Welford et al., 1998; Frohme et al., 2000; Ismail et al., 2000; Geschwind et al., 2001). The main advantages of this experimental design are to allow the isolation of yet unknown sequences through the RDA and the reduction of the size of the arrays. A smaller number of genes is analysed, but these genes have been selected for the question of interest. Furthermore, it allows the study of species for which very few or no EST or cDNA microarrays are available today, i.e. species other than mice, rats or human.

1.6 Hypothesis and aims

Several experimental approaches support the hypothesis that white and brown adipocytes are distinct cell types and that they have distinct precursor cells, the white and brown preadipocytes. These preadipocytes are morphologically identical and no functional difference is known between them. Few is known about the specificity of the differentiation process of brown preadipocytes. The aim of this study was to use a systematic approach to identify differences in gene expression between the white and the brown preadipocytes and during their differentiation.

To do so, RDA was chosen as a method allowing to isolate not only genes specific for a given cell type, but also genes that are only up-regulated in these cells. To screen the isolated cDNA libraries and allow a large-scale gene expression analysis, microarrays were used. These enabled to compile a large data set of gene expression levels during preadipocytes differentiation in primary cell culture and *in vivo*, questioning particularly the comparison of white and brown preadipocytes differentiation.

2 MATERIALS AND METHODS

2.1 Materials

2.1.1 Chemicals

If not specified otherwise, all chemicals were obtained from Merck, Fluka or ICN in “p.a.” (analytical grade) quality.

2.1.2 Media and solutions

2.1.2.1 Water

For microarray manufacturing and hybridisation, water was purified by Millipore filtration; for all other applications it was purified using the “Reinstwasser-System Clear SG”.

2.1.2.2 Buffers and solutions

50x TAE	2 M Tris.HCl, 1 M acetic acid, 0.1 M EDTA (Sigma)
10x TBE	0.89 M Tris.HCl, 0.89 M boric acid, 20 mM EDTA
20x SSC	3 M NaCl, 0.3 M NaCitrate, pH 7.5
10xMOPS	0.2 M 3-Morpholino-propane-sulfonic acid, 0.05 M NaAcetate, 0.01 M EDTA, pH 7
1x TE	10 mM Tris.HCl, pH 8, 1 mM EDTA
1x TNE	10 mM Tris.HCl, pH 8, 1 mM EDTA, pH 8, 100 mM NaCl
3x EE buffer	30 mM EPPS (Sigma), 3 mM EDTA, pH 8
5x RDA PCR buffer	335 mM Tris.HCl, pH 8.8, 20 mM MgCl ₂ , 80 mM (NH ₄) ₂ SO ₄ , 166 µg/ml BSA
PBS	200 mM NaCl, 100 mM Na ₂ HPO ₄ , 20 mM NaH ₂ PO ₄
NaPi	1 M NaH ₂ PO ₄ , adjusted to pH 7 with 85 % H ₃ PO ₄
50x Denhardt's reagent	10 g/l Ficoll, 10 g/l polyvinylpyrrolidone, 10 g/l BSA (Sigma)

2.1.2.3 Medium and solutions for cell culture

Collagenase buffer	100 mM HEPES (pH 7.4), 123 mM NaCl, 5 mM KCl, 1.3 mM CaCl ₂ , 5 mM glucose, 1.5 % (w/v) BSA (Sigma), 1 mg/ml collagenase (Sigma)
Cell culture medium	50% modified Eagle's medium (Gibco BRL) and 50% Ham's F12 medium (Gibco BRL) supplemented with 1.2 g/l Na HCO ₃ , 4 mg/l biotin, 2 mg/l Ca-pantothenate, 5 mM glutamine, 4.5 g/l glucose, 15 mM Hepes (pH 7.4), 6.25 mg/l penicillin G, 5 mg/l streptomycin

2.1.2.4 Media for bacterial cultures

LB Medium	1 % (w/v) NaCl, 1 % (w/v) casein hydrolysate (Gibco BRL), 0.5 % (w/v) Bacto yeast extract (Gibco BRL), pH 7
LB Agar/ampicillin	LB Medium with 1.5 % (w/v) agar and 75 mg/l ampicillin
SOC Medium	0.05 % (w/v) NaCl, 2 % (w/v) casein hydrolysate (Gibco BRL), 0.5 % (w/v) Bacto yeast extract (Gibco BRL), 2.5 mM KCl, 10 mM MgCl ₂ , 20 mM glucose, pH 7

2.1.3 E.coli strain and plasmid

JM109 competent cells (Promega)

DH5- α competent cells (Gibco BRL)

pGEM®-T Vector (Promega) was used for all cloning experiments

2.1.4 Oligonucleotides

2.1.4.1 Gene specific PCR primers

name	target gene	species	sequence (5' - 3')
UCP1-1	UCP1	hamster	TGGAGGTGTGGCAGTATTC
UCP1-2	UCP1	hamster	AGCTCTGTACAGTTGATGATGAC
pRA2-1f	RAMP2	hamster	ATTCTCTTCCCACTGAGGACAGCTTGC
pRA2-2f	RAMP2	hamster	GATCGCGGCTTGCTATGACC
pRA2-3f	RAMP2	hamster	CTCCGCTGCTGCTGGTGCTGGTG
pRA2-4f	RAMP2	hamster	GACTCTGTCAGGGACTGGTGCAACTGGA
pRA2-1r	RAMP2	hamster	TGCAGGTCGCTGTAATGCCTGCTAAT
pRA2-2r	RAMP2	hamster	TGGGAAACCCAGGCCAAACCTCTCG
pRA2-3r	RAMP2	hamster	CCGGCGCGGGTCATAGCAAG
pRA2-4r	RAMP2	hamster	TGGGAAGAGATTGATTCGGGGAGGT
mRA1-f	RAMP1	mouse	GGCTCACCATCTCCTCATGG
mRA1-r	RAMP1	mouse	AGTCATGAGCAGCGTGACC
mRA2-f	RAMP2	mouse	TCTCACCCAAGGCGTGATG
mRA2-r	RAMP2	mouse	ATGGCTGCTGAGAAATGGAC
mRA3-f	RAMP3	mouse	TGCACCTTCTTCCACTGTTG
mRA3-r	RAMP3	mouse	CACAGCAGCCGATCAGTGT
mRCP-f	RCP	mouse	CAGCAACTATGAGGTGTTCCA
mRCP-r	RCP	mouse	CTTTTCTACCATCAGCTGGATCT
mCRLR-f	CRLR	mouse	ACAGCACGCATGAGAAAGTG
mCRLR-r	CRLR	mouse	CCTCTGCAACCTTTCTTCA
mADM-f	ADM	mouse	CCGAAAGAAGTGAATAAGTGG
mADM-r	ADM	mouse	TAGCCTTGAGGGCTGATCTT

Table 1. List of the gene specific primers used, with indication of the target gene, the species and the sequence.

2.1.4.2 Other oligonucleotides

name	sequence (5' - 3')
M13uni	TGTA AACGACGGCCAGT
M13rev	CAGGAAACAGCTATGACC
1F-mod	AGGCGATTA ACTTGGGTAAC
3R-mod	AGCGGATAACAATTCACAC
R-Bgl-12	GATCTGCGGTGA
R-Bgl-24	AGCACTCTCCAGCCTCTCACCGCA
J-Bgl-12	GATCTGTTCATG
J-Bgl-24	ACCGASCGTCGACTATCCATGAACA
N-Bgl-12	GATCTTCCCTCG
N-Bgl-24	AGGCAACTGTGCTATCCGAGGGAA

Table 2. List of other oligonucleotides used: M13uni, M13rev, 1F-mod and 3R-mod are primers for amplification of inserts in plasmids; the R-, J- and N-Bgl oligonucleotides are the adapters used for RDA.

2.1.5 Animals

2.1.5.1 Breeding colony of Djungarian dwarf hamster

Djungarian (also termed Siberian) dwarf hamsters (*Phodopus sungorus*) were obtained from the German Institute of Human Nutrition's breeding colony. Animals were kept at 23 °C (thermoneutrality) in long photoperiod (18:6, light:dark). Hamsters aged 4 to 6 weeks were used for primary cell cultures. They were anaesthetized with CO₂ and killed by cardiac puncture.

For the isolation of tissue RNA, animals aged 10 to 30 weeks were used. They were eventually exposed to 4°C for 18 hours prior to tissue preparation.

2.1.5.2 Mouse strain

The mice used for tissue isolation were female mice from the FVB strain. They were aged approximately 6 months.

2.2 Isolation of cells and primary cell culture of preadipocytes

2.2.1 Primary cell culture of preadipocytes

For the parallel primary cell cultures of white and brown preadipocytes, the largest subcutaneous depot of white fat, the inguinal white fat, and several subcutaneous depots of brown fat (axillar, suprasternal, interscapular, dorsal-cervical) from Djungarian hamsters were used. For each cell culture, fat depots from 4 to 6 animals were pooled in order to minimize possible artefacts resulting from differences between different fat depots and individual differences.

The stromal-vascular fraction, containing the preadipocytes, was then isolated (Klaus et al., 1991). The prepared fat depots were maintained at 37 °C in cell culture medium and cut in small pieces with

preparation scissors before collagenase digestion. The minced, pooled tissue samples were incubated in collagenase buffer (around 10 ml for 1.5 g tissue) for 20 to 30 minutes at 37 °C, being vortexed every 5 minutes. The digest was then filtered twice on nylon membranes of pore size 250 µm and 70 µm successively, and let to incubate 5 to 10 minutes at room temperature to allow the formation of an upper fat layer containing the mature adipocytes. This fat layer was discarded. To stop the digestion, some medium supplemented with 10 % (v/v) Foetal Calf Serum (FCS, Bio Whittaker) was added. Finally, the cells from the stromal-vascular fraction were washed twice in medium with 10% FCS by centrifugation at 700g.

The cells were diluted and inoculated in petri dishes (10 cm diameter) at approximately 1500-2000 cells/cm². Cells were grown at 37 °C in air with 5 % CO₂ content and 100 % relative humidity in cell culture medium supplemented with 10 % FCS. Medium was changed after one day, mainly in order to wash away all cells or cell debris that did not succeed to attach to the culture dish. The cells reached confluence at day 4 or 5. Semi-confluent preadipocytes (pAd4) were harvested at day 4, confluent preadipocytes (pAd6) at day 6 (table 3).

To induce differentiation, medium was changed at day 3. Insulin (17 nM, Sigma) and triiodothyronine (T3, 1 nM, Sigma) were added and FCS supplement was reduced to 7 %. For chronic β-adrenergic stimulation isoproterenol (10 µM, Sigma) or CL 316,243 (disodium(R,R)-5-[2-[[2-(3-chlorophenyl)-2-hydroxyethyl]-amino]propyl]-1,3-benzodioxole-2,2-dicarboxylate) (CL, 0.1 µM, Bloom JD et al., 1992) were also added at day 3, at the start of differentiation. These concentrations have been shown to be maximally effective for long term stimulation of UCP1 expression, whereas acute effects could be seen at much lower concentrations (Klaus et al., 1991; Klaus et al., 2001c). Differentiating adipocytes (Ad6) (i.e. cells treated with insulin but not fully differentiated) were harvested at day 6; mature adipocytes (Ad10) at day 10. The isoproterenol (Adiso) and the CL (AdCL) treated adipocytes were also harvested at day 10.

	WAT	BAT	differentiation state	culture day	insulin / T3	isoproterenol	CL
pAd 4	pW4	pB4	semi-confluent preadipocytes	4	-	-	-
pAd 6	pW6	pB6	confluent preadipocytes	6	-	-	-
Ad 6	W6	B6	preadipocytes beginning differentiation	6	+	-	-
Ad 10	W10	B10	mature adipocytes	10	+	-	-
Ad iso	Wiso	Biso	adipocytes treated with isoproterenol	10	+	+	-
Ad Cl	WCl	BCl	adipocytes treated with Cl 316,243	10	+	-	+

Table 3. List of the kind of cells harvested for RNA isolation. The abbreviations used for cells originating from WAT and BAT are reported in the first columns. The day of culture when cells were harvested as well as the treatment given at day 3 are reported.

2.2.2 Isolation of adipocytes and of stromal-vascular fraction

For direct RNA preparation from cells, adipocytes and stromal-vascular fraction were isolated from the fat depots described above. For this application, in order to limit damages to mature adipocytes, the collagenase digestion was performed in a more gentle way. The digestion mixtures were incubated at 37 °C, shaken gently for 30 to 45 min. After filtration with a 250 µm nylon membrane, the digests were placed on ice for 10 minutes to allow the adipocytes to form an upper fat fraction. The stromal-vascular fraction was transferred to another reaction tube using glass Pasteur pipettes. The fat fraction was shock frozen in liquid nitrogen. The stromal-vascular fraction was washed, pelleted and frozen as well. Cells were stored at -80 °C.

2.3 Basic molecular biology methods

2.3.1 Phenol/chloroform extraction and precipitation

RNA or DNA solutions were mixed with an equal volume of phenol/chloroform/isoamylalcohol (IAA) 50:49:1 (phenol from Roth), vortexed and centrifuged. The supernatant was carefully removed, mixed with an equal volume of chloroform/IAA 49:1, vortexed and centrifuged again. 1/10 volume of a 3 M NaAcetate solution (pH 5.2) and 2.5 to 3 volumes ethanol were added to the supernatant. RNA or DNA was precipitated 20 minutes at -20 °C. The precipitate was washed with 75 % ethanol, air dried and resuspended.

Alternatively, the precipitation was carried out with 1/5 volume of 10 M NH₄OAcetate instead of NaAcetate, which strongly reduces the coprecipitation of dNTPs, or with 1 volume of isopropanol instead of ethanol.

2.3.2 Measurement of DNA and RNA concentrations

DNA and RNA concentrations were determined using 1 ml and 50 µl quartz cuvettes in a DU640 spectrophotometer (Beckmann).

For low concentration RNA samples, a fluorescent nucleic acid stain, the RiboGreen™ RNA Quantitation Reagent (Molecular Probes), was used, following the protocol of the manufacturer. A standard curve was established and the RNA concentrations were determined in a spectrofluorometer at 480 nm excitation and 520 nm emission.

For low concentration DNA samples, the Hoechst fluorescent dye was used. DNA was added to 2 ml of the following assay solution: 0.2 µl Hoechst dye in 1x TNE. The spectrofluorometer was calibrated with a standard DNA and concentrations were determined in a spectrofluorometer at 360 nm excitation and 460 nm emission.

2.3.3 Agarose gel electrophoresis

Solutions of agarose (Hybaid AGS) in TAE (or TBE) were melted in a microwave oven and cooled down to 60 °C before addition of 25 µg ethidium bromide per 50 ml agarose solution. DNA samples were mixed with following 5x loading buffer: 50 % (v/v) glycerol, 25 mM EDTA, 0.25 % (w/v) xylexyanol and 0.25 % (w/v) bromophenolblue. Electrophoresis was run in TAE (or TBE) buffer and DNA was visualised on a UV transilluminator Eagle EyeTMII (Stratagene).

2.3.4 Southern blotting

200 or 300 ng DNA were run in a 2 % TAE agarose gel. Prior to blotting, the DNA was denatured by soaking the gel for 45 min in a 1.5 M NaCl, 0.5 M NaOH solution, gently shaken, and the gel was subsequently neutralised by soaking in a 1 M Tris (pH 7.4), 1.5 M NaCl solution for 30 min and a second time for 15 min. The gel was blotted over night by upward capillary transfer to a Hybond N nylon membrane (Amersham). 10x SSC was used as a transfer buffer. After the transfer, DNA was crosslinked to the membrane with a UV crosslinker (Biometra) by application of 0.120 J/cm².

2.3.5 RNA isolation from tissue or cells

Total RNA from cultured cells, isolated cells and tissue was extracted using the single step acid phenol/guanidine protocol (Chomczynski et al., 1987).

Cells from cell culture were washed with ice cold PBS and harvested with a rubber policeman in 1.8 ml solution D (4 M Guanidinthiocyanate, 25 mM NaCitrate, pH 7, 0.5 % Lauroyl Sarcosine, 0.1 M 2-mercaptoethanol) per petri dish. The lysate was eventually shock frozen in liquid nitrogen and stored at -80 °C. Frozen tissue samples or cell samples (isolated adipocytes and stromal vascular fraction) were homogenized with a mortar under liquid nitrogen. Rapid and complete lysis was then achieved by homogenisation in solution D using an 'Ultra Turrax® T25 basic' homogeniser (IKA® Labortechnik).

To 1 ml lysate, 100 µl 2 M NaAcetate (pH 4), 1 ml acidic Phenol and 200 µl chloroform/IAA (49:1) were added. The mixture was strongly vortexed, centrifuged for 40 min at 4000x g at 4 °C. The aqueous phase was precipitated by addition of an equal volume of isopropanol and another centrifugation for 40 min at 4000x g at 4 °C. The pellet was resuspended in 300 µl solution D and reprecipitated with 400 µl isopropanol and centrifugation for 20 min at 13000x g at 4 °C. The pellet was resuspended in water by incubation at 65 °C for 5 min, and the RNA was stored at -80 °C.

2.3.6 Northern blotting

10 µg of total RNA were mixed with an equal volume of denaturing buffer (1x MOPS, 6.5 % (v/v) formaldehyde, 50 % (v/v) formamide) and 2 µl of RNA stain (0.5 mg/ml ethidium bromide). The mixture was denatured at 65 °C for 20 minutes. The following loading buffer was added: 50 % (v/v) glycerol, 1x MOPS, 0.25 % (w/v) bromophenolblue, and the RNA was then separated by

electrophoresis in a 1 % (w/v) agarose gel containing 1.2 % formaldehyde in MOPS. It was blotted over night by upward capillary transfer to a Hybond N nylon membrane (Amersham). 10x SSC was used as a transfer buffer. After the transfer, RNA was crosslinked to the membrane with a UV crosslinker (Biometra) by application of 0.120 J/cm².

2.3.7 PCR

2.3.7.1 RT-PCR

Prior to cDNA synthesis, 10 µg of total RNA were digested for 30 minutes at 37 °C with 2.5 units RNase-free DNase (Promega) in the provided buffer supplemented with 1 mM DTT and 40 units RNase inhibitor (Promega) in a final volume of 50 µl. RNA was phenol/chloroform extracted as described above and resuspended in 20 µl water.

RNA was then heat denatured 10 min at 65 °C and chilled on ice. The oligo-dT primed first-strand cDNA synthesis reaction was performed with 4 to 5 µg RNA as template using a kit from Boehringer Mannheim and following the instructions of the manufacturer. The reaction mixture was incubated 10 min at 25 °C, 1 hr at 42 °C, and the reaction was stopped by heat inactivation, 5 min at 95 °C.

The PCRs were performed in a PTC-200 thermal cycler (MJ Research). The template consisted of 1 µl of cDNA. The total reaction volume was 50 µl, containing 50 pmol of each primer, 2 mM MgCl₂ (Gibco BRL), 1x PCR buffer (Gibco BRL), 0.2 mM dNTPs, 5.2 % (v/v) DMSO and 1 U Taq polymerase (Gibco BRL). The PCR conditions consisted of: (i) initial denaturation, 2 min at 94 °C, (ii) denaturation, 40 sec at 94 °C, (iii) annealing, 40 sec at 58 °C, (iv) extension, 1 min 30 sec at 72 °C, the steps ii to iv being repeated 35 times, and (v) final extension, 5 min at 72 °C. The PCRs were stopped at 4 °C.

2.3.7.2 3' RACE PCR

RACE PCR was performed following the protocol of the SMARTTM RACE cDNA amplification Kit (Clontech), in parallel for preadipocytes and adipocytes. A 1 µg template of pW4 or W10 mRNA was used as template for cDNA synthesis. The 3'-RACE-Ready cDNA was prepared as suggested by the manufacturer using the SuperScript II reverse transcriptase (Gibco BRL) and with one modification. To improve denaturation of RNA, the mixture of mRNA and 3'-CDS primer was submitted to the following program: 1 min at 70 °C, 1 min at 85 °C, 30 sec at 4 °C, 3 min at 85 °C, 1 min at 70 °C, followed by a chilling of the tubes on ice. RACE PCR was then performed with mRA2-1f as gene specific primer, using the Advantage 2 PCR kit (Clontech), as suggested by the manufacturer. A touch-down PCR program with a total of 40 cycles was run.

2.3.7.3 Amplification of cloned DNA fragments

For difference products, the RDA adapters J-Bgl-24 (for DP3) and N-Bgl-24 (for DP2) were used as forward and reverse primers; for other cloned DNA fragments, the universal forward and reverse plasmid specific M13 primers. The template consisted of 5 to 10 ng plasmid DNA. The total reaction volume was 100 μ l, containing 2 μ g of J-Bgl-24 or N-Bgl-24, or 100 pmol of each universal primer, 2 mM MgCl₂ (Gibco BRL), 1x PCR buffer (Gibco BRL), 0.3 mM dNTPs, 2.5 U Taq polymerase (Gibco BRL). The PCR conditions consisted of: (i) initial denaturation, 1 min at 95 °C, (ii) denaturation, 1 min at 95°C, (iii) annealing, 1 min at 52 °C, (iv) extension, 2 min at 72 °C, the steps ii to iv being repeated 35 times, and (v) final extension, 10 min at 72 °C. For difference products, with J-Bgl-24 or N-Bgl-24 as primers, the annealing and the denaturation steps were replaced by one annealing/extension step with 3 min 72 °C for DP3 and 3 min 70 °C for DP2. The PCRs were stopped at 4 °C.

2.3.7.4 Purification of PCR products

For certain applications (sequencing, labelling of DNA), PCR products were purified using the QIAquick PCR purification kit (Qiagen).

2.3.8 Gel purification of DNA fragments

Agarose gel electrophoresis with 1 % (w/v) agarose (Hybaid AGS) in TAE buffer was performed. Bands of interest were excised and DNA was extracted using the QIAquick Kit (Qiagen). DNA was resuspended in the elution buffer supplied by the manufacturer.

2.3.9 DNA cloning

The gel purified DNA fragments to clone were PCR products, thus with a deoxyadenosine overhang at their 3' ends. They were ligated into a TA cloning vector (pGEM-T, Promega), the reaction mixture of 10 μ l being incubated 1 hour at room temperature, according to the manufacturer's instructions.

For the transformation, competent cells were thawed on ice. 5 μ l ligation mixture were added to 50 μ l cell suspension. After incubation on ice, a heat shock was performed at 42°C for 45 sec, and the cells were put back on ice. 950 μ l of SOC medium was added, and the mixture was incubated 1 hr at 37 °C, vigorously shaken. Bacteria were plated on LB Agar/ampicillin plates on which 40 μ l of a 2 % (w/v) X-gal solution (in dimethylformamide) and 40 μ l of a 100 mM IPTG solution (in water) had been spread for blue/white screen. Only white colonies were picked for further analysis.

2.3.10 Isolation of plasmid DNA

Bacteria were cultured over night in 5 ml LB medium with 1 mg ampicillin. Eventually 850 μ l cell suspension were mixed with 150 μ l glycerol and stored at -80 °C. The rest of the culture was

centrifuged, the medium was carefully withdrawn and the cell pellet was resuspended in 100 µl of a 50 mM Glucose, 25 mM Tris.HCl, 10 mM EDTA, pH 8 solution. After 5 min the cells were lysed with 200 µl of a 0.2 M NaOH, 1 % (w/v) SDS solution. The tubes were gently shaken and after another 5 min, 150µl of a 5 M KAcetate, 200 mM acetic acid solution were added. After 5 min incubation, the supernatant was cleared from proteins and genomic DNA by centrifugation. Plasmid DNA was digested with 10 µg RNase for 1 hour at 37 °C and phenol/chloroform extracted as described above. The DNA pellets were washed 3 times with 75 % ethanol. After air drying, they were resuspended in 15 µl water.

1 µl of the isolated DNA was subjected to restriction digestion as a control. Restriction endonucleases were obtained from New England Biolabs and Fermentas. The digests were performed according to the manufacturers' instructions using the appropriate buffer.

2.3.11 Preparation and labelling of probes

³²P-labeled probes were prepared with the RediprimeTMII random prime labelling system (Amersham) and α-³²P dCTP (3000 Ci/mmol, ICN) according to the manufacturer's protocol. 25 ng purified PCR product were used. After 30 min incubation at 37 °C, the probe was purified with Quick SpinTM columns (Boehringer Mannheim) in order to remove non-incorporated nucleotides. It was denatured 5 min at 99 °C and chilled on ice prior to hybridisation.

2.3.12 Northern blot hybridisation

The blots were prehybridised in a solution containing 0.5 M NaPi, 1 mM EDTA, 7 % (w/v) SDS and 1 % (w/v) BSA (Sigma) at 63 °C for at least 2 hours. For the hybridisation, 14 µl of labelled probe was added per 5 ml hybridisation solution. The blots were hybridised at 63 °C over night.

After hybridisation, they were washed twice with 2× SSC-0.1 % SDS for 10 min at room temperature, twice with 0.1× SSC-0.1 % SDS for 20 min at 42 °C and eventually twice with 0.1× SSC-0.1 % SDS for 20 min at 68 °C. They were exposed for various times depending on the signal intensity. A phosphoimager (BAS2000, Fuji) was used for analysis and quantification of radiolabelled signals.

2.3.13 DNA sequencing

DNA fragments were sequenced by SeqLab (Göttingen, Germany) using the M13 universal or reverse primers. Sequence homologies were detected using standard BLAST (basic local alignment search tool) at the NCBI (<http://www.ncbi.nlm.nih.gov/>).

2.4 cDNA representational difference analysis

RDA was applied as described (Lisitsyn et al., 1993; Hubank et al., 1994; Klingenspor et al., 1999), following the protocol of Hubank and Schatz (1994). Figure 2 is a schematic representation of the procedure that will be detailed in this paragraph.

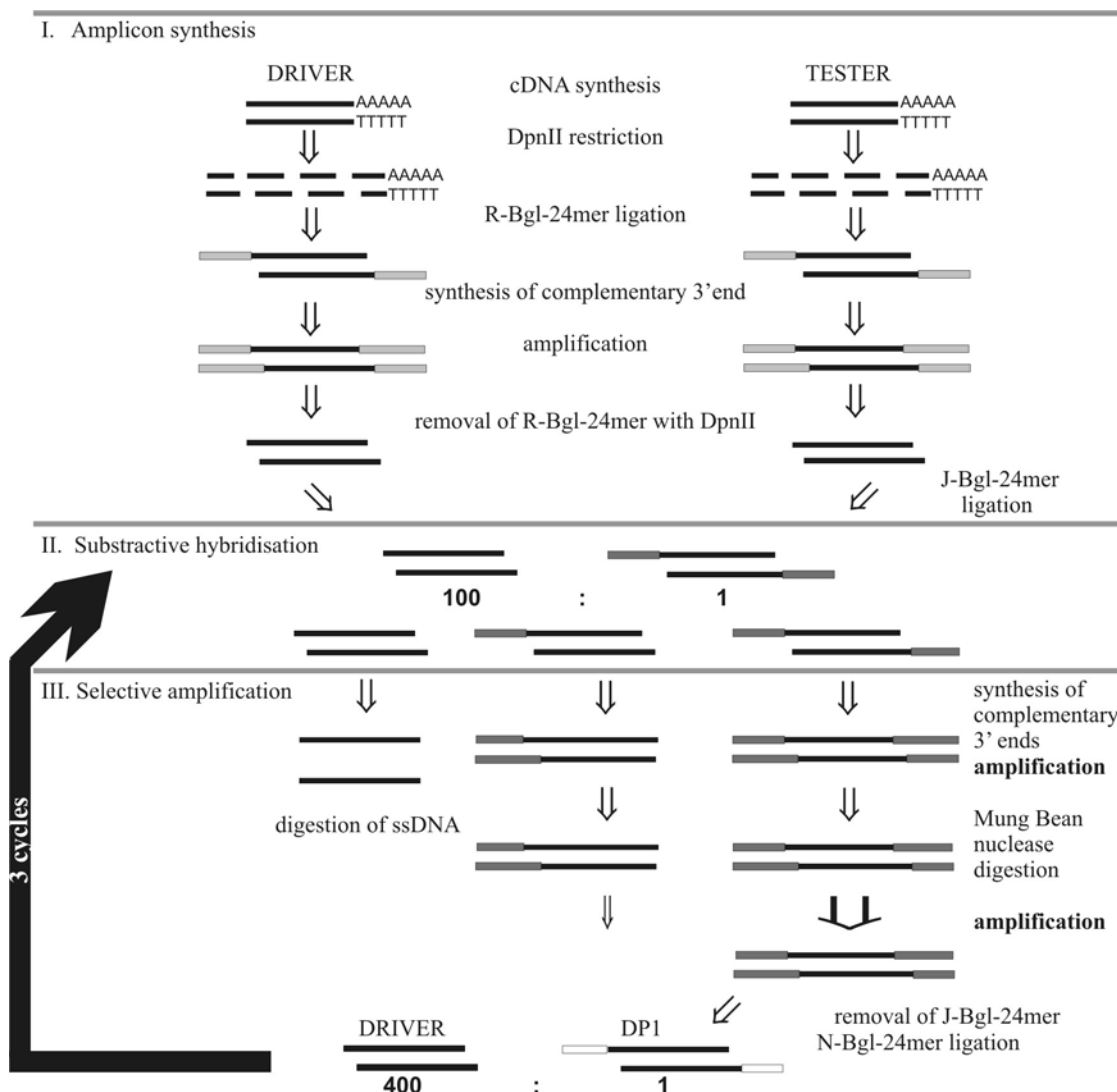


Figure 2. Schematic representation of the RDA protocol based on Hubank and Schatz (1994). After mRNA isolation and cDNA synthesis, the first step of RDA consists in the synthesis of the amplicons, the cDNA populations that will really be compared afterwards. These were subjected to 3 cycles of subtractive hybridisation and selective amplification. The difference products 2 and 3, obtained after 2 and 3 cycles respectively, were cloned. Dark grey boxes represent the J-Bgl oligonucleotides, light grey boxes the R-Bgl oligonucleotides and white boxes the N-Bgl oligonucleotides.

2.4.1 Preparation of the RNA probes

200 μ g RNA from white semi-confluent preadipocytes (pW4) and 140 μ g RNA from brown semi-confluent preadipocytes (pB4), originating from 2 separate cell cultures, were used for RDA. All the following steps were carried out in parallel with the pW4 and the pB4 RNA probes.

As an initial purification step in order to reduce the risk of RNase contamination, RNA probes were precipitated 20 min at -20°C in 1/10 volume NaAcetate (3 M, pH 5.2) and 2.5 volumes isopropanol. The pellet was resuspended in 600 μ l solution D. RNA was phenol/chloroform extracted as follows:

60 μ l of 3 M NaAcetate (pH 5.2), 600 μ l acidic phenol and 120 μ l chloroform/IAA (49:1) were added, and after centrifugation, the upper aqueous phase was transferred to a fresh tube. The RNA was precipitated over night at -20 $^{\circ}$ C with 600 μ l of isopropanol. The pellet was washed and resuspended in 150 μ l water.

The RNAs were then digested with RNase-free DNase (Promega) to remove eventual traces of genomic DNA. 3 μ g RNA were saved for documentation and all the remaining probe was incubated 45 min at 37 $^{\circ}$ C in the following reaction mixture : 1x DNase buffer (400 mM Tris.HCl, 100 mM NaCl, 60 mM $MgCl_2$), 15 U RNase-free DNase (Promega) and 120 U RNase inhibitor (Boehringer Mannheim) in a total volume of 300 μ l. The reaction was stopped with 30 μ l termination mix (1 mg/ml glycogen, 0.1 M EDTA). The RNA was phenol/chloroform extracted twice, chloroform extracted once and precipitated with 1/5 volume of 7.5 M NH_4O Acetate and 3 volumes of ethanol. The pellet was resuspended in 150 μ l water.

The quality of RNA before and after the digestion was checked on a 1 % agarose gel (figure 3). Although the conditions of the digestion had been optimised, a certain degree of degradation of the RNA could not be avoided, as can be seen from the reduction of the intensity of the 28S bands.

Furthermore, 1 μ g of each RNA probe before and after the digestion were subjected to PCR amplification with primers located on two adjacent exons of the hamster UCP1 gene (primers UCP1-1 and UCP1-2, table 1), and the products were compared to the products of the amplification of 10 ng, 1 ng and 0.1 ng of genomic DNA (figure 4). In the white preadipocytes before the digestion, only a very weak signal could be seen; the signal was higher in the brown preadipocytes, corresponding to about 1 ng DNA. After the digestion, there was no detectable signal, suggesting that the digestion had been efficient.

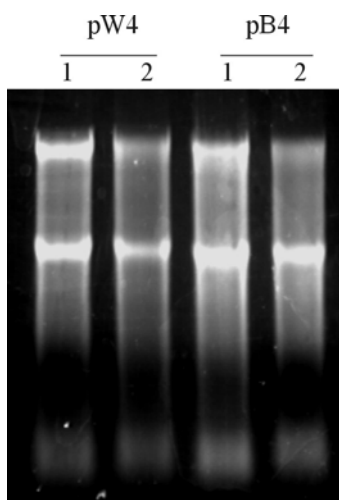


Figure 3. RNA from white and brown preadipocytes before (lanes 1) and after (lanes 2) DNase digestion. 2 μ g RNA were loaded on a 1 % agarose TAE gel.

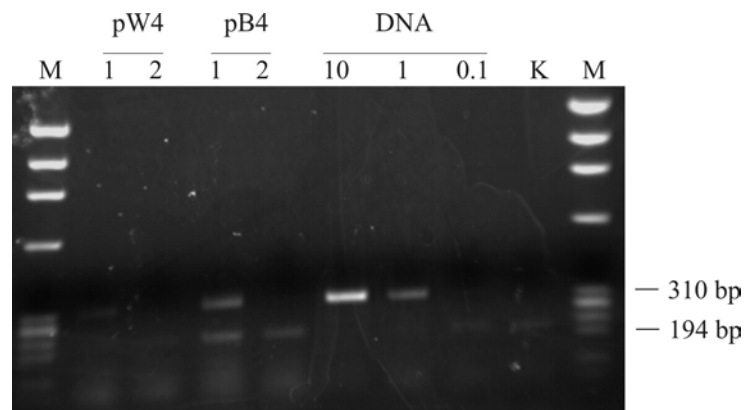


Figure 4. Detection of genomic DNA in RNA probes. The following templates, 1 μ g RNA from white and brown preadipocytes before (lanes 1) and after (lanes 2) DNase digestion and 10 ng, 1 ng and 0.1 ng genomic DNA, were PCR amplified with UCP1 specific primers. The spliced sequence produces a PCR product of 207 bp, so that the PCR product originating from genomic DNA can be identified as the upper band of approximately 300 bp length. (K: negative control with water as template; M: DNA marker HaeIII fragments (Gibco-BRL))

2.4.2 mRNA isolation and reverse transcription

mRNA was isolated by poly (A)⁺ selection using magnetic beads (PolyAtract System IV, Promega). The resulting mRNA dissolved in 250 μ l elution buffer was precipitated overnight at -80°C with 4 μ g glycogen as a carrier. The pellet was resuspended in 10 μ l water. The isolation yielded 1.64 μ g pW4 mRNA and 1.49 μ g pB4 mRNA.

Double stranded cDNA was synthesized with oligo-dT primer using the cDNA-synthesis-system (Gibco BRL) and following the instructions of the manufacturer. The resulting cDNA was phenol/chloroform extracted, precipitated with addition of glycogen and resuspended in 20 μ l TE. Thus 792 ng pW4 cDNA and 940 ng pB4 cDNA have been synthesized.

2.4.3 Generation of the amplicon

The cDNAs were digested at 37°C for 4 hours by 50 U DpnII (Biolabs) in 1x DpnII buffer (Biolabs) in a volume of 100 μ l. 100 μ l TE were added and the cDNAs were extracted twice with phenol/chloroform/IAA, once with chloroform/IAA and precipitated with addition of glycogen carrier in NH_4OAc and ethanol. The pellet was resuspended in 20 μ l TE.

Followed the ligation of the R-Bgl-24 and R-Bgl-12 adapter oligonucleotides (table 2). The whole digested cDNAs were mixed with 8 μ g R-Bgl-24, 4 μ g R-Bgl-12 and 1x ligase buffer (Gibco BRL) in 57 μ l water. The oligonucleotides were annealed in PCR machine by 1 min incubation at 50°C followed by stepwise cooling down to 10°C during 1 hour. Ligation was performed over night at 15°C by addition of 1200 U T4 DNA ligase (Gibco-BRL). The ligations were diluted to a volume of 200 μ l in TE.

For the generation of the amplicons, which are also the representations, different dilutions of the ligated cDNAs were tested as templates for PCR. After optimisation, the amplification was performed in 44 single PCRs for each probe. The template consisted of 4 μ l of the ligated cDNA solution. The total reaction volume was 100 μ l, containing 2 μ g of R-Bgl-24, 1x RDA PCR buffer, 0.34 mM dNTPs, 2.5 U Taq polymerase (Gibco BRL). The polymerase was added after an initial step of 3 min at 72 °C, aiming to melt away the R-Bgl-12 oligonucleotides. After addition of the Taq polymerase, the PCR conditions consisted of: (i) initial extension, 5 min at 72 °C, in order to fill in the 3' ends, (ii) denaturation, 1 min at 95°C, (iii) annealing/extension, 3 min at 72 °C, the steps ii and iii being repeated 20 times, and (iv) final extension, 10 min at 72 °C. The PCRs were stopped at 4 °C.

6 reactions were combined in one tube for 2 phenol/chloroform/IAA extractions, one chloroform/IAA extraction and precipitation in NaAcetate and isopropanol, 20 min on ice. Each amplicon was finally dissolved in a total volume of 440 μ l. The amplification yielded 162 μ g of pW4 amplicon and 187 μ g of pB4 amplicon.

2.4.4 The cycles of subtractive hybridisation and selective amplification

2.4.4.1 Preparation of the drivers

The whole amplicons were digested at 37 °C for 4 hours by 540 U DpnII in 1x DpnII buffer in a volume of 1 ml. The digests were extracted twice with phenol/chloroform/IAA, once with chloroform/IAA and precipitated in NaAcetate and isopropanol on ice for 20 min. The pellet was resuspended in TE at approximately 350 ng/ μ l. These digested cDNAs are the cut drivers. They will be used as drivers for the 3 cycles of subtractive hybridisation.

2.4.4.2 Preparation of the testers

5 μ g of each driver were run in 1.2 % agarose TAE preparative gels, until the bromophenol blue had migrated about 2 cm. The amplicon-containing gel slices were excised, leaving behind the digested adapters. The DNA was extracted using the QIAquick Kit (QIAGEN). DNA was eluted with the provided elution buffer and precipitated with addition of glycogen in NH₄OAcetate and ethanol. The pellet was resuspended in 10 μ l.

1 μ g of purified tester DNA was ligated to the J-Bgl oligonucleotides. The following reaction mixture was prepared: 4 μ g J-Bgl-24, 2 μ g J-Bgl-12, 1x ligation buffer and 1 μ g DNA in 28.5 μ l water. The oligonucleotides were annealed in PCR machine by 1 min incubation at 50 °C followed by stepwise cooling down to 10 °C during 1 hour. Ligation was performed over night at 13 °C by addition of 600 U of T4 DNA ligase. The ligations were diluted to a volume of 90 μ l in TE.

These ligated DNAs are the testers for the first subtractive hybridisations. 1.615 μ g pW4 tester and 1.579 μ g pB4 tester were produced.

2.4.4.3 Subtractive hybridisation

To achieve a tester:driver ratio of 1:100, 0.4 µg of the pW4 and of the pB4 tester were mixed to 40 µg of the pB4 and of the pW4 driver respectively. Both mixtures were once phenol/chloroform extracted, once chloroform extracted and precipitated in NH₄OAcetate and ethanol for 10 min at -70 °C. The pellets were washed twice, dried and resuspended very thoroughly in 4 µl 3x EE buffer by pipetting for at least 2 min, then warming the reaction tube to 37 °C for 5 min, vortexing and spinning the content to the bottom of the tube. 35 µl mineral oil were overlaid, the hybridisation mixtures were denatured for 5 min at 98 °C in PCR machine and cooled down to 67 °C. When this temperature was reached, 1 µl of 5 M NaCl was immediately added to the DNA. The mixture was left to hybridise at 67 °C over night.

Mineral oil was removed and the DNAs were stepwise diluted by adding successively and pipetting vigorously between each step 8 µl TE containing 5 µg/µl tRNA, 25 µl TE and 362 µl TE.

2.4.4.4 Selective amplification

Each hybridisation mix was split into 8 PCRs. The template consisted of 10 µl of the hybridisation mix. The total reaction volume was 100 µl, containing 2 µg of J-Bgl-24, 1x RDA PCR buffer, 0.3 mM dNTPs, 5 U Taq polymerase. The polymerase was added after an initial step of 3 min at 72 °C, aiming to melt away the J-Bgl-12 oligonucleotides. Only after (i) the initial extension, 5 min at 72 °C, in order to fill in the 3' ends, the J-Bgl-24 was added to the reaction mixture. Followed the usual steps: (ii) denaturation, 1 min at 95°C, (iii) annealing/extension, 3 min at 70 °C, the steps ii and iii being repeated 10 times, and (iv) final extension, 10 min at 72 °C. The PCR reactions were stopped at 4 °C. The PCR products were pooled for 2 phenol/chloroform/IAA extractions, one chloroform/IAA extraction and precipitation in NaAcetate and isopropanol with addition of glycogen, 20 min on ice. The pellets were resuspended in 40 µl 0.2x TE.

To remove not annealed single stranded DNA, the PCR products were digested with Mung Bean nuclease (NEB). 20 µl DNA were mixed in 1x Mung Bean nuclease buffer (NEB) and 20 U Mung Bean nuclease in a total volume of 40 µl. After 35 min incubation at 30 °C, the reaction was stopped by addition of 160 µl 50 mM Tris.HCl (pH 8.9) and incubating 5 min at 98 °C, then chilling on ice.

The second part of the amplification was performed with a template of 10 µl digested DNA, each subtraction being split into 8 PCRs. The total reaction volume was 100 µl, containing 1 µg of J-Bgl-24, 1x RDA PCR buffer, 0.3 mM dNTPs, 2.5 U Taq polymerase (Gibco-BRL). The polymerase was added after an initial denaturation step of 1 min at 95 °C. After addition of the Taq polymerase, the PCR conditions consisted of: (i) denaturation, 1 min at 95°C, (ii) annealing/extension, 3 min at 70 °C, the steps ii and iii being repeated 18 times, and (iii) final extension, 10 min at 72 °C. The PCRs were stopped at 4 °C. For the pB4 subtraction, 2 additional cycles were performed.

These amplified DNAs are the difference products 1 (DP1). They were phenol/chloroform/IAA extracted twice, chloroform/IAA extracted once and precipitated in NaAcetate and isopropanol with addition of glycogen, 20 min on ice. The pellets were resuspended in 50 μ l TE. The amplification yielded 6 μ g pW4 DP1 and 1.85 μ g pB4 DP1.

2.4.4.5 Generation of DP2

To generate the new tester, the whole pB4 DP1 and 3 μ g of the pW4 DP1 were digested with DpnII. The digested DNAs were purified from digested adapters by excision in agarose gel. 400 ng DP1 were then ligated to N-Bgl-12 and N-Bgl-24 (ligation temperature: 15 $^{\circ}$ C). A different adapter than in the previous cycle was used in order to avoid “contamination” from one cycle to the next.

The subtractive hybridisation was performed at a tester:driver ratio of 1:400, mixing 100 ng of N-Bgl ligated pW4 DP1 to 40 μ g pB4 driver and vice versa. N-Bgl-24 was used as a primer for selective amplification (annealing/extension temperature of 72 $^{\circ}$ C). In the second amplification step, 20 cycles were performed for the pW4 subtraction and 28 for the pB4 subtraction. The amplification yielded 27.7 μ g pW4 DP2 and 54.6 μ g pB4 DP2.

2.4.4.6 Generation of DP3

10 μ g pB4 DP2 and 10 μ g of the pW4 DP2 were digested with DpnII and gel purified. 1 μ g DP2 was then ligated to J-Bgl-12 and J-Bgl-24 (ligation temperature: 13 $^{\circ}$ C), thus generating the new tester.

The subtractive hybridisation was performed at a tester:driver ratio of 1:16000, mixing 2.5 ng of J-Bgl ligated pW4 DP2 to 40 μ g pB4 driver and vice versa. J-Bgl-24 was used as a primer for selective amplification (annealing/extension temperature of 70 $^{\circ}$ C). In the second amplification step, 30 cycles were performed for both subtractions. The amplification yielded 15 μ g pW4 DP3 and 15.5 μ g pB4 DP3.

2.4.5 Cloning of the difference products

DP2 and DP3 were chosen to be cloned. The difference products of the brown preadipocytes had a size range of 200 to 900 kb. The pW4 and pB4 DP2s and DP3s were added a deoxyadenosine overhang at their 3' ends for a subsequent ligation in a TA cloning vector. 2 μ g template were used for this tailing reaction. The reaction mixture consisted of 2.5 mM MgCl₂, 0.2 mM dATP, 1x PCR buffer (Gibco BRL) and 5 U Taq polymerase in a volume of 40 μ l. It was incubated for 15 min at 72 $^{\circ}$ C, and the reaction was stopped on ice. The whole reaction mixture was separated on a 3% agarose gel (Metaphor agarose, FMC), cut into 5 or 6 size fractions and extracted from the gel slices, in order to reduce redundancy of highly abundant cDNAs and avoid bias towards small fragments in the subsequent cloning step. The fractions were ligated into a TA cloning vector (pGEM-T, Promega),

transformed into DH5- α competent cells and plated on LB-Agar/ampicilin plates, using the blue/white screen to select clones of interest. The colonies were harvested with a rubber policeman in 2 ml LB medium and stored at -80°C with 30 % glycerol. Thereby 12 cDNA libraries for brown preadipocytes and 11 for white preadipocytes have been established. From each of them, 10 clones were isolated and analysed by restriction digestion. From those libraries that seemed particularly heterogeneous some more clones were isolated.

2.5 Microarrays

2.5.1 Experimental design

The aim of the microarray hybridisations performed was not only to screen the difference products obtained by RDA, but also to allow a large-scale gene expression analysis during the differentiation of preadipocytes in cell culture and in tissue samples. To be able to compare multiple hybridisation, a double labelling method was used (Schena et al., 1996) with one channel being affected to a reference cDNA which was identical for all hybridisations (Figure 5).

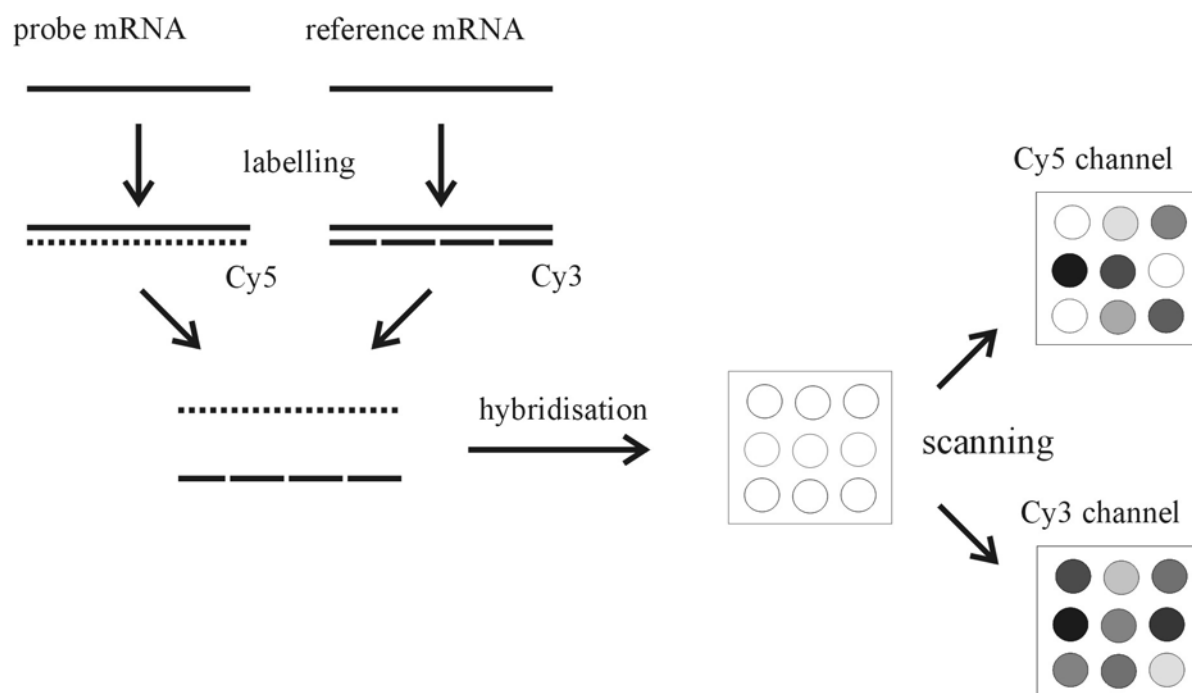


Figure 5. Schematic representation of the double labelling method. The probe mRNA is compared to a reference which is the same for all hybridisations and will allow the comparison of multiple hybridisation. Probe and reference mRNA are labelled with Cy5 and Cy3 respectively. The labelled cDNAs are mixed and hybridised to an array. After hybridisation, the array is scanned at the wavelengths corresponding to the Cy5 and the Cy3 signals, providing on two separate channels the probe and the reference signal.

					array #	
			Cy5	Cy3	1st hybr.	replicate
cell culture	white	semi-confluent preadipocytes	pW4	reference	1	29
	brown		pB4	reference	2	30
	white	confluent preadipocytes	pW6	reference	3	31
	brown		pB6	reference	4	32
	white	preadipocytes beginning differentiation	W6	reference	5	33
	brown		B6	reference	6	34
	white	mature adipocytes	W10	reference	7	35
	brown		B10	reference	8	36
	white	adipocytes treated with isoproterenol	Wiso	reference	9	37
	brown		Biso	reference	10	38
	white	adipocytes treated with Cl 316.243	WCL	reference	11	39
	brown		BCL	reference	12	40
tissue pool	white	adipose tissue from animals exposed to 4 °C	WATC	reference	15	
	brown		BATC	reference	16	
individual tissue Samples	white	adipose tissue male 1	Wm1	reference	17	
	brown		Bm1	reference	18	
	white	adipose tissue male 2	Wm2	reference	19	
	brown		Bm2	reference	20	
	white	adipose tissue male 3	Wm3	reference	21	
	brown		Bm3	reference	22	
	white	adipose tissue female 1	Wf1	reference	41	
	brown		Bf1	reference	42	
	white	adipose tissue female 2	Wf2	reference	43	
	brown		Bf2	reference	44	
	white	adipose tissue female 3	Wf3	reference	45	
	brown		Bf3	reference	28	

Table 4. List of the hybridisations performed (see table 3 for a more precise description of the cell culture probes). The cell or tissue probes were labelled with Cy5 and mixed to a Cy3 labelled reference cDNA for hybridisation. All hybridisations with cell culture probes were replicated once.

Table 4 is a list of the hybridisations performed. All the arrays were hybridised to an aliquot of the Cy3 labelled reference cDNA and to a probe labelled with Cy5. The arrays were hybridised to probes from cells at different states of differentiation (pAd4, pAd6, Ad6, Ad10) and cells treated with β -agonists (Adiso, AdCL): all these hybridisations with cell culture probes were replicated once. Furthermore, arrays were hybridised in single experiments to probes from a pool of adipose tissues from animals kept at 4 °C for 18 hours and from individual tissue samples from 6 animals, 3 males and 3 females.

2.5.2 Choice and preparation of clones for the screening on microarrays

256 clones were chosen for being screened on microarrays: 71 from pW4 DP3, 50 from pW4 DP2, 75 from pB4 DP3 and 60 from pB4 DP2. This corresponds to at least 10 clones from each size fraction cDNA library. When one of these libraries appeared to be very heterogeneous in its content, more

clones were selected. These clones were cultured over night in 5 ml LB medium and stored in glycerol stocks.

species	sequ.	accession	function	gene description
mouse	pOB24	X62332	structure	pOB24
Djung.h.	UCP1	AF271263	mitochondrial	UCP1
Djung.h.	UCP3	AF271265	mitochondrial	UCP3
Djung.h.	PPARg	-	transcription factor	PPAR gamma
rat	P55CDC	U05341	cell cycle	cell division cycle protein p55CDC
rat	PKC	M13707	signal transduction	protein kinase C
rat	rheb	U08227	signal transduction	Sprague-Dawley Ras-related protein (rheb)
rat	ODC	NM_012615	protein metabolism	Ornithine decarboxylase
rat	cycB	NM_012615	cell cycle	cyclin B
rat	GAPDH	AF106860	metabolism	glyceraldehyde-3-phosphate-dehydrogenase
Rat	ACS	D30666	metabolism	acyl CoA synthetase II
rat	APC	D38629	ECM	APC protein
rat	GCGR	D38629	receptor	glucagon receptor
rat	D123	U34843	cell cycle	cell cycle progression related D123
rat	p27kip1	NM_031762	cell cycle	cyclin-dependent kinase inhibitor 1B (p27, kip1)
rat	GluR6	Z11548	receptor	glutamate receptor subunit (GluR6)
rat	PPARd	U40064	transcription factor	Peroxisome proliferator activator receptor, delta
rat	PCNA	Y00047	replication	proliferating cell nuclear antigen (PCNA/cyclin)
rat	MLH1	NM_031053	DNA repair	mismatch repair protein
rat	P53	X13058	signal transduction	nuclear oncoprotein p53
rat	PPARg	AB011365	transcription factor	PPAR gamma
rat	MSH2	NM_031058	DNA repair	mismatch repair protein
rat	HOX	J02722	microsomal	heme oxygenase
rat	TIMP1	U06179	secreted	tissue inhibitor of metalloproteinase 1
rat	GST	M25891	antioxidant	glutathione S-transferase
rat	TACBP49	U15734	synaptic	taipoxin-associated calcium binding protein 49
rat	u-PA	X63434	secreted	urokinase-type plasminogen activator
rat	PLAT	NM_013151	secreted	plasminogen activator, tissue
rat	24KG	M75153	secretory pathway	p21-like small GTP-binding protein (24KG)
rat	BAD	AF003523	apoptosis	Bcl-2 associated death promoter (BAD)
rat	PAI-1	M24067	secreted	plasminogen activator inhibitor-1
rat	OB-Rb	U52966	receptor	leptin receptor isoform b
rat	cdc25A	D16236	cell cycle	cell division cycle 25A
rat	PB-cadh	D83349	cell adhesion	short type PB-cadherin
rat	CT-ATPas	M99223	Ca transport	Calcium transporting ATPase
rat	met	X83537	ECM	membrane type matrix metalloproteinase
rat	rad	U12187	signal transduction	ras related protein (rad)
rat	CRLR	L27487	receptor	calcitonin receptor-like receptor
rat	CnA	D90035	signal transduction	calcineurin A alpha
rat	HO2	J05405	microsomal	heme oxygenase-2
rat	TACE	AJ012603	protein metabolism	TNF-alpha converting enzyme
rat	Cts1	NM_013156	lysosomal	cathepsin L
rat	Ca-PK2	NM_012519	signal transduction	Ca ⁺⁺ /calmodulin-dependent protein kinase II
rat	N-myc	X63281	transcription factor	N-myc
rat	CCND1	D14014	cell cycle	cyclin D1

Table 5. List of the standard clones from Djungarian hamster and from rat spotted on the arrays. The accession number and an indication about the function are given.

Additionally, 41 rat reference clones with established functional relevance to adipocyte development (Research Genetics, <http://www.resgen.com>, vector: pT7T3D-PAC w/ modified polylinker) as well as 3 available hamster clones and one mouse clone were chosen for arraying.

As a negative control, Salmonella cDNA was arrayed, and as a positive control, a set of luciferase clones (the complete luciferase sequence, the 5' end, the middle part and the 3' end). The latter served also as a control for the quality of the labelling reaction, as luciferase mRNA was spiked into all mRNA samples prior to labelling.

2.5.3 Microarray manufacturing

The cDNA fragments to be arrayed were prepared by PCR amplification of bacterial glycerol stocks. For amplification the following primers were used: J-Bgl-24 for DP3, N-Bgl-24 for DP2 and 1F-mod and 3R-mod as forward and reverse plasmid specific primers for the reference and control clones (table 2). The primers used were all modified by addition of a hexamine group at their 5' ends. The PCR reactions were performed in a total volume of 100 μ l, containing 80 pmol primer (for the reference clones 40 pmol 1F-mod and 40 pmol 3R-mod), 1.5 mM MgCl₂ (Gibco BRL), 1x PCR buffer (Gibco BRL), 0.2 mM dNTPs, 5 U Taq polymerase (Gibco BRL) and 1 μ l of the bacterial glycerol stock. The PCR conditions for the reference and control clones consisted of: (i) initial denaturation, 2 min at 94 °C, (ii) denaturation, 40 sec at 94 °C, (iii) annealing, 1 min at 55 °C, (iv) extension, 2.5 min at 72 °C, the steps ii to iv being repeated 35 times, and (v) final extension, 10 min at 72°C. For the DPs, the annealing and the extension steps were replaced by one annealing/extension step of 3.5 min at 72 °C for DP3 and 3.5 min at 70 °C for DP2. As a control for the quality of the PCR products, 1 μ l of each PCR product was run on a 1 % agarose TBE gel. For each clone 2 PCRs were performed and the PCR products were pooled prior to purification by Qiaquick purification kit (Qiagen). Water was used as an elution buffer. The eluted DNAs were pipetted in 384 well plates and evaporated overnight on a hot plate (30 °C). The PCR products were then resuspended in 10 μ l spotting buffer (5xSSC).

Microarrays were produced as described by Franssen-van Hal et al. (2002). They were printed on silylated slides (CELAssociates, Houston, Texas, USA) using a PixSys 7500 arrayer (Cartesian Technologies, Durham, NC, USA). Arrays were spotted by passive dispensing using 4 quill pins (Chipmaker 3; Telechem), resulting in a spot diameter of 0.12 mm at a volume of about 0.5 nl. All clones were printed in duplicate onto the arrays. After printing, microarrays were allowed to dry at room temperature for at least 3 days. Free aldehyde groups were blocked according to the method of Schena et al (1996): the glass slides were washed twice in 0.2 % SDS for 2 min, twice in water for 2 min prior to denaturation of DNA by 2 min boiling in water. Once the slides had dried, they were incubated for 5 min in a 2.5 g/l NaBH₄ and 25 % ethanol solution, causing the reduction of the free aldehyde groups. The slides were then washed 3 times for 1 min in 0.2 % SDS, once in water and

poured for 30 sec in boiling water before they were dried by centrifugation. The arrays were then ready for hybridisation.

2.5.4 Sample preparation and labelling

All RNAs from cultured cells used for array hybridisation were pooled from at least two different cell cultures. The RNAs from animals exposed to 4 °C for 18 hours (WATC and BATC) were pooled from 3 animals. The reference RNA was a mixture of RNAs from the WAT of 16 adult animals and from the BAT of 18 adult animals. mRNA for microarray hybridisation was isolated using a mRNA purification kit (Amersham Pharmacia). It was eluted in 1 ml of the provided elution buffer and precipitated following the instructions of the manufacturer. The pellet was resuspended in 25 µl water. The yield was of 1 to 2 % mRNA per weight of total RNA.

The mRNAs were labelled by incorporation of either Cy3-dCTP or Cy5-dCTP during a reverse transcription (Schena et al., 1996). 1 to 2.5 µg of poly(A⁺) RNA was mixed with 2 µg oligo-dT primer (21-mer) and 0.5 ng luciferase mRNA in a final volume of 13.5 µl, heated for 3 min at 65 °C for denaturation of the RNA and for 10 min at 25 °C in order to anneal the oligo-dT primer. It was then immediately put on ice. The reverse transcription reaction was performed for 2 hours at 37 °C in a reaction mixture contained the mRNA template with the annealed oligo-dT primer, 1x first strand buffer (Gibco BRL), 10 mM DTT, 0.5 mM dATP, 0.5 mM dGTP, 0.5 mM dTTP, 0.04 mM dCTP, 0.04 mM Cy3-dCTP (or Cy5-dCTP), 15 U RNase OUT (Gibco BRL) and 150 U SuperScript II reverse transcriptase (Gibco BRL) in a total volume of 25 µl. The labelled cDNA was then purified by a NaAcetate/ethanol precipitation performed at room temperature. The pellet was dried in a speedvac and resuspended in 10 µl TE (pH 8.0). After a 3 min boiling step, the cDNA was immediately put on ice and 2.5 µl 1 M NaOH were added. This mixture was incubated for 10 min at 37 °C to break down the remaining RNA. To neutralize the pH, 2 µl 1M HCl and 2.5 µl 1 M Tris-HCl (pH 6.8) were added. Finally, a second ethanol precipitation at room temperature was performed and the resulting cDNA pellet was resuspended in 20 µl hybridisation buffer containing 5xSSC, 0.2 % SDS, 5x Denhardt's, 50 % (v/v) formamide, 0.2 mg/ml denatured herring sperm DNA. Compared to other solutions, this buffer should lead to higher signal to background ratios (Cheung et al., 1999). Prior to hybridisation, the labelled cDNA was denatured for 3 min at 65°C and spun for 2 min at 12000x g to remove non dissolved debris.

2.5.5 Microarray hybridisation

The microarrays were prehybridised at 42 °C for several hours in a 20 ml hybridisation volume in hybridisation buffer (5x SSC, 0.2 % SDS, 5x Denhardt's, 50 % (v/v) formamide, 0.2 mg/ml denatured

herring sperm DNA). After prehybridisation, the slides were rinsed twice in Millipore filtered water, once in isopropanol, and dried by centrifugation (2 min, 470x g). The hybridisation was performed in a GeneFrame (1x1 cm², 25 µl hybridisation volume; Westburg, Leusden, The Netherlands) which, due to the size of the spotted area, was enlarged to reach a hybridisation volume of 32 µl. A 1:1 (v/v) mixture of Cy3 and Cy5 labelled cDNAs was applied to each array. Arrays were hybridised overnight at 42 °C in a humid hybridisation chamber. After hybridisation, the gene frames were removed and the slides were washed at room temperature in 1x SSC-0.1 % SDS for 5 min, in 0.1x SSC-0.1 % SDS for 5 min, in 0.1x SSC for 1 min and then were dried by centrifugation (2 min, 470x g).

As a preliminary set of experiments, WAT and BAT mRNAs were compared on several arrays, using different amounts of mRNA template for the labelling reactions. WAT cDNA was labelled with Cy3 and BAT with Cy5, and vice versa for a second set of hybridisations. 2 µg, 1 µg, 0.5 µg and 0.25 µg mRNA templates were used for the labelling reactions. This procedure allowed hybridisations with reasonable signal to background ratios for the arrays hybridised to probes resulting from the labelling of 2 µg or of 1 µg of mRNA. In these arrays, more than 90 % of the spots produced signals significantly higher than the background. With lower amounts of template, the quality of the arrays degraded and the number of spots with signals similar to the background raised dramatically. For this reason, it was decided to use 1 µg templates for all the further labelling reactions.

Thus the probe mRNAs were labelled with Cy5 as described in 2.5.4, 1 µg mRNA being used for each hybridisation. The reference mRNA was labelled with Cy3. It was split in 26 aliquots containing each approximately 2.5 µg mRNA, and 26 individual labelling reactions were performed. The labelled cDNAs were pooled prior to the precipitation steps and finally dissolved in 1300 µl hybridisation solution, corresponding to the same dilution as for the probes. The labelled cDNA reference was stored at -20°C in the dark.

2.5.6 Microarray scanning

The microarrays were scanned using a confocal laser scanner ScanArray 3000 (General Scanning Inc.) containing a GreNe 543 nm laser for Cy3 measurement and a HeNe 633 nm laser for Cy5 measurement. Scans were made with a pixel resolution of 10 micron, a laser power of 90 % and a PMT voltage of 55 %. The software package ArrayVision (Imaging Research, Ontario, Canada) was used for image analysis of the TIFF-files as generated by the scanner. Average spot intensities were collected for each individual spot and stored for further data processing in Microsoft Excel®. Prior to any further analysis, the quality of the data was controlled. Spots covered by stains or bleached, areas with too high background were removed from the data set.

2.5.7 Data analysis and normalisation

2.5.7.1 Comparison of multiple hybridisations

In the preliminary experiment referred to in 2.5.5, microarrays were used to compare 2 hybridisations, i.e. to compare 2 different mRNA populations. Microarray hybridisations are carried out with a large excess of immobilised DNA compared to the labelled probe. This allows to perform two colour hybridisations without competition between the two labelled probes. The kinetics of hybridisation are pseudo-first order and there is a linear correlation between RNA expression levels and hybridisation signals (Van Hal et al., 2000). “Under these conditions, the linear differences arising from exact amount of applied target, extent of target labelling, efficiencies of fluor excitation and emission, and detector efficiency can be compounded into a single variable and the information from each detection channel normalised” (Duggan et al., 1999). This gives the possibility for a statistical sound comparison of two simultaneous hybridisations.

The aim of the series of microarray hybridisations performed here was not only to screen the difference products for real differences in gene expression in brown and white preadipocytes, but also to follow the expression of these genes during differentiation of the adipose cells and in vivo. To be able to compare multiple hybridisations, the following experimental design was used: a pool of mRNAs from the BAT of 18 animals and the WAT of 16 animals was used as a reference. Cy3 labelled cDNA was synthesised and all the arrays were hybridised simultaneously with this reference and with a Cy5 labelled probe. For each hybridisation, the Cy5/Cy3 ratios was calculated, representing the expression levels in the probe relatively to the tissue mix of the reference. These normalised ratios can then be compared to other arrays hybridised to the same reference. Preliminary experiments indicated that over 90 % of the clones show significant signals with such a reference so that only few data will be lost because of the absence of a reference signal.

2.5.7.2 Statistical model for the data normalisation

Various sources of fluctuation should be expected in microarray experiments (Schuchhardt et al., 2000):

- (i) for each spot, random fluctuations between different arrays in the amount of DNA immobilised, due to fluctuations in the spotted volume and in the fixation of DNA on the array
- (ii) random fluctuations in the amount of labelled cDNA used for hybridisation, due to differences in the mRNA preparation, in the reverse transcription and labelling efficiencies for each sample
- (iii) random fluctuations in the hybridisation efficiencies, which are local, within different areas on one array, and global, between two different arrays.

Furthermore, the background level (non-specific radiation) should be taken into account.

This results in the following statistical model: the measured signal intensity of a particular spot on an array depends on the amount of labelled cDNA used for hybridisation, the amount of DNA in the spot, the true expression level of the gene and an error due to local fluctuations. The local background inside the spot is added to this.

Statistical model

This model is derived from Yang et al. (2001).

For the fluorescent dye i , the spot j and the array n , let t_{ijn} represent the measured target signal intensity, b_{ijn} the background intensity inside the spot j , a_{in} the total amount of labelled cDNA used, d_{jn} the amount of DNA in spot j , θ_{ijn} the true expression level of the gene from spot j in the probe of array n and dye i , and ε_{ijn} a random variable with ideal value 0.

As Yang et al. show that background noise is additive, the observed target intensity is

$$\begin{aligned} t_{ijn} &= a_{in} \cdot d_{jn} \cdot \theta_{ijn} \cdot e(\varepsilon_{ijn}) + b_{ijn} \\ &= \omega_{ijn} \cdot e(\varepsilon_{ijn}) + b_{ijn} \\ &\text{with } \omega_{ijn} = a_{in} \cdot d_{jn} \cdot \theta_{ijn} \end{aligned}$$

Thus, the fluctuations in the amount of immobilised DNA (i) are included in the d_{jn} component, the fluctuations in the amount of labelled cDNA (ii) and the global hybridisation efficiency (iii) in a_{in} , and the local fluctuations (iii) in ε_{ijn} .

2.5.7.3 Correction for the background

The difficulty with the correction for the background comes from the impossibility to assess the true background: the background intensity inside a spot (b_{ijn}). It can only be estimated by the background level in the non spotted area. Yet, there can be a large local heterogeneity in the background levels, making this estimation difficult. We measured background fluorescence intensities around each of the 96 spots blocks of the arrays, so that only a general information about the mean background level on the array is available. Due to the narrowness of the space between the spots, it seemed difficult to estimate local background levels, as suggested by Yang et al. (2001).

A good opportunity to test the quality and reproducibility of the signals are the 40 hybridisations with the Cy3 reference cDNA. For each array, the Cy3 signals were normalised with their median, to correct for different hybridisation efficiencies. The Cy3 signals for each spot were then compared. Their variability reflect the fluctuation in the amount of DNA spotted and the local differences in hybridisation efficiency. Figure 6 shows the distribution of the coefficients of variation ($CV = SD / \text{mean}$) in % of the Cy3 signals relatively to the mean of the Cy3 signals without correction for the background (A) and with correction for the background (B). The mean Cy3 background of all arrays is 0.19, the lowest 0.1. For spots with high mean signals, the two methods are equivalent and the CV is

ranging from 10 to 30 %. With lower signals, the CV rise till about 50 % when no background correction is performed and till almost 100 % when the signals are corrected for the background.

Thus, the background correction seems to induce additional errors for low signals. We have only a rough estimation of the background level. When considering low signals not much higher than the background, a correction through this estimate of the background can induce high levels of error. Therefore, this background estimate should only be used as an indicator, not as a correction factor. Furthermore, signal intensities too close to the background produce no reliable data and should not be considered for data analysis. We have chosen to consider as not significant all spots with a mean Cy3 and Cy5 signal lower than twice the mean background of the slide.

Applying this method, 68 % of the spots have a variation of their Cy3 signals lower than 20 %, 90 % lower than 30 % (figure 6.C). This variation reflects fluctuation in the amounts of DNA spotted and the local differences in hybridisation efficiency. It is slightly increased at lower intensities.

Nota bene: for each clone, the median values of the non normalised Cy3 signals were calculated and termed as “virtual slide” intensities. They will be used in further steps of the data analysis to rescale expression ratios.

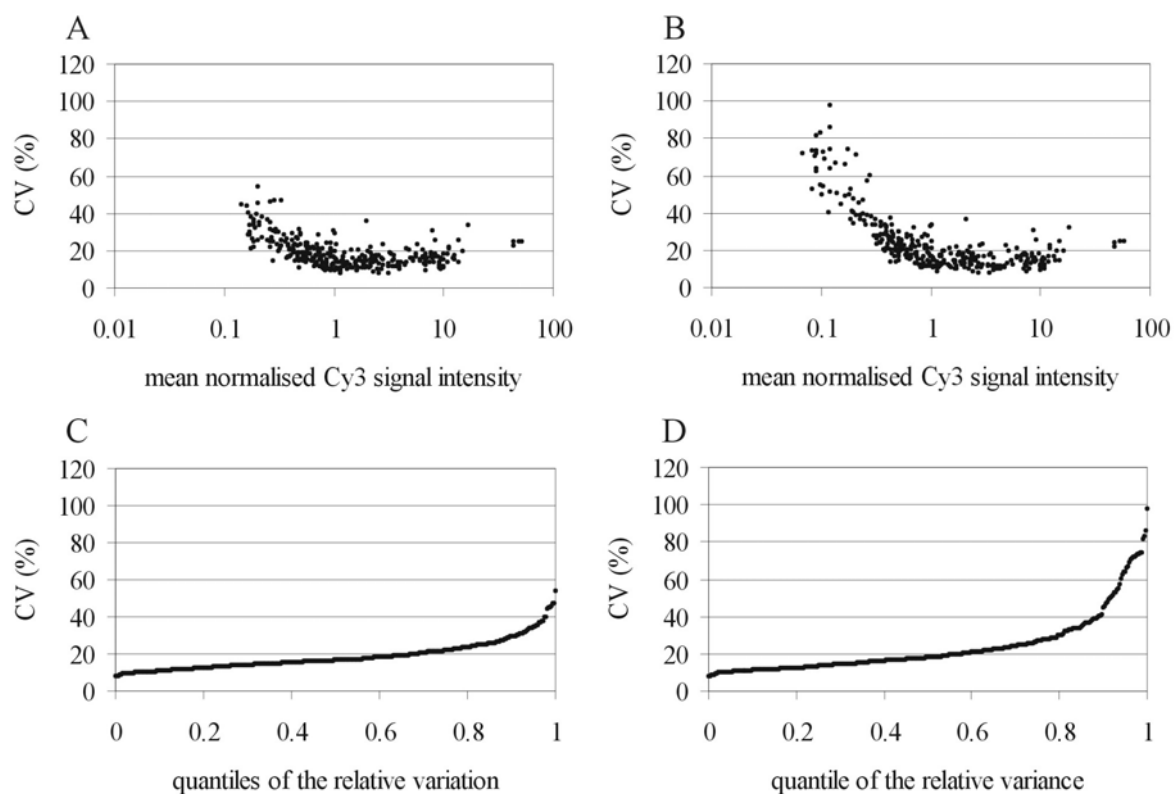


Figure 6. Comparison of the reference (Cy3) signals on all the arrays, using the signals without correction for the background (A and C) and the signals corrected for the background (B and D). A, B. For each spot, the CV ($CV = 100 \times SD$ divided by the mean) of all the Cy3 signals in % is plotted against the mean normalised Cy3 signal. C, D. The CV is plotted against its quantile.

2.5.7.4 Local normalisation

The local normalisation is the normalisation for local differences within one array. The reference signal is used for this purpose: the Cy5/Cy3 ratios are calculated. The Cy5 and Cy3 signals from one spot are compared, so that the Cy5/Cy3 ratio is no more dependent on the amount of DNA spotted. The statistical model shows that this ratio contains three components: the true signal / reference ratio (λ_{jn}), the ratio of the amounts of cDNA used in the Cy5 and Cy3 hybridisations (ρ_n) and an error. To assess the efficiency of this normalisation, the evaluation of the reproducibility of signals in duplicate spots is a good validation. For duplicate spots, the 2 first components of the Cy5/Cy3 ratio are identical, so that by comparing duplicate spots, the error in this normalisation can be assessed. This error is in part linked to the background level, so that it is decreasing with higher signal intensities.

Statistical model

Lets take the logarithm of the measured intensity,

$$\ln(t_{ijn}) = \ln(a_{in}) + \ln(d_{jn}) + \ln(\theta_{ijn}) + \varepsilon_{ijn} + \gamma_{ijn}$$

$$\text{with } \gamma_{ijn} = \ln(1 + b_{ijn} / (\omega_{ijn} \cdot e(\varepsilon_{ijn})))$$

For high signals ($t_{ijn} \gg b_{ijn}$), γ_{ijn} is close to 0. Let y_{jn} represent the logarithm of the Cy5/Cy3 ratio,

$$y_{jn} = \ln(t_{5jn} / t_{3jn}) = \ln(a_{5n} / a_{3n}) + \ln(r_{jn}) + \varepsilon_{5jn} - \varepsilon_{3jn} + \gamma_{5jn} - \gamma_{3jn}$$

where $r_{jn} = \theta_{5jn} / \theta_{3jn}$ is the true signal / reference ratio. Lets define $\rho_n = \ln(a_{5n} / a_{3n})$, $\lambda_{jn} = \ln(r_{jn})$ and $\tau_{jn} = \varepsilon_{5jn} - \varepsilon_{3jn} + \gamma_{5jn} - \gamma_{3jn}$

$$y_{jn} = \rho_n + \lambda_{jn} + \tau_{jn}$$

If we compare the duplicate spots j' and j'' on one array corresponding to the clone j ,

$$\lambda_{j'n} = \lambda_{j''n}$$

and

$$\Delta y_{jn} = y_{j'n} - y_{j''n} = \tau_{j'n} - \tau_{j''n}$$

Yang et al. show that the $\varepsilon_{5jn} - \varepsilon_{3jn}$ are independent and identical normal distributions for each spot j . The remaining term is $\gamma_{5j'n} - \gamma_{3j'n} - \gamma_{5j''n} + \gamma_{3j''n}$, linked to the background.

What is the distribution of the $\tau_{j'n} - \tau_{j''n}$?

Figure 7 shows the comparison of the signal / reference ratios of duplicate spots from the slide 29, not corrected (A, C, E) and corrected (B, D, F) for the background. This array was chosen because it has one of the highest background levels. The low signals have been removed as explained in 2.5.7.3. In the scatter plots (figure 7.A and B) the signal / reference ratios were rescaled by multiplication to the virtual slide intensities. The difference between duplicates is not affected by this, but the ratios are scaled according to signal intensities. It can be seen that the dots are rather tightly gathered around the $x=y$ axis. Ideally, they would lie on the diagonal. The dispersion of the dots is higher for low intensity

signals, especially when the data were corrected for the background. Without background correction, there are only 5 outliers (duplicates ratio > 2); with background correction 22.

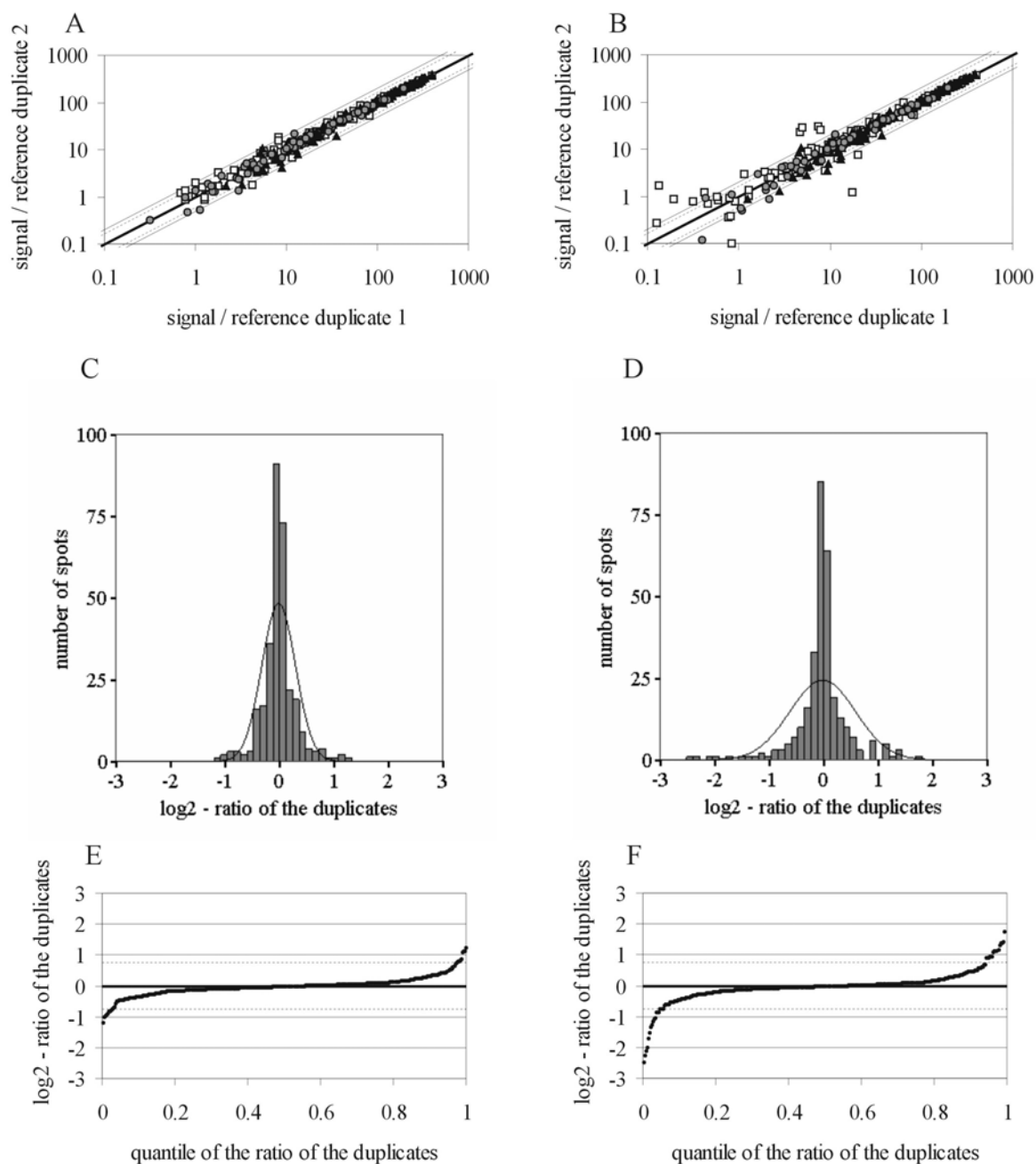


Figure 7. Reproducibility of duplicates in slide 29, using the signals without correction for the background (A, C and E) and the signals corrected for the background (B, D and F). A, B. Scatter plot of the signal / reference ratios (Cy5/Cy3) rescaled with the virtual slide intensities. For each clone, the ratio from one spot is plotted against its duplicate's ratio. The thick solid line is the $x=y$ axis; the thin solid lines are the $x=2y$ and the $x=y/2$ axis; the thin dashed lines are the $x=3y/5$ and the $x=5y/3$ axis. The white squares \square correspond to the clones from the pW4 DPs, the black triangles \blacktriangle to the clones from the pB4 DPs and the grey circles \bullet to the reference clones. C, D. Histogram of the distribution of the \log_2 of the duplicate 1 / duplicate 2 ratios. The best fitting Gauss curve is shown. E, F. The \log_2 of the duplicate 1 / duplicate 2 ratio is plotted against its quantile. The dashed lines correspond to the ratios duplicate 1 / duplicate 2 = 3/5 and 5/3.

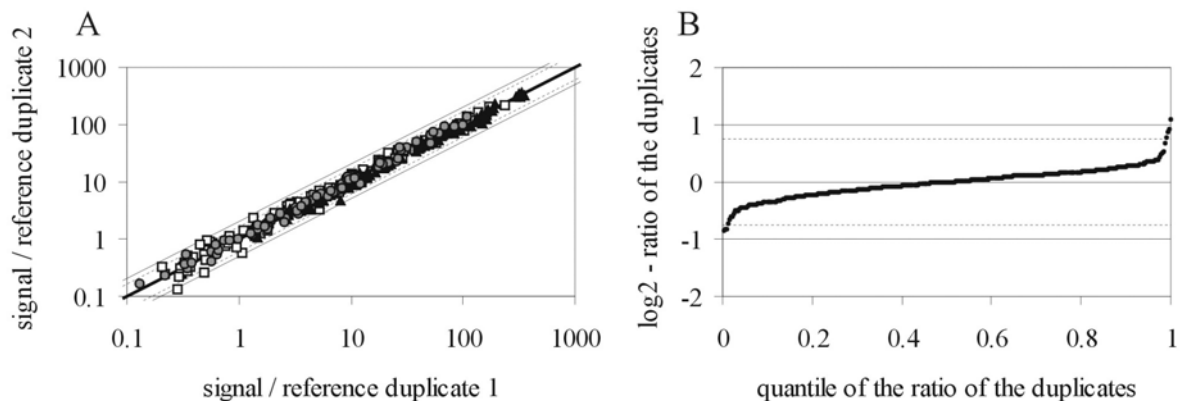


Figure 8. Reproducibility of duplicates in slide 02, using the signals without correction for the background. A. Scatter plot of the signal / reference ratios (Cy5/Cy3) rescaled with the virtual slide intensities. For each clone, the ratio from one spot is plotted against its duplicate's ratio. The thick solid line is the $x=y$ axis; the thin solid lines are the $x=2y$ and the $x=y/2$ axis; the thin dashed lines are the $x=3y/5$ and the $x=5y/3$ axis. The white squares \square correspond to the clones from the pW4 DPs, the black triangles \blacktriangle to the clones from the pB4 DPs and the grey circles \bullet to the reference clones. B. The \log_2 of the duplicate 1 / duplicate 2 ratio is plotted against its quantile. The dashed lines correspond to the ratios duplicate 1 / duplicate 2 $3/5$ and $5/3$.

The histograms (C, D) and the quantile graphs (E, F) show the distribution of the logarithms in base 2 of the ratios of the duplicates (Δy_j). The mean of the \log_2 - ratios are close to 0 in both cases (without background correction: 0.01; with background correction: 0.02), the standard deviation is much higher when a background correction was performed (without background correction: 0.31; with background correction: 1.38).

Similar results were found for other arrays, with closer distributions around the line of identity when the background is lower (figure 8, slide 02: only 1 outlier). These results confirm what was found previously about the background correction. When no background correction is effected, the duplicates are highly reproducible. Due to the presence of the γ_{ijn} term in Δy_j , the ratios of the duplicates are not independent of the mean of the duplicates, i.e. of the signal intensity. For low signals, there is a small error due to the lack of background correction. This affects a low proportion of the spots: for slide 29, the signal intensity at the first 10th percentile was higher than 6 times the background, meaning that only 10 % of the spots including the rejected low intensity spots have an intensity lower than 6 times the background. For slide 02, the 10th percentile was at 10 times the background.

To avoid taking into account inconsistent data, a further restriction was introduced to accept spots for analysis: only clones with a difference between the duplicates lower than half the mean signal were accepted (Schena et al., 1996). This is equivalent to a duplicate ratio between $3/5$ and $5/3$. In figures 7.E and 8.B it can be seen that only very few spots are concerned by this: the mean number of rejected clones is 10 (3 % of all clones on the array).

To recapitulate, spots were rejected if duplicates showed too low signals compared to the background or if the difference between the duplicates was lower than half the mean signal. The mean of the not corrected signal / reference ratios of the accepted duplicate spots was calculated and used for further data analysis.

2.5.7.5 Global normalisation

The global normalisation is the normalisation for global differences between arrays. As shown previously, the Cy5/Cy3 ratios are dependant on the amounts of cDNA used for hybridisation. Because of these global differences of intensities of the Cy5 and Cy3 signals in different arrays, the Cy5/Cy3 ratios have to be normalised prior to the comparison of arrays. Different methods of normalisation exist. We tested some of them in the preliminary experiments referred to in 2.5.5.

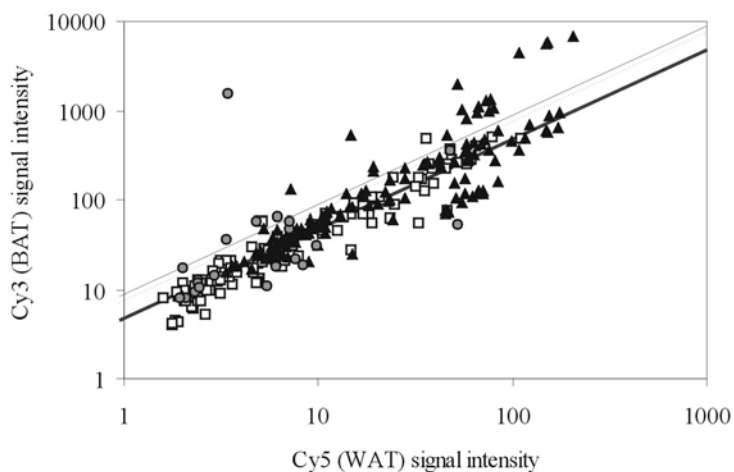


Figure 9. Scatter plot of the hybridisation intensities for each spot of an array hybridised with a WAT probe (Cy5 signal) and a BAT probe (Cy3 signal). The white squares \square correspond to the clones from the pW4 DPs, the black triangles \blacktriangle to the clones from the pB4 DPs and the grey circles \bullet to the reference clones. The thick solid line represents the points where y/x is equal to the median of all the Cy3/Cy5 ratios; the thin solid line where y/x is equal to the mean of all the Cy3/Cy5 ratios and the thin dashed line where y/x is equal to the mean of the Cy3/Cy5 ratios of the luciferase clones.

Figure 9 is the graphical representation on a scatter plot of one of these hybridisations performed with probes deriving from 1 μ g templates. For each clone, the mean of the duplicate spots was calculated. The WAT (Cy5) signal and the BAT (Cy3) signal were not normalised. Most of the dots are gathered around a diagonal of the graph. There are several outliers, one of them is the UCP1 dot with, as expected, a much higher BAT signal (coordinates 3.42; 1578.7). 3 different methods were tested for the normalisation of the data:

- (i) 0.5 ng luciferase RNA was spiked in the mRNA templates prior to labelling. 12 spots of luciferase cDNA fragments were printed on the arrays. The mean of the luciferase Cy3/Cy5 ratios was used to normalise the Cy3/Cy5 ratios of all clones.
- (ii) the mean of all Cy3/Cy5 ratios was used for normalisation.
- (iii) the median of all Cy3/Cy5 ratios was used for normalisation.

On the logarithmic scaled graph, the normalisation of the data with a constant is equivalent to a shift of the dots. The thin dashed line represents the position of the $x=y$ axis if the data were normalised with the luciferase signal (i), the thin solid line with the mean (ii) and the thick solid line with the median (iii). Thus it appears that the normalisation with the median fits best. It places the majority of the dots around the $x=y$ axis. The spiking with luciferase as attempted here proved to be not precise enough for normalisation of data: the pipetting error is too large. The mean of the Cy3/Cy5 ratios is more influenced by outliers than the median and thus also not proper for normalisation.

Thus, the median of the Cy5/Cy3 ratios was used for global normalisation. The efficiency of this procedure can be validated by assessment of the reproducibility of signals in replicated hybridisations.

Statistical model

The logarithm of the Cy5/Cy3 ratio is

$$y_{jn} = \rho_n + \lambda_{jn} + \tau_{jn}$$

where λ_{jn} is the true Cy5/Cy3 ratio for spot j . To estimate λ_{jn} , ρ_n has to be estimated (capital letters indicate the estimates):

$$\Lambda_{jn} = y_{jn} - P_n$$

We have chosen as an estimate of ρ_n , $P_n = \text{median}_j (y_{jn})$. Thus, the expression is adjusted in a way that the median values of the λ_{jn} are the same for the two arrays to compare. This is equivalent to make the assumption that a majority of genes have similar expression levels in the probes to compare or that the number of genes up-regulated is similar to the number of genes down-regulated.

When comparing two arrays a and b hybridised with the same probe, for the clone j

$$\lambda_{ja} = \lambda_{jb}$$

and

$$\Delta y_j = y_{ja} - y_{jb} = \rho_a - \rho_b + \tau_{ja} - \tau_{jb}$$

i.e.

$$\Delta y_j - \rho_a + \rho_b = \tau_{ja} - \tau_{jb}$$

The variance of $\tau_{ja} - \tau_{jb}$ can be estimated by the variance of Δy_j . Therefore, the distribution of the $\Delta y_j - P_a + P_b$ was examined.

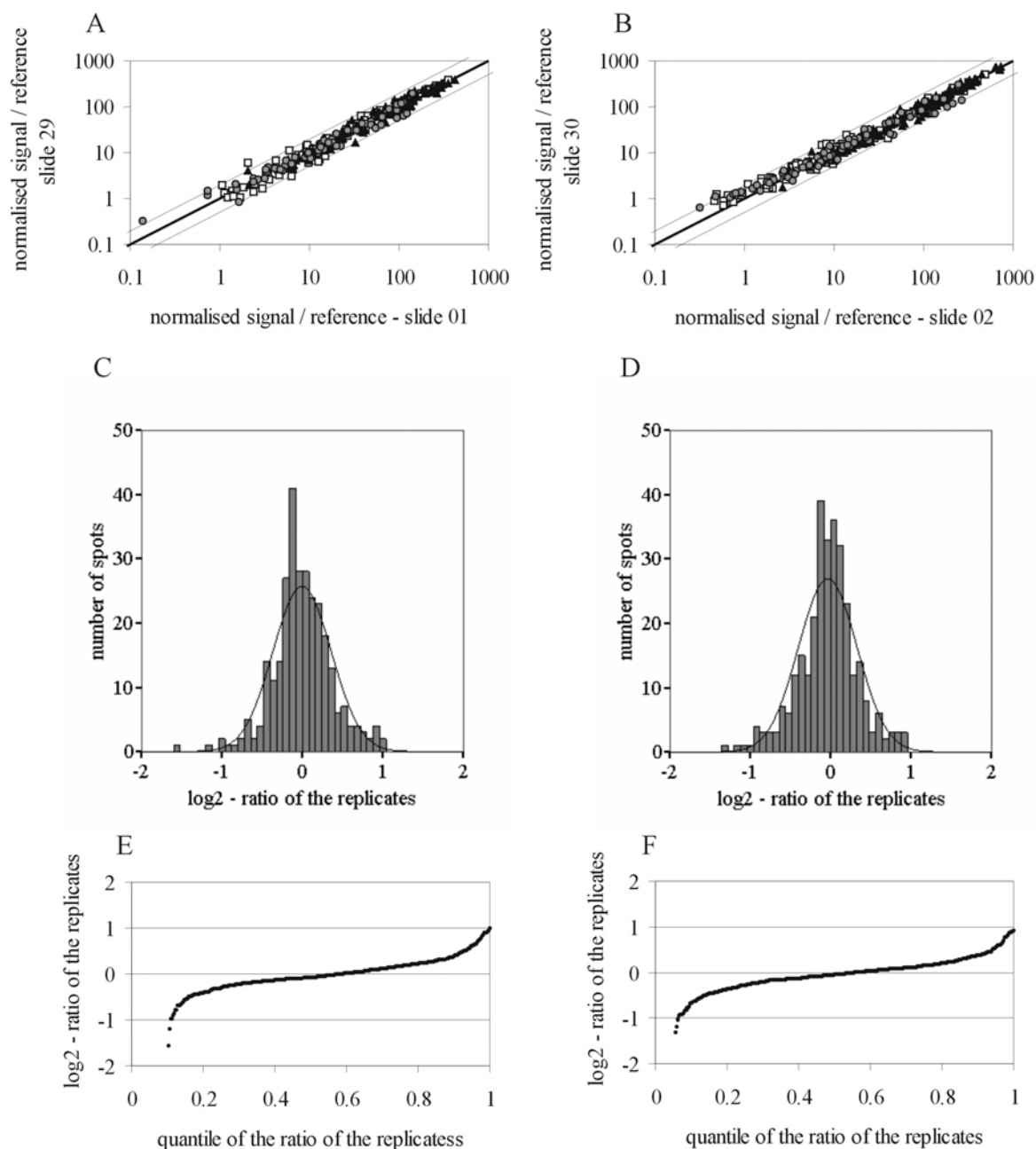


Figure 10. Reproducibility of replicated hybridisations with pW4 probes (slide 01 and 29; A, C and E) and with pB4 probes (slide 02 and 30; B, C and D). A, B. Scatter plot of the normalised signal / reference ratios (Cy5/Cy3) rescaled with the virtual slide intensities. For each clone, the ratio from one array is plotted against its replicate's ratio. The thick solid line is the $x=y$ axis; the thin solid lines are the $x=2y$ and the $x=y/2$ axis. The white squares \square correspond to the clones from the pW4 DPs, the black triangles \blacktriangle to the clones from the pB4 DPs and the grey circles \bullet to the reference clones. C, D. Histogram of the distribution of the \log_2 of the replicate 1 / replicate 2 ratios. The best fitting Gauss curve is shown. E, F. The \log_2 of the replicate 1 / replicate 2 ratio is plotted against its quantile. Clones with too high background or poor reproducibility of the duplicate spots have been removed, explaining the gaps on the left side of these graphs.

Figure 10 shows the comparison of replicated experiments: 2 hybridisations with pW4 probes (slide 01 and 29, A, C, E) and 2 hybridisations with pB4 probes (slide 02 and 30, B, D, F). The distribution of the dots in the scatter plots (figure 10.A and B) is tight around the $x=y$ axis: there are 4 outliers for pW4 (replicates ratio > 2), 3 for pB4. This is less than 2 % of all spots. There is only a slightly higher dispersion of dots in the low intensities. The \log_2 ratios are sharply distributed around 0: for pW4 and pB4 the standard deviation is 0.36 and the mean lower than 0.04. This indicates a good reproducibility of the hybridisations and the absence of bias introduced by the estimation of ρ_n when comparing replicate experiments. As there were no dramatic differences in gene expression between the probes examined, there should also be no bias when comparing different arrays.

In all further analysis, for one mRNA probe, the signal / reference ratio was therefore estimated by the mean of the normalised ratios from the replicate hybridisations.

2.6 Cluster analysis and statistics

All standard data analysis was performed in Microsoft Excel® and SPSS.

The K-means clustering was performed with the programs Cluster and TreeView, available at <http://rana.stanford.edu/software> (Eisen et al., 1998). K-means clustering is a good method to categorise the expression patterns of genes in multiple hybridisation experiments. It groups genes with similar patterns of expression in K clusters, the number of clusters K being chosen by the user. Additionally, the different hybridisation datasets used for the clustering can be assigned a weight. It was chosen to use as input the mean expression levels corresponding to each cell type with 2 as weight, the mean tissue expression levels from the 6 animals with 2 as weight and the WATC and BATC data with 1 as weight. In order to normalise for differences in expression level, the expression levels relatively to the expression in pW4 were calculated and their \log_2 subjected to K-means clustering. K=10 was found to give the most explicit results.

3 RESULTS

3.1 Primary cell cultures of preadipocytes

The cells to be compared by RDA were obtained from primary cell cultures of white and brown preadipocytes from the Djungarian dwarf hamster *Phodopus sungorus*. Preadipocytes were let to proliferate for 4 days, until they reached semi-confluence.

As a control of the fitness of the preadipocytes and of their ability to differentiate normally, from each cell culture a few plates were grown further and cells were brought to differentiate. Two factors were controlled: adipogenesis was evaluated optically and UCP1 expression in the brown adipocytes was assessed by northern blot analysis (figure 11). There was no expression in the preadipocytes, a high expression level in brown adipocytes and low expression in white adipocytes: the expected expression profile for UCP1 in cell culture (Klaus et al., 1995).

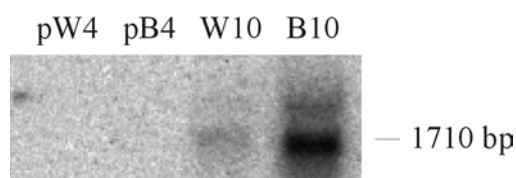


Figure 11. Northern blot analysis of the UCP1 expression in cell culture. 10 μ g of pW4, pB4, W10 and B10 total RNA were blotted and hybridised to a hamster UCP1 radiolabelled probe (see table 3 for nomenclature). The blot was exposed over night.

3.2 Representational Difference Analysis

Figure 2 is a schematic representation of the RDA protocol. The pW4 and pB4 amplicons are the two populations of PCR amplified cDNA fragments that will be compared through RDA. They were obtained by splitting the pW4 and pB4 digested cDNA fragments in 44 templates for PCRs (see 2.4.3). In figure 12, the products of 3 of each of these reactions are shown. The range of the cDNA fragments' sizes from 200 bp to over 1000 bp corresponds to what is expected from a 4-cutter restriction enzyme (Hubank and Schatz, 1994). The PCR products were then pooled, phenol extracted and precipitated. Thus 162 μ g pW4 amplicon and 187 μ g pB4 amplicon were synthesised. This is enough for 3 cycles of subtractive hybridisation and selective amplification performed in both directions, with once pW4 as a tester and once pB4 as a tester.

The first subtractive hybridisation was performed with a tester:driver ratio of 1:100. For the next cycles, the difference products were compared again to the drivers from the other cell type. The tester:driver ratios 1:400 and 1:16000 were used for the second and the third cycles respectively. The last ratio is lower than suggested by Hubank and Schatz. This low stringency should lead to the

isolation of cDNA fragments from genes with low differences in expression between the two cell types.

200 ng of the amplicons and of the 6 difference products were run in a 2 % agarose gel (figure 13). Whereas the amplicons are continuous smears, discrete bands appear already in DP1 for the pW4 and in DP2 for the pB4. The background decreases with the number of cycles. The pattern of bands of pW4 and of pB4 are clearly distinct. There is no systematic brightening of the individual bands from one DP to the next: some of them also lose of their intensity, especially from DP2 to DP3.

The amplicons and difference products were transferred to nylon membranes for Southern analysis (figure 14). Two blots were hybridised with radiolabelled probes synthesised from two cloned difference products: a pW4 DP, complement factor B (factB) and a pB4 DP, hepatocellular carcinoma associated protein (HCAP). There is a higher level of factB in the pW4 amplicon than in the pB4 amplicon. It is already amplified in the pW4 DP1 and is present in all 3 difference products. It could be identified as being the upper strong band in the gel figure 6, suggesting a lower signal in pW4 DP3. The signal in the pB4 amplicon decreases in DP1 and DP2, but in DP3 there is again a detectable amount of factB. HCAP is not present in the pW4 DP2 and DP3, it is detected mainly in the pB4 DP2, the level in the DP3 being much lower. These results show that difference products were not just amplified from cycle to cycle, but that some of them underwent more complex kinetics.

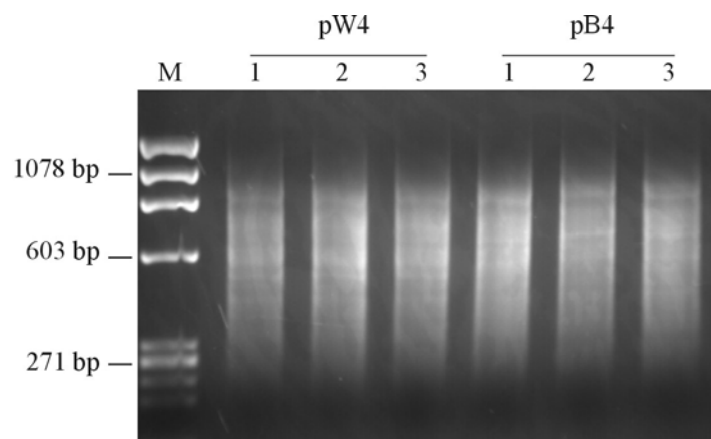


Figure 12. Gel electrophoresis of the amplified representations of mRNA from white and the brown preadipocytes. The amplicon was synthesised by splitting the ligated cDNA fragments in 44 templates for PCR amplification. From each amplicon, 3 of these PCR products were loaded in a 2 % agarose gel. M: DNA marker HaeIII fragments (Gibco-BRL)

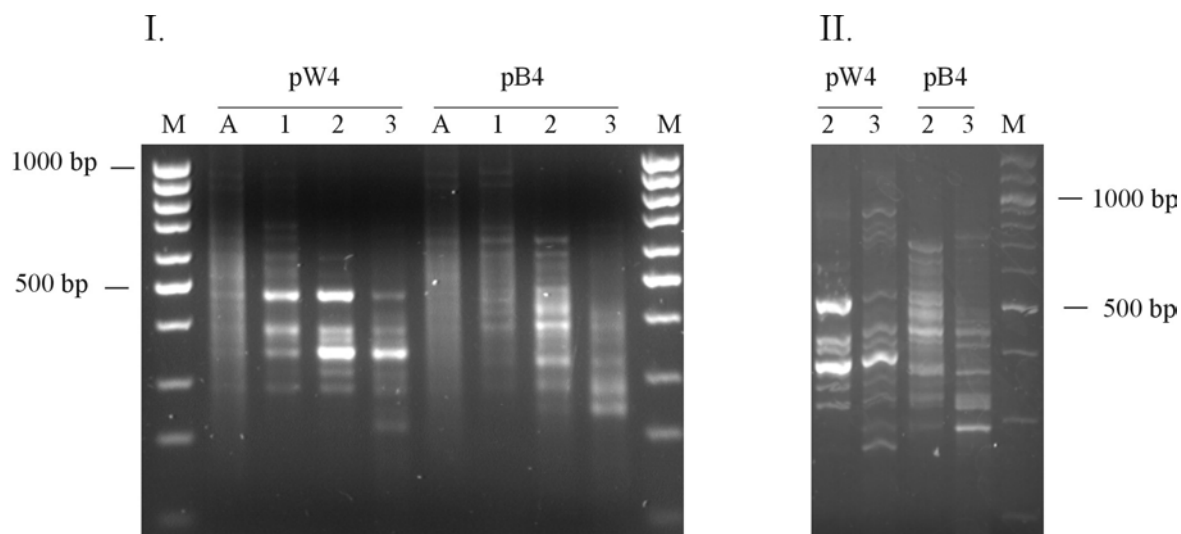
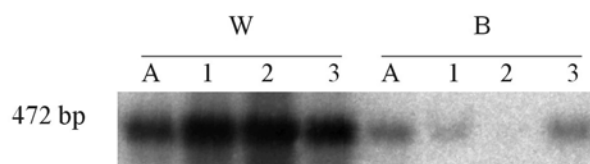


Figure 13. Gel electrophoresis of the amplicons and difference products. I. The pW4 and pB4 amplicons (A), DP1 (1), DP2 (2) and DP3 (3) were loaded in a 2 % agarose gel. II. The DP2 and DP3 from both cell types were loaded in a 3 % Metaphor gel. M: 100 bp ladder (Gibco-BRL)

A. Complement factor B



B. Hepatocellular carcinoma associated protein

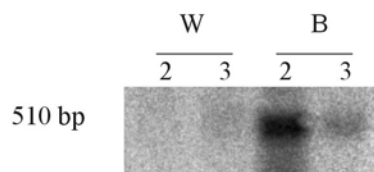


Figure 14. Southern blot analysis of the amplicons and difference products. A. The pW4 and pB4 amplicons (A), DP1 (1), DP2 (2) and DP3 (3) were blotted on a nylon membrane and hybridised to a radiolabelled cDNA probe from the complement factor B gene. B. The pW4 and pB4 DP2 and DP3 were blotted and hybridised to a radiolabelled cDNA probe from the hepatocellular carcinoma associated protein gene. Cloned difference product were amplified by PCR and radiolabelled as probes for hybridisation. The blots were exposed for 1 hour.

3.3 Differential gene expression in white and brown preadipocytes

3.3.1 Microarray data

Because of these differences we found between DP2 and DP3, both difference products were cloned. 110 clones from DP2 and 146 clones from DP3 were spotted on microarrays, as well as 45 reference clones representing genes of potential interest in adipocyte function and differentiation. On each array, all the clones were spotted in duplicate.

The primary aim of this project was to isolate genes expressed differentially in white and brown preadipocytes, so let us first focus on the hybridisations with the pW4 and pB4 probes. Figure 15 shows a scatter plot of the comparison of the pW4 and pB4 hybridisations. Most of the dots are gathered around the $x=y$ axis, but a part of them are clearly outliers, thus showing different expression levels in white and brown preadipocytes. Table 6 shows the distribution of the pW4/pB4 and pB4/pW4 ratios. 20.6 % of the spots have a ratio of expression levels higher than 2; 8 % between 1.75 and 2; 14.7 % between 1.5 and 1.75 and 55.5 % under 1.5. We have chosen to consider as significant differences in expression higher than 2. This is a standard choice (Schena et al., 1996; Frohme et al., 2000). Our reproducibility results (see 2.5.7.5 and figure 12) show that an error rate of not more than 2 % should be expected for the identification of two-fold differences.

All the clones with a more than two-fold difference between pW4 and pB4 were sequenced and the sequences matched to databases. Table 7 is the list of the thus identified differentially expressed genes in preadipocytes. Some of them are represented several times on the array in different clones with identical inserts, some of them are also represented by different cDNA fragments (complement factor C3 and fibronectin). Highest differences in expression were found in the genes higher expressed in pW4: 3 members of the complement system, a fatty acid desaturase and a cDNA fragment that could not be clearly attributed to a specific gene. It is homologous to ribosomal RNAs and to the non coding sequences of different genes, among them tensin. The genes higher expressed in pB4 showed lower differences in expression levels, the ratio is not exceeding 3. 3 genes are linked to cell structure or ECM (fibronectin, α actinin 4 and metargidin), 3 to the control of transcription at different levels (necdin, vigilin and snrpA) and 2 are of unknown function, one of them being new, i.e. not matching to any known sequence.

Additionally, 2 standard clones, not included in this table, showed significant differences between pW4 and pB4: UCP1, at a very low level of expression, and cyclin D1, both up-regulated in pB4.

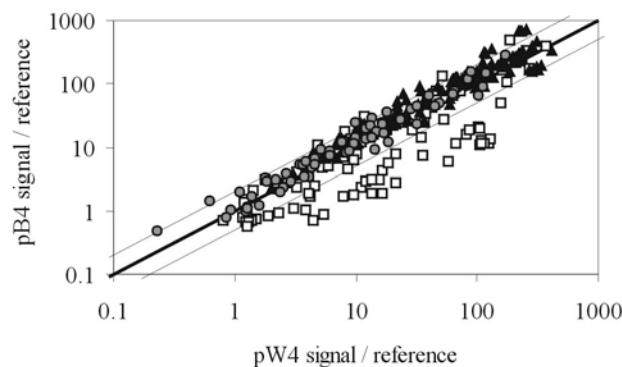


Figure 15. Comparison of white and brown preadipocytes (pW4 vs. pB4): the scatter plot of the signal / reference ratios (Cy5/Cy3) rescaled with the virtual slide intensities is shown. The white squares \square correspond to the clones from the pW4 DPs, the black triangles \blacktriangle to the clones from the pB4 DPs and the grey circles \bullet to the reference clones. The thick solid line is the $x=y$ axis; the thin solid lines are the $x=2y$ and the $x=y/2$ axis.

	total		pW4				pB4				standards	
			DP2		DP3		DP2		DP3			
	#	%	#	%	#	%	#	%	#	%	#	%
$2 < pW4/pB4$	38	12.6	29	58.0	9	12.7	0	0.0	0	0.0	0	0.0
$1.75 < pW4/pB4 < 2$	9	3.0	5	10.0	1	1.4	0	0.0	3	4.0	0	0.0
$1.5 < pW4/pB4 < 1.75$	8	2.7	1	2.0	3	4.2	0	0.0	2	2.7	2	4.4
$2 < pB4/pW4$	24	8.0	0	0.0	6	8.5	14	23.3	2	2.7	2	4.4
$1.75 < pB4/pW4 < 2$	15	5.0	0	0.0	1	1.4	11	18.3	1	1.3	2	4.4
$1.5 < pB4/pW4 < 1.75$	36	12.0	1	2.0	6	8.5	8	13.3	11	14.7	10	22.2
ratios < 1.5	167	55.5	11	22.0	45	63.4	27	45.0	56	74.7	28	62.2
total	301		50		71		60		75		45	

Table 6. Distribution of the white vs. brown preadipocytes expression ratios in the difference products: listed are number (#) and percentage (%) of clones from the different cell types and difference products (DP) according to their expression ratios. 'ratios < 1.5 ' corresponds to all spots with $pW4/pB4 < 1.5$ and $pB4/pW4 < 1.5$.

higher expression in white preadipocytes

cluster	ratio	sequ.	accession	gene description	putative function	#
CW2	8.86	W1	NM_008198	complement factor B	complement	11
CW2	3.94	W5	NM_004265	delta 6 fatty acid desaturase	metabolism	1
CW1/ 2	3.53	W8/19/24	M29866	complement component C3	complement	13
CW2	3.29	W17	AF225896	tensin	structure	2
CW2	2.10	W18	NM_000063	complement component C2	complement	2

higher expression in brown preadipocytes

cluster	ratio	sequ.	accession	gene description	putative function	#
CB2	2.88	B27/28	NM_019143	fibronectin	structure	9
CB1	2.39	B32	NM_010882	necdin	cell cycle	1
CB1	2.29	B34	NM_021895	alpha actinin 4	structure	1
CB3	2.21	W12	NM_005336	high density lipoprotein binding protein (vigilin)	transcription	1
CB3	2.19	BW1	NM_006787	hepatocellular carcinoma associated protein	unknown	2
CB2	2.12	B33	NM_015782	small nuclear ribonucleoprotein polypeptide A	RNA processing	1
CB2	2.08	W20	AJ251198	metargidin	ECM	4
CB1	2.00	B26	-	new	unknown	1

Table 7. Genes with a more than two-fold difference in expression between white and brown preadipocytes (pW4 and pB4). The ratios indicated (ratio pW4/pB4 for the white preadipocytes difference products and pB4/pW4 for the brown preadipocytes difference products) are the mean of the ratios from all the spots corresponding to identical clones. For complement component C3, represented by 3 different cDNA fragments on the array, and fibronectin, represented by 2, the mean of the ratios from all fragments was calculated. The sequences from the pW4 DPs are nomenclatured with W, the sequences from the pB4 DPs with B and the sequences found in both DPs with BW. The number of clones (#) spotted on the array for each sequence is indicated in the last column. Except for the sequence W18 (complement component C2), the homology to the quoted sequence (accession number) covers the whole RDA amplified cDNA fragment. For the sequence W18, a homology to complement component C2 was found on 122 bp only. In these domains, the homologies to BLAST records were all higher than 80 %. For the sequence W17 (tensin) indicated in grey both ribosomal sequences and sequences from the non coding region of different genes were found homologous.

3.3.2 Confirmation on Northern blots

Northern blot analysis was used to confirm with another method the differences in expression levels found with the microarrays. RNAs from white and brown preadipocytes and adipocytes grown in the same conditions as for the microarrays were blotted. For the synthesis of the labelled probes, the cloned difference products were PCR amplified using the N-Bgl-24 oligonucleotide for the DP2 and the J-Bgl-24 for the DP3 as primers. The purified PCR products were then radiolabelled and hybridised to the northern blots. Representative autoradiograms are shown in figure 16. For the 5 DPs tested, the differences in gene expression could be confirmed. There is a 1.95 fold up-regulation of the *factB* expression in white preadipocytes, and a 3.8 fold up-regulation of the complement component C2 expression. Alpha actinin 4 is 2.63, HCAP 2.12 and fibronectin 1.86 times higher expressed in brown preadipocytes. These ratios are all similar to or lower than those estimated with the microarray hybridisations.

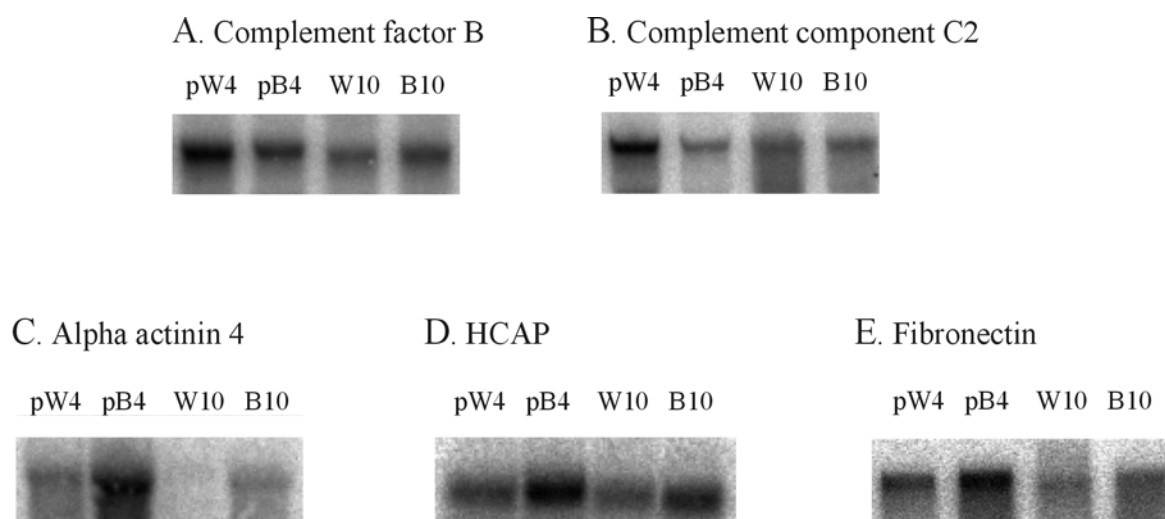


Figure 16. Northern blot analysis of the expression in cell culture of 5 difference products: A. complement factor B (size of the mouse transcript: 2443 bp), B. complement component C2 (2587 bp), C. alpha actinin 4 (6867 bp), D. hepatocellular carcinoma associated protein (2064 bp) and E. fibronectin (4430 bp). 10 μ g of pW4, pB4, W10 and B10 total RNA were blotted and hybridised to the corresponding hamster radiolabelled probe. The estimated size of the detected transcripts was close to the size of the mouse transcripts indicated before. The blots were exposed over night.

3.4 Cluster analysis of gene expression

3.4.1 Characterisation of the clusters

To analyse all expression data, K-means clustering was applied to them with $K=10$ (see 2.6). The 10 gene clusters were classified in 3 groups, depending on the relative expression of pW4 vs. pB4 (figure 17):

- (i) two clusters have a mean \log_2 pB4/pW4 lower than -1 . This difference was found to be significant in each cluster ($P < 0.001$, students t-test). They were termed CW1 and CW2.
- (ii) three clusters have a mean \log_2 pB4/pW4 higher than 0.49 (significant difference, $P < 0.001$). They were termed CB1, CB2 and CB3.
- (iii) the 5 other clusters have low differences between pB4 and pW4 (lower than 0.35). Two of them, termed CN1 and CN2, show high variations in gene expression (higher than two-fold), the three others, CN3, CN4 and CN5 show only low variations in gene expression during the differentiation and in vivo.

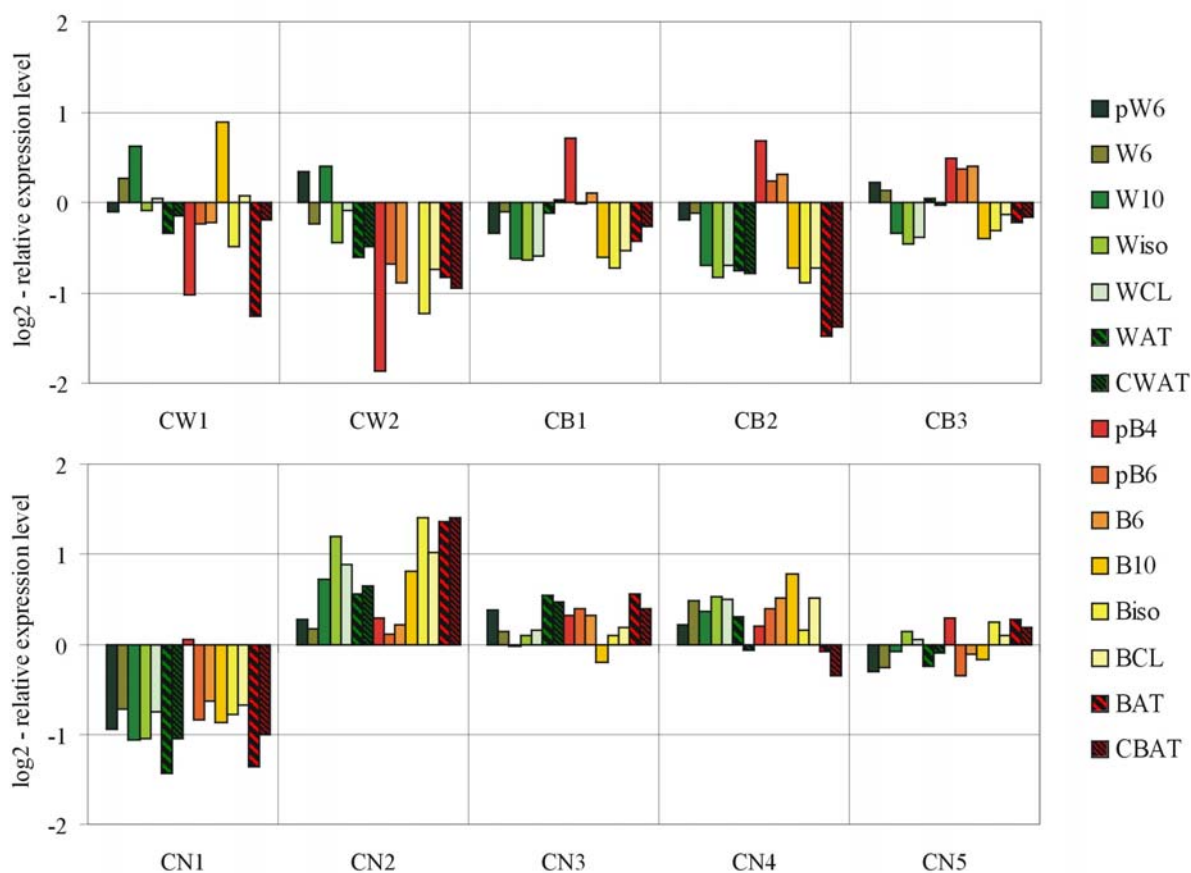
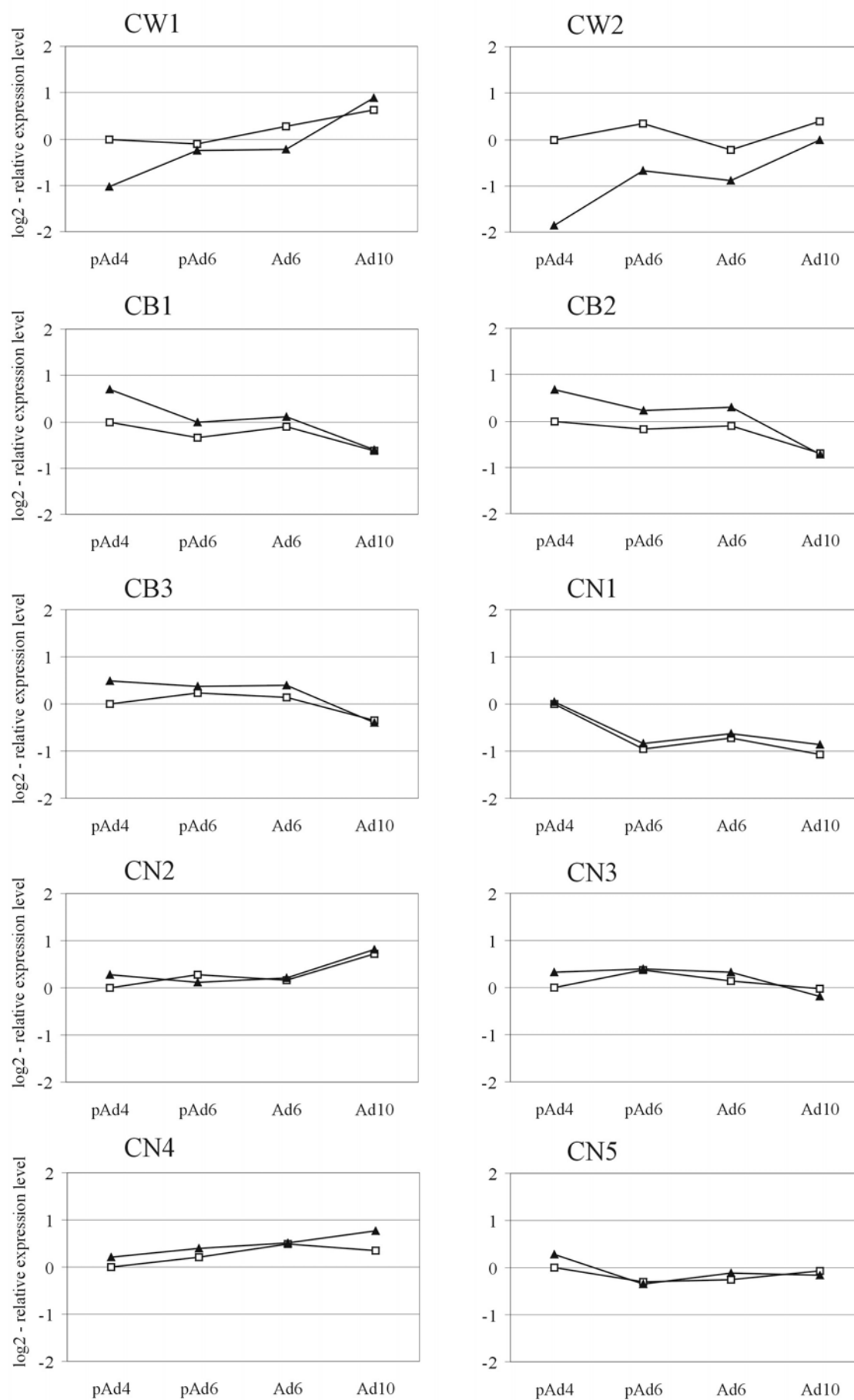


Figure 17. Mean gene expression levels in each of the 10 clusters. The mean of the \log_2 of the expression level divided by the pW4 expression level was calculated for each cell or tissue type in each cluster. See table 4 for further explanations about cell and tissue types.

Figure 18 shows the mean expression patterns during differentiation in the 10 clusters.

- (i) CW clusters: the clones represented in CW1 show a significant difference between white and brown preadipocytes (figure 18), but this difference disappears during the further steps of differentiation. There is also a lower expression in BAT than in WAT (figure 17). In CW2, the difference between pW4 and pB4 is higher and is reduced more slowly during differentiation (figure 18). In both clusters, the expression in white adipose cells is rather stable, whereas the expression in brown adipose cells is increasing during differentiation. In CW2, expression levels are down-regulated by β -agonist treatment and are lower in vivo than in vitro (figure 17).
- (ii) CB clusters: the 3 clusters have similar expression patterns in cell culture, a low expression level in white adipose cells, particularly in mature adipocytes and for the brown adipose cells, a higher expression level in the preadipocytes getting lower during differentiation to reach the same level as white adipocytes after differentiation (figure 18). The β -agonist treatment has no effect. In CB1, expression in vivo is similar to expression in cell culture, whereas it is much lower in CB2. In CB3, the differences between white and brown adipose cells are lower than in CB1 and 2 (figure 17).
- (iii) CN clusters: in CN1, expression is decreasing during differentiation, whereas it is increasing in CN2 (figure 18). In CN3, 4 and 5, there are only very low differences in gene expression between the different cell and tissue types.

Figure 18. (next page) Mean gene expression levels during differentiation in each of the 10 clusters. The mean of the log₂ of the expression level divided by the pW4 expression level was calculated for each cell type in each cluster. The white squares \square correspond to the hybridisations with white adipose cell probes and the black triangles \blacktriangle to hybridisations with brown adipose cell probes. See table 4 for further explanations about cell and tissue types.



3.4.2 Distribution of genes in the clusters

The distribution of the clones in the 10 clusters is shown in table 8. The sizes of the clusters are very different, from 6 clones in cluster CN5 to 81 in cluster CN2. The main clusters, according to their size are CW2, CB2, CN2 and CN3. Table 9 is a list of all the sequenced genes found on the array. 156 clones were sequenced (60.9 % of all clones). The degree of redundancy of the clones varied between uniqueness and 12 copies of one sequence.

- (i) CW clusters: all the genes with higher expression in white preadipocytes are in cluster CW2. CW1, a smaller cluster, contains a part of the complement component C3 clones. The difference between the expression patterns in both clusters is low, explaining the possibility to find a gene in both of them.
- (ii) CB clusters: the genes higher expressed in pB4 are distributed among the 3 clusters. It can be noticed that a lot of structure related genes are found in these clusters.
- (iii) CN clusters: almost all the standard genes are in these 5 clusters. Only CN2 and CN3 also have a certain number of DPs.

cluster	total		pW4				pB4				standards	
	#	%	#	%	#	%	#	%	#	%	#	%
CW1	15	5.0	12	24.0	2	2.8	0	0.0	0	0.0	1	2.2
CW2	44	14.6	24	48.0	14	19.7	0	0.0	6	8.0	0	0.0
CB1	22	7.3	0	0.0	9	12.7	9	15.0	3	4.0	1	2.2
CB2	44	14.6	0	0.0	12	16.9	19	31.7	12	16.0	1	2.2
CB3	21	7.0	0	0.0	2	2.8	7	11.7	10	13.3	2	4.4
CN1	19	6.3	1	2.0	3	4.2	7	11.7	2	2.7	6	13.3
CN2	81	26.9	8	16.0	13	18.3	12	20.0	24	32.0	24	53.3
CN3	39	13.0	3	6.0	14	19.7	4	6.7	13	17.3	5	11.1
CN4	10	3.3	2	4.0	2	2.8	1	1.7	2	2.7	3	6.7
CN5	6	2.0	0	0.0	0	0.0	1	1.7	3	4.0	2	4.4

Table 8. Distribution of the clones from the difference products (DPs) and the standard clones in the gene clusters: listed are number (#) and percentage (%) of clones in each cluster.

cluster CW1 15 clones

sequ.	#	accession	species	putative function	homology	gene description
W8	5	M29866	rat	complement	fragment	complement component C3 (fragment 1)
W19	3	M29866	rat	complement	fragment	complement component C3 (fragment 2)
W24	5	M29866	rat	complement	fragment	complement factor C3 (fragment 3)
rad	1	U12187	rat	signal transduction	-	ras related protein (rad)

cluster CW2 44 clones

sequ.	#	accession	species	putative function	homology	gene description
W1	11	NM_008198	mouse	complement	fragment	complement factor B
W3	1	A1100835	rat	unknown	fragment	EST
W5	1	NM_004265	human	metabolism	fragment	delta 6 fatty acid desaturase (FADSD6)
W17	2	AF225896	human	structure	fragment *	tensin
W18	2	NM_000063	human	complement	122 bp	complement component C2
W25	12	NM_021713	mouse	unknown	fragment *	melanocyte proliferating gene 1 (Myg1) or GAMM1
BW4	8	X54966	mouse	lysosomal	206 bp	partial homology with cathepsin B
W8	5	M29866	rat	complement	fragment	complement component C3 (fragment 1)
W19	3	M29866	rat	complement	fragment	complement component C3 (fragment 2)
W24	5	M29866	rat	complement	fragment	complement factor C3 (fragment 3)

cluster CB1 22 clones

sequ.	#	accession	species	putative function	homology	gene description
W6	1	M90364	mouse	ECM	fragment	beta-catenin
B3	1	A1157995	mouse	unknown	fragment	EST
B26	1	-	-	unknown	-	new
B32	1	NM_010882	mouse	cell cycle	fragment	necdin
B34	1	NM_021895	mouse	structure	fragment	alpha actinin 4 (Actn4)
BW3	2	AF104033	mouse	metabolism	fragment	MUEL protein
BW8	3	Y00169	rat	structure	62 bp	TM-4 gene for fibroblast tropomyosin 4
W16	5	U27340	mouse	lysosomal	fragment	sulfated glycoprotein (Sgp1) or prosaposin
pOB24	1	X62332	mouse	structure	-	pOB24

cluster CB2 44 clones

sequ.	#	accession	species	putative function	homology	gene description
W10	2	NM_017356	rat	unknown	fragment	neural visinin-like Ca ²⁺ -binding protein type 3 (NVP 3)
W20	4	AJ251198	rat	ECM	fragment	metargidin (MDC15 gene)
W21	1	NM_015784	mouse	structure	fragment	osteoblast specific factor 2 (OSF2)
W22	2	AF014364	hamster	structure	fragment	β-actin
B15	1	X61381	rat	ECM	fragment	interferon inducible protein
B22	1	U60318	mouse	DNA repair	fragment	putative endo/exonuclease MmMRE11b
B27	3	NM_019143	rat	structure	fragment	fibronectin (fragment 1)
B28	5	NM_019143	rat	structure	fragment	fibronectin (fragment 2)
B30	1	NM_012025	mouse	unknown	74 bp	Rac GTPase-activating protein 1
B33	1	NM_015782	mouse	RNA processing	fragment	small nuclear ribonucleoprotein polypeptide A (Snrpa)
BW6	4	X58251	mouse	structure	140 bp	pro-alpha 2 (I) collagen
B2	2	A1103440	rat	unknown	fragment	EST
u-PA	1	X63434	rat	secreted	-	urokinase-type plasminogen activator

cluster CB3 21 clones

sequ.	#	accession	species	putative function	homology	gene description
W12	1	NM_005336	human	transcription	fragment	high density lipoprotein binding protein (vigilin)
B5	1	D63423	mouse	anticoagulant	fragment	annexin V
B9	1	NP_002879	human	unknown	120 bp	retinoic acid receptor responder 1 (TIG1)
B11	3	-	-	unknown	-	new
B12	2	AW742402	mouse	unknown	fragment	EST
B29	1	M24554	mouse	inflammatory	fragment	lipocortin 1 (annexin 1)
BW1	2	NM_006787	human	unknown	fragment	hepatocellular carcinoma associated protein
B2	2	A1103440	rat	unknown	fragment	EST
PCNA	1	Y00047	rat	replication	-	proliferating cell nuclear antigen (PCNA/cyclin)
TACBP	1	U15734	rat	synaptic	-	taipoxin-associated calcium binding protein 49

cluster CN1 19 clones

sequ.	#	accession	species	putative function	homology	gene description
W14	1	X74401	rat	signal transduction	fragment	GDP dissociation inhibitor beta
B20	3	U50842	rat	protein folding	fragment	ubiquitin ligase (Nedd 4)
cycB	1	NM_012615	rat	cell cycle	-	cyclin B
TIMP1	1	U06179	rat	secreted	-	tissue inhibitor of metalloproteinase 1
PAI-1	1	M24067	rat	secreted	-	plasminogen activator inhibitor-1
met	1	X83537	rat	ECM	-	membrane type matrix metalloproteinase
Cts1	1	NM_013156	rat	lysosomal	-	cathepsin L
Ca-PK2	1	NM_012519	rat	signal transduction	-	Ca ⁺⁺ /calmodulin-dependent protein kinase II

cluster CN2 82 clones

sequ.	#	accession	species	putative function	homology	gene description
W11	1	AF146523	mouse	signal transduction	fragment	RAMP 2
W16	5	U27340	mouse	lysosomal	fragment	sulfated glycoprotein (Sgp1) or prosaposin
W23	1	NM_010216	mouse	growth factor	fragment	c-fos induced growth factor (FIGF)
B1	1	AAC05812	human	unknown	fragment	gene product with similarity to ubiquitin binding enzyme
B4	1	AF083214	mouse	cell cycle	fragment	SCF complex protein Skp1
B6	1	M74227	mouse	protein metabolism	214 bp	cyclophilin C (peptidylpropyl isomerase C)
B13	5	U97674	Syrian h.	mitochondrial	fragment	cytochrome-c oxidase chain I
B14	1	L16842	human	mitochondrial	fragment	ubiquinol cytochrome-c reductase core I protein
B19	1	U05784	rat	structure	fragment	microtubule-associated proteins 1 light chain 3 subunit
B21	1	X05300	rat	glycosylation	fragment	ribophorin 1
B23	1	X54467	rat	lysosomal	fragment	preprocathepsin D
B25	1	-	-	unknown	-	new
BW2	5	M13964	mouse	signal transduction	fragment	stimulatory G protein of adenylate cyclase alpha chain
UCP1	1	AF271263	Djung. h.	mitochondrial	-	UCP1
UCP3	1	AF271265	Djung. h.	mitochondrial	-	UCP3
PPARg	1	-	Djung. h	transcription factor	-	PPAR gamma
rheb	1	U08227	rat	signal transduction	-	Sprague-Dawley Ras-related protein (rheb)
ODC	1	NM_012615	rat	protein metabolism	-	Ornithine decarboxylase
GAPDH	1	AF106860	rat	metabolism	-	glyceraldehyde-3-phosphate-dehydrogenase
ACS	1	D30666	rat	metabolism	-	acyl CoA synthetase II
APC	1	D38629	rat	ECM	-	APC protein
GCGR	1	D38629	rat	receptor	-	glucagon receptor
D123	1	U34843	rat	cell cycle	-	cell cycle progression related D123
p27kip1	1	NM_031762	rat	cell cycle	-	cyclin-dependent kinase inhibitor 1B (p27, kip1)
GluR6	1	Z11548	rat	receptor	-	glutamate receptor subunit (GluR6)
PPARd	1	U40064	rat	transcription factor	-	Peroxisome proliferator activator receptor, delta
MLH1	1	NM_031053	rat	DNA repair	-	mismatch repair protein
PPARg	1	AB011365	rat	transcription factor	-	PPAR gamma
MSH2	1	NM_031058	rat	DNA repair	-	mismatch repair protein

BAD	1	AF003523	rat	apoptosis	-	Bcl-2 associated death promoter (BAD)
OB-Rb	1	U52966	rat	receptor	-	leptin receptor isoform b
cdc25A	1	D16236	rat	cell cycle	-	cell division cycle 25A
PB-cadh	1	D83349	rat	cell adhesion	-	short type PB-cadherin
CRLR	1	L27487	rat	receptor	-	calcitonin receptor-like receptor
CnA	1	D90035	rat	signal transduction	-	calcineurin A alpha
HO2	1	J05405	rat	microsomal	-	heme oxygenase-2
CCND1	1	D14014	rat	cell cycle	-	cyclin D1

cluster CN3 40 clones

sequ.	#	accession	species	putative function	homology	gene description
W2	1	Z46372	rat	DNA topology	55 bp	DNA topoisomerase II
W4	1	M13444	mouse	structure	fragment	tubulin alpha chain
W13	1	D87909	mouse	protein metabolism	fragment	proteasome activator PA28 alpha subunit
W15	1	U47024	mouse	unknown	fragment	maternal embryonic 3 (Mem3)
B8	1	NP_002880	human	unknown	160 bp	retinoic acid receptor responder 2 (TIG2)
B10	1	A45259	human	differentiation	fragment	neuroblast differentiation associated protein AHNAK
B17	1	AJ002390	mouse	anticoagulant	fragment	annexin VIII
B18	1	-	-	unknown	-	new
B24	1	-	-	unknown	-	new
B31	1	NM_011424	mouse	transcription	fragment	nuclear receptor co-repressor 2 (Ncor2)
BW5	2	X06407	mouse	unknown	fragment	tumor protein, translationally controlled
BW7	3	U35142	mouse	transcription	fragment	retinoblastoma binding protein 7
P55CDC	1	U05341	rat	cell cycle	-	cell division cycle protein p55CDC
PKC	1	M13707	rat	signal transduction	-	protein kinase C
PLAT	1	NM_013151	rat	secreted	-	plasminogen activator, tissue
TACE	1	AJ012603	rat	protein metabolism	-	TNF-alpha converting enzyme
N-myc	1	X63281	rat	transcription factor	-	N-myc

cluster CN4 10 clones

sequ.	#	accession	species	putative function	homology	gene description
W26	1	AF132045	rat	unknown	fragment	foocen-m2 mRNA
BW9	2	-	-	unknown	-	new
HOX	1	J02722	rat	microsomal	-	heme oxygenase
GST	1	M25891	rat	antioxidant	-	glutathione S-transferase
CT-A	1	M99223	rat	Ca transport	-	Calcium transporting ATPase

cluster CN5 6 clones

sequ.	#	accession	species	putative function	homology	gene description
B16	1	U06179	rat	ECM	fragment	tissue inhibitor of metalloproteinase 1 (TIMP1)
P53	1	X13058	rat	signal transduction	-	nuclear oncoprotein p53
24KG	1	M75153	rat	secretory pathway	-	p21-like small GTP-binding protein (24KG)

Table 9. List of all genes classified by cluster analysis. The accession number and the species of the sequence from the database matching the best to the cDNA fragment are indicated, as well as the putative function of the gene. If the homology covers the whole cDNA fragment, 'fragment' is quoted in the homology column, if it is only on a shorter domain, the length of the homologous sequence is indicated. In these domains, the homologies to BLAST records were all higher than 80 %. For the new sequences, no homology to any database record was found. For these sequences, as well as for the standard sequences, no indication about homology has to be given. The sequences from the pW4 DPs are nomenclatured with W, the sequences from the pB4 DPs with B, the sequences found in both DPs with BW and the standard genes with gene specific names. The number of clones corresponding to one sequence (#) is indicated. Some sequences were found in two different clusters and are reported twice in this table. * for these 2 clones, both ribosomal sequences and sequences from the non coding region of different genes were found.

3.4.3 Characterisation of the difference products

In order to evaluate RDA and the difference products, the distribution of clones corresponding to differentially expressed genes in the difference products 2 and 3 was examined (table 6). In the pW4 DP2, 70 % of the clones have at least a 1.5 times higher signal in white preadipocytes, only one spot has a higher signal in brown preadipocytes. In the pB4 DP2 the situation is similar: 55 % of the clones have a higher signal in brown preadipocytes and none in white. Both DP2 consist of spots with higher signals in the corresponding cell type (more than 50 %) or with no difference at all. In contrast to this, in the DP3s there are more spots without any difference in the signals and there are spots with higher signals in both cell types.

A similar observation can be made when considering the distribution of the clones from different DPs in the expression clusters (table 8). Most of the pW4 DP2 spots are in the CW clusters and none in the CB clusters, and vice versa for the pB4 DP2 spots. The spots from both DP3s are more spread among the clusters.

Finally, it should be noticed that only 2 of the identified differentially expressed genes were present only in DP3, the others were already present in DP2. These results seem to indicate that the 3rd cycle of RDA was not as effective as expected. Compared to DP2, DP3 brings little new information.

3.5 Gene expression in cell culture

3.5.1 Expression of the genes differentially expressed in preadipocytes

The genes listed in table 7, all from the CW and CB clusters, have significant differences in gene expression between white and brown preadipocytes. The comparison of all the hybridisations performed gives the possibility to examine the expression pattern of single genes in cell culture and in tissue samples.

Figure 19 shows the expression patterns of two genes higher expressed in white preadipocytes: complement factor B and $\Delta 6$ fatty acid desaturase. The expression patterns from these two genes from CW2 are very similar. In brown adipose cells, the expression level is higher in mature cells than in undifferentiated cells, whereas for white adipose cells there are high expression levels in both preadipocytes and adipocytes. For both kind of cells, the expression is repressed by isoproterenol. The other genes from the same cluster have similar expression patterns but with lower differences.

Figure 20 shows the expression patterns of genes higher expressed in brown preadipocytes. Necdin and the new sequence B26 are in cluster CB1. The expression level in white adipose cells does not change significantly during differentiation. In brown preadipocytes, the expression level is high and diminishes during differentiation. In mature cells, the expression level of brown adipocytes has reached the level of the white adipocytes and no effect of β -adrenergic stimulation is found either in white nor in brown adipocytes. In tissue, there is no significant difference between WAT and BAT. Fibronectin (C), from cluster CB2, shows a similar expression pattern with a higher difference of expression in preadipocytes and lower expression levels in vivo. The hepatocellular carcinoma associated protein (HCAP, D) is in cluster CB3. Its expression pattern is also similar to the previously described ones, but with lower differences between cell types.

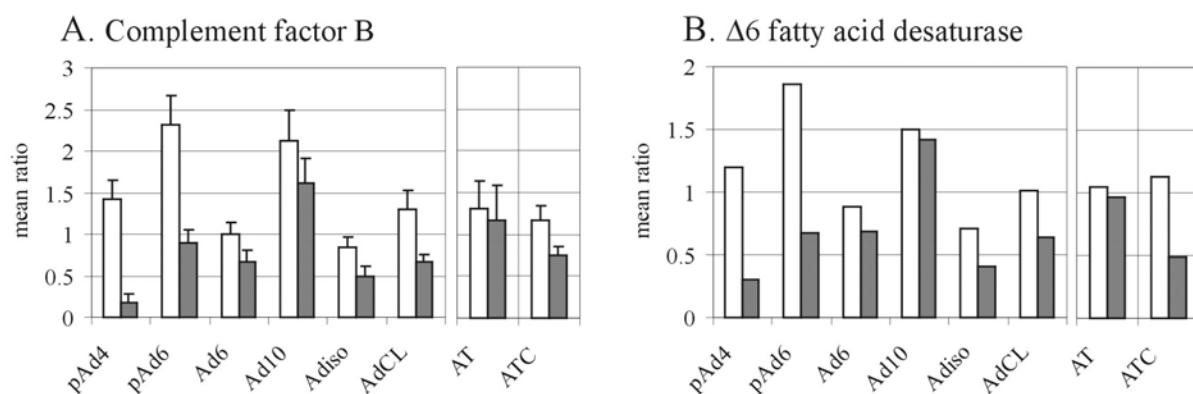


Figure 19. Expression patterns of complement factor B (A) and $\Delta 6$ fatty acid desaturase (B) in cell culture and in vivo. The abbreviations are explained in table 3 and 4. For in vitro data, the mean corrected ratios Cy5/Cy3 (\pm SD) from two hybridisations and from several clones are plotted. For the adipose tissue from animals at room temperature (AT), the mean from the 6 animals is plotted; for the adipose tissue from animals at 4°C (ATC), the ratio from a single hybridisation is shown. As $\Delta 6$ fatty acid desaturase was present only once on the array, no error bars can be shown.

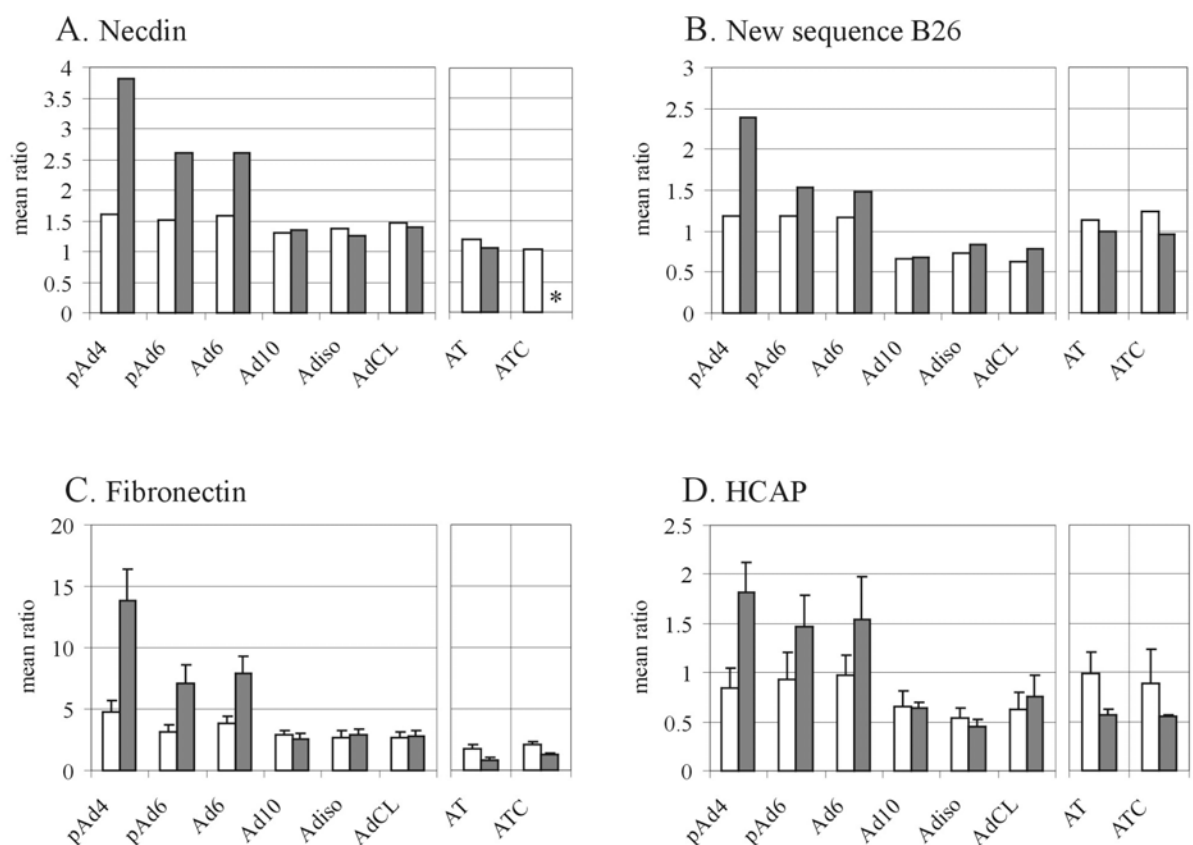


Figure 20. Expression patterns of necdin (A), the new sequence B26 (B), fibronectin (C) and hepatocellular carcinoma associated protein (D) in cell culture and in vivo. The abbreviations are explained in table 3 and 4. See figure 19 for further details. As necdin and the new sequence B26 were present only once on the array, no error bars can be shown. * These data are missing.

3.5.2 Gene expression during differentiation

We looked for the differences in gene expression between undifferentiated (pAd4) and mature (Ad10) cells. Table 10 is a list of the genes with significant differences occurring during differentiation. Some of these differences reflect what was seen in the expression patterns presented in the previous paragraph: in the CB clusters, expression decreases during the differentiation of brown adipose cells, and in CW2, for some clones, an increase in gene expression is observed during the differentiation of the brown adipose cells. Furthermore, this table shows that the clusters CN1 and CN3 contain genes with decreasing expression during differentiation, whereas CN2 contains genes with increasing expression.

In figure 21, the expression of two clones down-regulated during differentiation is shown: plasminogen activator inhibitor 1 and tissue inhibitor of metalloproteinase 1. The expression of both genes is very high in semi-confluent preadipocytes and decreases rapidly: it is already at a low level in confluent preadipocytes.

In figure 22, expression patterns are shown for 4 genes from CN2: UCP1, cytochrome-c-oxidase chain I (COX), peroxisome proliferator-activated receptor γ (PPAR γ) and GAPDH. UCP1 is found to be expressed only in mature cells, at a higher level in brown than in white adipocytes (A). This expression is strongly inducible by isoproterenol. In vivo, UCP1 expression is only detectable in BAT. This expression pattern is in total agreement with previous data (Klaus et al., 1995; Klaus et al., 1991). COX is expressed at low levels in immature cells and at a higher level in mature adipocytes (B). Its expression is strongly induced by isoproterenol treatment. Only in tissue, there is a difference in expression between WAT and BAT: COX is expressed at a much higher level in brown adipose tissue. The expression of PPAR γ increases during differentiation equally in white and brown adipose cells whereas its expression in vivo is higher in BAT (C). The expression of GAPDH (D) is induced in final differentiation. Several genes have expression patterns very similar to those of PPAR γ and GAPDH: the leptin receptor OB-Rb, ornithine decarboxylase, acyl CoA synthetase II, glutathione S-transferase and cell division cycle 25A.

cluster	W ratio	B ratio	sequ.	accession	gene description	putative function	#
CN1	- 4.500	- 4.551	PAI-1	M24067	plasminogen activator inhibitor-1	secreted	1
CN1	- 2.660	- 5.418	TIMP1	U06179	tissue inhibitor of metalloproteinase 1	secreted	1
CN1	- 1.680	- 2.041	cycB	NM_012615	cyclin B	cell cycle	1
CN1	- 2.153	- 1.770	met	X83537	membrane type matrix metalloproteinase	ECM	1
CN2	+ 126.746	+ 262.359	UCP1	AF271263	UCP1	mitochondrial	1
CN2	+ 3.848	+ 3.860	B13	U97674	cytochrome-c oxidase chain I	mitochondrial	5
CN2	+ 3.739	+ 2.687	OB-Rb	U52966	leptin receptor isoform b	receptor	1
CN2	+ 2.095	+ 2.634	PPAR γ	AB011365	PPAR gamma (rat)	transcription factor	1
CN2	+ 3.058	+ 2.011	GAPDH	AF106860	glyceraldehyde-3-phosphate-dehydrogenase	metabolism	1
CN2	+ 2.981	+ 1.930	ODC	NM_012615	Ornithine decarboxylase	protein metabolism	1
CN2	+ 2.540	+ 1.450	cdc25A	D16236	cell division cycle 25A	cell cycle	1
CN2	+ 2.537	+ 1.551	B23	X54467	preprocathepsin D	lysosomal	1
CN2	+ 2.481	+ 2.060	ACS	D30666	acyl CoA synthetase II	metabolism	1
CN2	+ 2.174	+ 1.930	PPAR γ	-	PPAR gamma (Dj. hamster)	transcription factor	1
CN2	+ 2.123	+ 1.192	W23	NM_010216	c-fos induced growth factor (FIGF)	growth factor	1
CN3	- 1.015	- 2.052	B24	-	new	unknown	1
CN3	- 1.258	- 2.003	BW7	U35142	retinoblastoma binding protein 7	transcription	3
CN4	+ 4.962	+ 2.876	GST	M25891	glutathione S-transferase	antioxidant	1
CB1	- 1.485	- 3.730	B34	NM_021895	alpha actinin 4 (Actn4)	structure	1
CB 1	- 1.792	- 3.468	B26	-	new	unknown	1
CB 1	- 1.948	- 3.312	BW8	Y00169	TM-4 gene for fibroblast tropomyosin 4	structure	3
CB 1	- 1.241	- 2.840	B32	NM_010882	neccin	cell cycle	1
CB 1	- 1.713	- 2.409	BW3	AF104033	MUEL protein	metabolism	2
CB 2	- 2.396	- 2.669	BW6	X58251	pro-alpha 2 (I) collagen	structure	4
CB 2	- 1.687	- 5.265	B27	NM_019143	fibronectin	structure	4
CB 2	- 1.744	- 2.998	W20	AJ251198	metargidin (MDC15 gene)	ECM	4
CB 2	- 1.684	- 2.705	W22	AF014364	β -actin	structure	2
CB 2	- 1.243	- 2.275	B30	NM_012025	Rac GTPase-activating protein 1	unknown	1
CB 2	- 1.148	- 2.268	B33	NM_015782	small nuclear ribonucleoprotein polypeptide A	RNA processing	1
CB 2	- 1.717	- 2.210	B22	U60318	putative endo/exonuclease MmMRE11b	DNA repair	1
CB 2	- 1.711	- 2.082	B2	AI103440	EST	unknown	2
CB 2	- 1.447	- 2.094	u-PA	X63434	urokinase-type plasminogen activator	secreted	1
CB 3	- 3.318	- 2.408	B5	D63423	annexin V	anticoagulent	1
CB 3	- 1.285	- 2.853	BW1	NM_006787	hepatocellular carcinoma associated protein	unknown	2
CB 3	+ 1.040	- 2.207	B29	M24554	lipocortin 1 (annexin 1)	inflammatory	1
CW2	+ 1.490	+ 10.152	W1	NM_008198	complement factor B	complement	11
CW2	+ 1.551	+ 6.122	W24	M29866	complement factor C3	complement	5
CW2	+ 1.253	+ 4.713	W5	NM_004265	delta 6 fatty acid desaturase (FADS6)	metabolism	1

Table 10. List of the genes with a more than two-fold difference in expression between preadipocytes (pAd4) and mature adipocytes (Ad10), classified according to their cluster. The ratios of expression levels between preadipocytes and adipocytes in white (W) and in brown (B) cells are indicated, '+' meaning an increase of expression level during differentiation and '-' a decrease. See table 9 for more details about the homologies of the sequences to BLAST records.

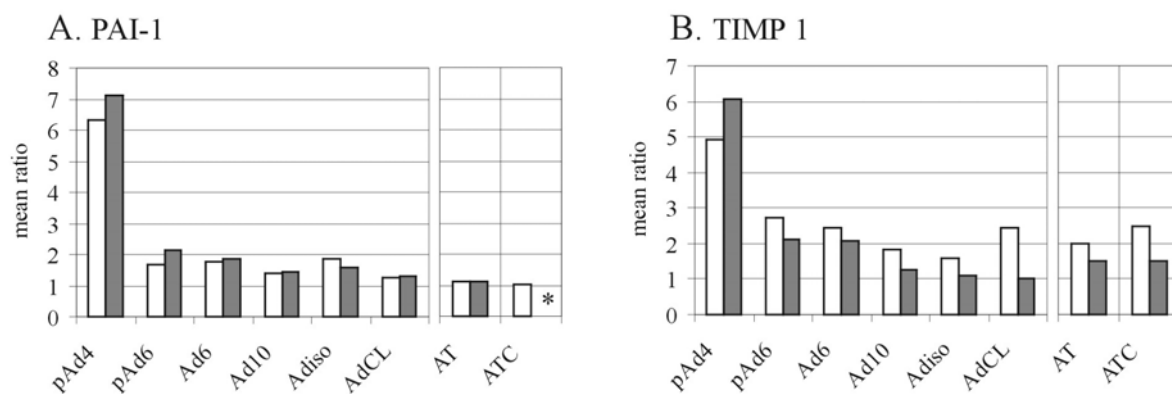


Figure 21. Expression patterns of plasminogen activator inhibitor 1 (A) and tissue inhibitor of metalloproteinase 1 (B) in cell culture and in vivo. The abbreviations are explained in table 3 and 4. See figure 19 for further details. * These data are missing.

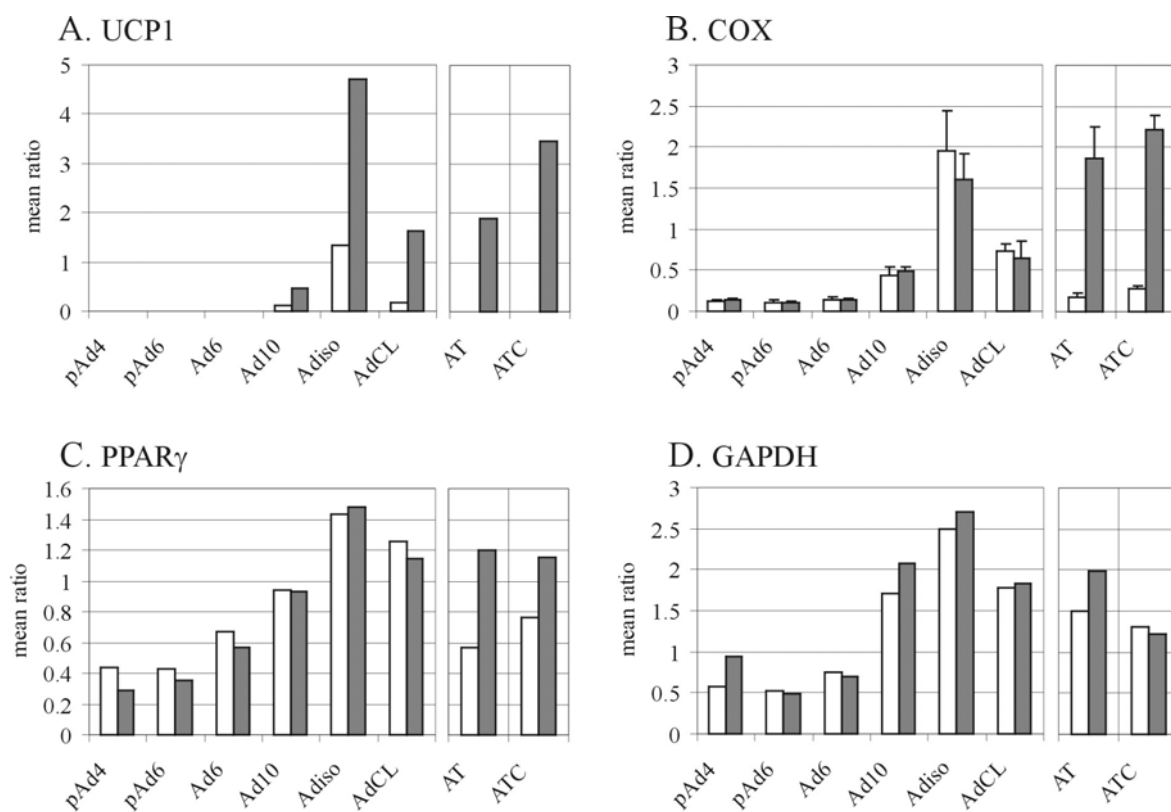


Figure 22. Expression patterns of UCP1 (A), cytochrome C-oxidase (B), djungarian hamster PPAR γ (C) and GAPDH (D) in cell culture and in vivo. The abbreviations are explained in table 3 and 4. See figure 19 for further details. As UCP1, PPAR γ and GAPDH were present only once on the array, no error bars can be shown.

3.5.3 Gene expression after β -agonist treatment

Gene expression was compared between adipocytes (Ad10) and adipocytes grown under β -agonist treatment. It was found that the CL treatment induced very few changes in gene expression, more changes were found after isoproterenol treatment: table 11 is a list of the genes with a more than two-fold difference in expression under isoproterenol treatment. These genes are all from the same two clusters: CW2 and CN2. As it can be seen from the examples shown in figure 19 and according to the mean cluster expression profile (figure 17), genes from both CW clusters are down-regulated by β -agonist treatment.

In opposition to this, the expression of genes from the cluster CN2 is stimulated by isoproterenol treatment. Two examples shown before (figure 22) are UCP1 and COX. In figure 23, two other genes with up-regulated expression after isoproterenol treatment are shown: UCP3 and the new sequence B25. For B25 this difference is significant only in the white adipocytes. For both genes, the expression is constant during differentiation. B25 is higher expressed in BAT than in WAT, both at room temperature and at 4 °C. The expression profile of the stimulatory G protein, specifically stimulated in brown adipocytes, is shown in figure 28.

cluster	W ratio	B ratio	sequ.	accession	gene description	putative function	#
CN2	+ 12.93	+ 10.38	UCP1	AF271263	UCP1	mitochondrial	1
CN2	+ 4.41	+ 3.28	B13	U97674	cytochrome-c oxidase chain I	mitochondrial	13
CN2	+ 2.20	+ 2.25	CRLR	L27487	calcitonin receptor-like receptor	receptor	1
CN2	+ 2.18	+ 4.36	UCP3	AF271265	UCP3	mitochondrial	1
CN2	-	+ 2.12	APC	D38629	APC protein	ECM	1
CN2	+ 1.36	+ 2.05	BW2	M13964	stimulatory G protein of adenylate cyclase alpha chain	signal transduction	5
CN2	+ 2.19	+ 1.99	B25	-	new	unknown	1
CN2	+ 2.11	+ 1.27	B1	AAC05812	gene product with similarity to ubiquitin binding enzyme	unknown	1
CW2	- 2.52	- 3.36	W1	NM_008198	complement factor B	complement	11
CW2	- 2.20	- 3.40	W24	M29866	complement factor C3	complement	5
CW2	- 2.13	- 3.51	W5	NM_004265	delta 6 fatty acid desaturase (FADSD6)	metabolism	1

Table 11. List of the genes with a more than two-fold difference in expression between adipocytes (Ad10) and adipocytes treated with isoproterenol (Adiso), classified according to their cluster. The ratios of expression levels between treated and untreated adipocytes in white (W) and in brown (B) cells are indicated, '+' meaning an increase of expression level with isoproterenol treatment and '-' a decrease. See table 9 for more details about the homologies of the sequences to BLAST records.

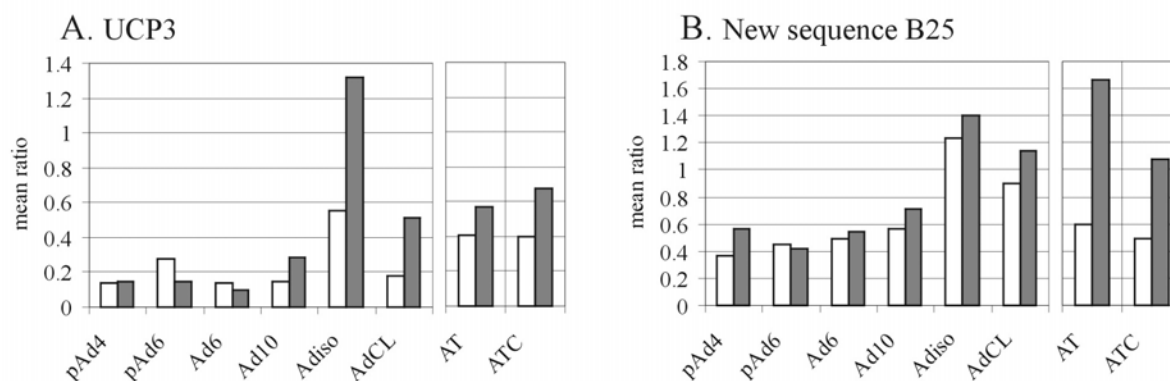


Figure 23. Expression patterns of UCP3 (A) and the new sequence B25 (B) in cell culture and in vivo. The abbreviations are explained in table 3 and 4. See figure 19 for further details.

3.6 Gene expression in vivo

The WAT and the BAT of six animals, 3 male and 3 female, were hybridised to the arrays without replication. Additionally, the adipose tissues from 3 animals exposed to 4 °C during 18 hours were pooled for another hybridisation. The aim of these hybridisations was to have an indication about the expression levels of the genes in vivo and to look for differences between the animals, eventually sex dependant differences.

3.6.1 Inter individual variability of gene expression

The first question addressed here is that of eventual sex dependant differences in gene expression. Therefore, the mean corrected signal / reference ratios from the 3 males and from the 3 females were calculated in WAT and in BAT. Figure 24 is a scatter plot comparing these expression levels in WAT (A) and in BAT (B). In both graphs, the dots are distributed rather closely along the line of identity. Only in the low expression levels are there a few outliers, corresponding to no significant difference between male and female animals.

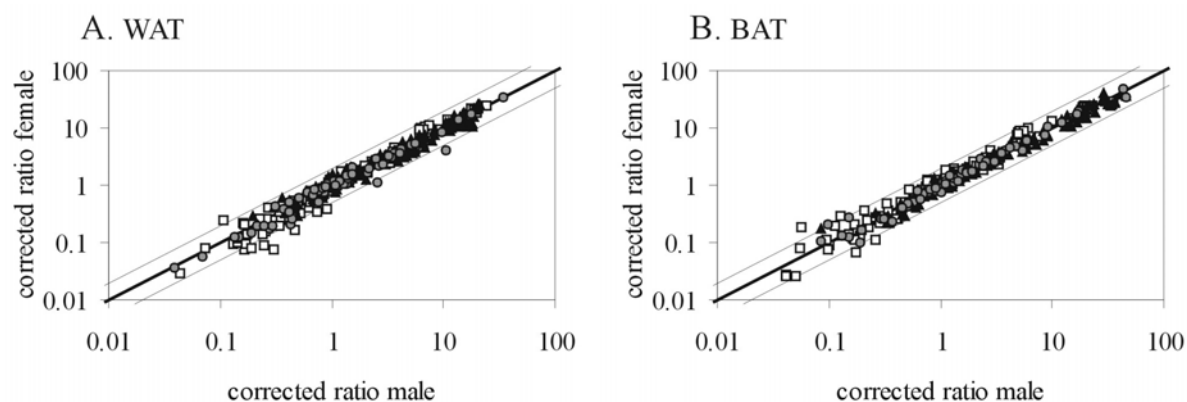


Figure 24. Comparison of the adipose tissues from male and female animals (WAT (A) and BAT (B)): scatter plots of the mean signal / reference ratios (Cy5/Cy3) from three animals, rescaled with the virtual slide intensities. The white squares \square correspond to the clones from the pW4 DPs, the black triangles \blacktriangle to the clones from the pB4 DPs and the grey circles \bullet to the reference clones. The thick solid line is the $x=y$ axis; the thin solid lines are the $x=2y$ and the $x=y/2$ axis.

Having established this, we were interested in the global homogeneity of the expression levels. Let us shortly go back to the statistical model presented in 2.5.7.2.

Statistical model

For the slide n , corresponding to animal n , and the spot j , the logarithm of the Cy5/Cy3 ratio is

$$y_{jn} = \rho_n + \lambda_{jn} + \tau_{jn}$$

Comparing two animals a and b ,

$$\Delta y_j = y_{ja} - y_{jb} = \rho_a - \rho_b + \lambda_{ja} - \lambda_{jb} + \tau_{ja} - \tau_{jb}$$

i.e.

$$\Delta y_j - \rho_a + \rho_b = \lambda_{ja} - \lambda_{jb} + \tau_{ja} - \tau_{jb}$$

Two components are involved in the variance of y_j : the noise $\tau_{ja} - \tau_{jb}$, which is depending on the mean signal intensity, and the inter-individual difference $\lambda_{ja} - \lambda_{jb}$, which should be independent of the signal intensity.

The distribution of CV of the expression levels from the 6 animals in % is shown in figure 25. Globally, the inter-individual variations of expression are rather low: most of the clones (86 % in WAT and 83 % in BAT) have a variation lower than 30 %. The median of the CV of the expression levels lies at 18.5 % in WAT and at 17.5 % in BAT. At the lower intensities, the variation reaches higher levels for some clones, which is certainly due to the measurement errors, but some clones with high expression levels also show higher variations, especially in BAT. In order to investigate this further, we looked at all the clones with a mean corrected ratio higher than the median of the ratios, in order to avoid high variations due to measurement errors, and with a CV in the highest 10 percentile of the variations (figure 26). For the WAT, the following genes were found to be represented in this area of the plot: COX, factB, membrane type matrix metalloproteinase and 6 unsequenced clones; and for the BAT, factB, UCP1, GAPDH, ACS, the Gs protein and 2 unsequenced clones. In WAT, COX has a mean variation of 26% and factB of 24.4 %, close to the 10th percentile limit. In the BAT, some genes have higher levels of CV: complement factor B and UCP1 have a variation close to 40 %. The variation of the Gs protein expression is also higher compared to the WAT (22 % vs. 16 %). In contrast to this, the variation of the COX expression decreases from about 7 %. The expression levels of complement factor B, Gs protein and UCP1 in the BAT of the 6 animals are shown in figure 27 A. There is a significant (at the level 0.05, Pearson) negative correlation between the UCP1 and the complement factor B expression levels (figure 27 B, slope of -0.44). When the data point from the pool of animals held at 4 °C for 18 hours is added, the same correlation is found. Between UCP1 and Gs protein expression levels, a positive but not significant correlation is found.

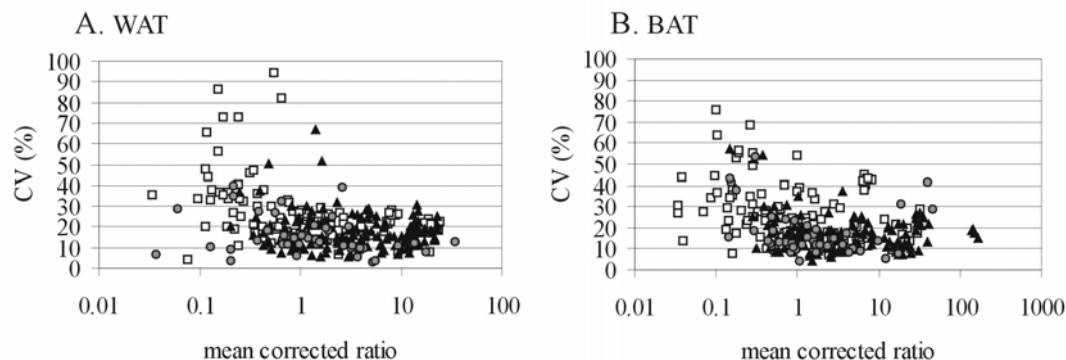


Figure 25. Inter-individual variation in % of the gene expression from 6 animals in WAT (A) and BAT (B). For each clone on the arrays, the CV of the 6 corrected signal / reference ratios in % is plotted against the mean ratio, rescaled with the virtual slide intensities. The white squares □ correspond to the clones from the pW4 DPs, the black triangles ▲ to the clones from the pB4 DPs and the grey circles ● to the reference clones.

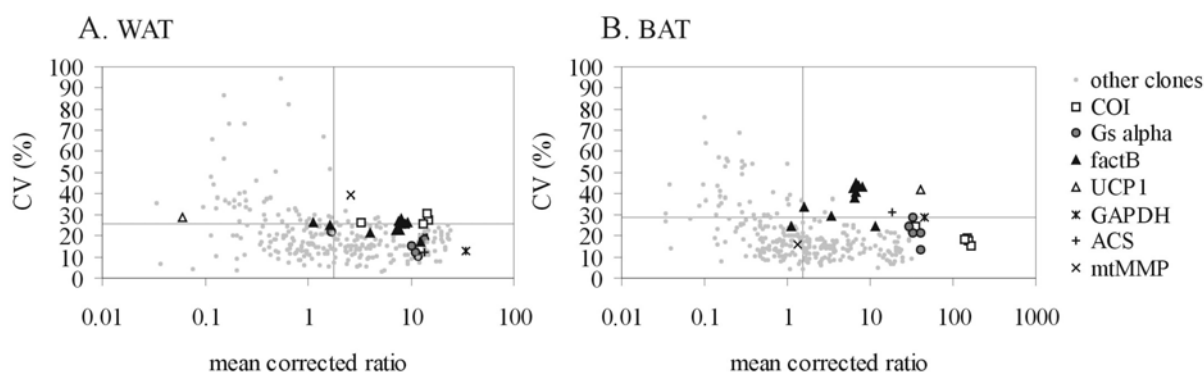


Figure 26. Inter-individual variation in % of different genes. The graphs are the same as in figure 25. The positions of the clones corresponding to □ cytochrome c-oxidase, ● stimulatory G protein, ▲ complement factor B, △ UCP1, * GAPDH, + acyl CoA synthetase II protein and x membrane type matrix metalloproteinase are shown. The other clones are represented with grey spots ●. The horizontal line represents the 90th percentile of the CV (25.9 % in WAT, 28.9 % in BAT) and the vertical line the median of the mean corrected ratios (1.8 in WAT, 1.56 in BAT).

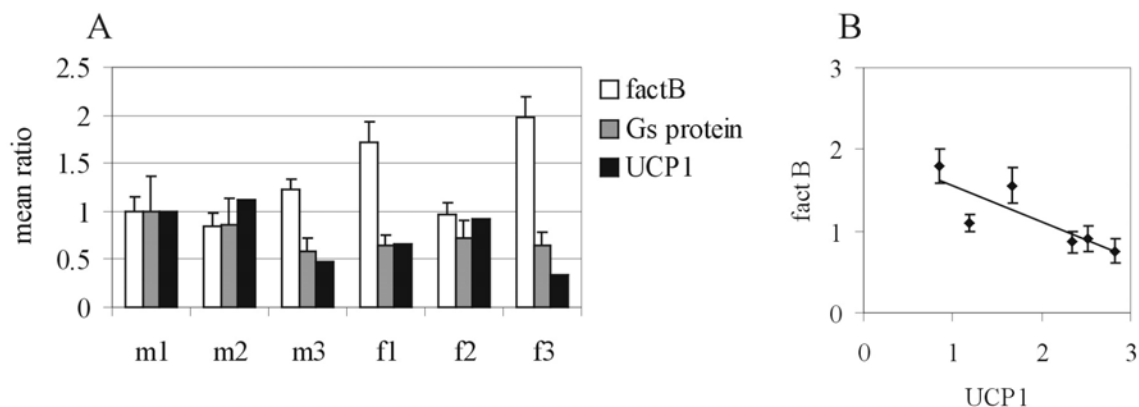


Figure 27. A. Expression levels (\pm SD) of complement factor B, stimulatory G protein and UCP1 in BAT of 6 animals. The expression levels in the animal m1 were arbitrarily set to 1 and the expression levels in the other animals calculated relatively to m1. As UCP1 was present only once on the array, no error bars can be shown. B. Expression levels of complement factor B vs. UCP1 in BAT, with the regression line.

3.6.2 Differential gene expression in WAT and BAT

The mean of the corrected signal / reference ratios of all the clones were calculated. A Mann-Whitney test was applied to recognise significant differences between WAT and BAT in the 6 animals kept at room temperature. Table 12 is a list of the genes showing a more than two-fold difference in gene expression between WAT and BAT and with a significance level lower than 0.004. The genes with more than two-fold differences in the pool of animals held at 4 °C for 18 hours are added. As expected, the highest differences were found with genes up-regulated in the BAT with UCP1 and COX (see figure 22 A and B). The expression pattern of the Gs protein is shown in figure 28 A. It is higher expressed in BAT than in WAT, but except an induction of expression in brown adipocytes after isoproterenol treatment, the expression of the Gs protein is constant during differentiation, and no differences are found between white and brown adipose cells. The expression of the new sequence B25 is shown in figure 23 B, the expression of PPAR γ in figure 22 C.

Several genes are up-regulated in WAT. Alpha 2 collagen is higher expressed in WAT both at room temperature and at 4 °C (figure 28 D). The expression pattern of the EST B2 is shown in figure 28 C: it is down-regulated during differentiation. Only in vivo and at room temperature is there a significant difference between WAT and BAT. For the expression profiles of fibronectin and Δ 6 fatty acid desaturase, see figure 20 C and 19 B.

higher expression in WAT

cluster	ratio		sequ.	accession	gene description	putative function	#
	RT	4 °C					
CB3	3.49	2.10	B29	M24554	lipocortin 1 (annexin 1)	inflammatory	1
CB2	2.38	2.18	BW6	X58251	pro-alpha 2 (I) collagen	structure	4
CB2	2.30	1.32	B2	AI103440	EST	unknown	2
CN3	2.26	1.51	PKC	M13707	protein kinase C	signal transduction	1
CB2	2.08	1.69	B27/28	NM_019143	fibronectin	structure	5
CW2	1.08	2.29	W5	NM_004265	delta 6 fatty acid desaturase (FADSD6)	metabolism	1
CB1	1.95	2.11	pOB24	X62332	pOB24	structure	1

higher expression in BAT

cluster	ratio		sequ.	accession	gene description	putative function	#
	RT	4 °C					
CN2	669.10	296.15	UCP1	AF271263	UCP1	mitochondrial	1
CN2	10.84	8.00	B13	U97674	cytochrome-c oxidase chain I	mitochondrial	5
CN2	2.97	2.49	BW2	M13964	stimulatory G protein of adenylate cyclase α chain	signal transduction	5
CN2	2.79	2.19	B25	-	new	unknown	1
CN1	3.66	*	cycB	NM_012615	cyclin B	cell cycle	1
CN2	2.22	1.61	PPARg	AB011365	PPAR gamma (rat)	transcription factor	1
CN2	2.10	1.52	PPARg	-	PPAR gamma (Dj. Hamster)	transcription factor	1
CN2	1.27	2.18	GluR6	Z11548	glutamate receptor subunit (GluR6)	receptor	1

Table 12. List of the genes with a more than two-fold difference in expression between WAT and BAT from animals held at room temperature (RT) and from animals held at 4 °C for 18 hours (4 °C). For the data at RT, the mean of 6 animals were used and only clones with a significant difference between WAT and BAT according to Mann-Whitney were used. The ratios indicated (ratio WAT/BAT for the WAT difference products and BAT/WAT for the BAT difference products) are the mean of the ratios from all the spots corresponding to identical clones. See table 9 for more details about the homologies of the sequences to BLAST records. * These data are missing.

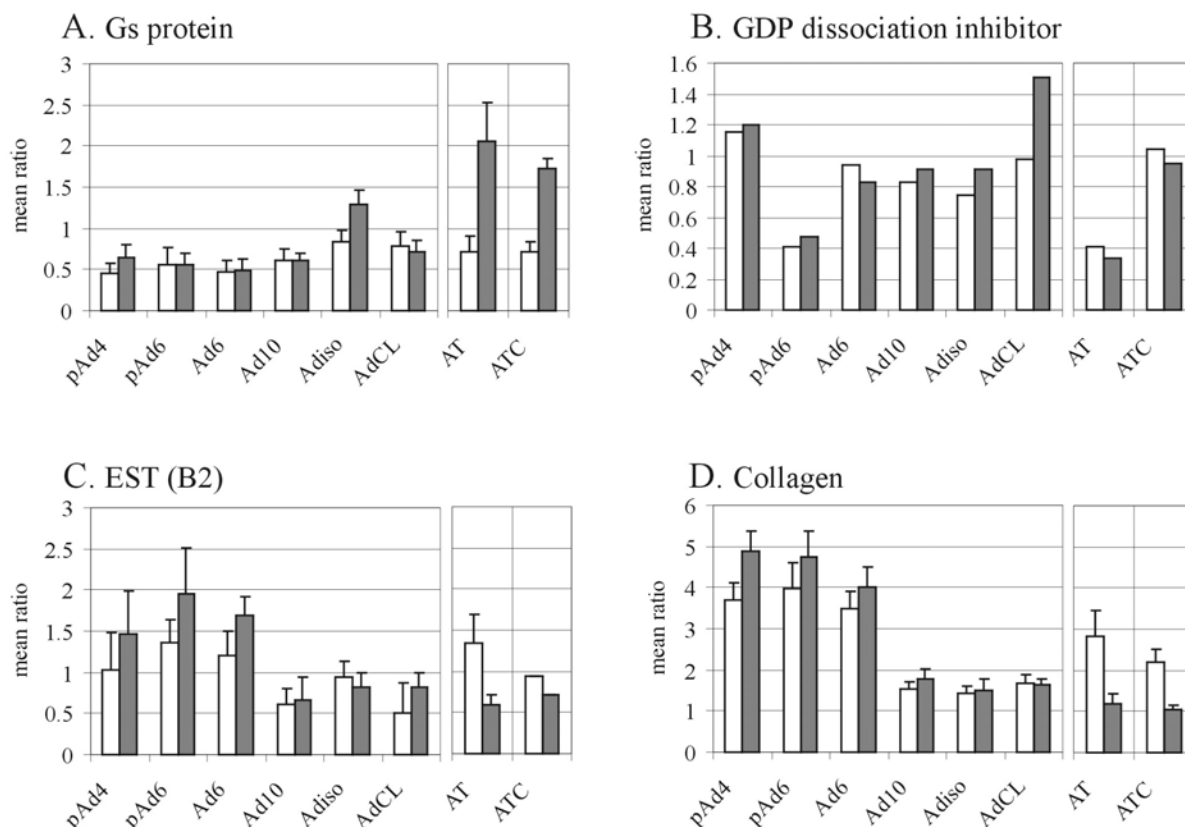


Figure 28. Expression patterns of stimulatory G protein (A), GDP dissociation inhibitor (B), the EST B2 (C) and alpha 2 collagen (D) in cell culture and in vivo. The abbreviations are explained in table 3 and 4. See figure 19 for further details. As GDP dissociation inhibitor was present only once on the array, no error bars can be shown.

3.6.3 Exposure to cold

There are only 3 genes with more than two-fold differences between the adipose tissues from the animals held at room temperature and the adipose tissue from the animals held at 4 °C (table 13). Only one is up-regulated in WAT and in BAT after cold exposure: the GDP dissociation inhibitor (figure 28 B). The expression level of UCP1 is more than four-fold increasing in WAT, but remains at a very low expression level compared to BAT (see table 12).

cluster	ratio		sequ.	accession	gene description	putative function	#
	WAT	BAT					
CN1	+ 2.521	+ 2.802	W14	X74401	GDP dissociation inhibitor beta	signal transduction	1
CN2	+ 4.114	+ 1.821	UCP1	AF271263	UCP1	mitochondrial	1
CN3	+ 3.128	*	N-myc	X63281	N-myc	transcription factor	1

Table 13. List of the genes with a more than two-fold difference in expression between adipose tissue from animals held at room temperature and animals exposed to 4 °C for 18 hours. The ratios of expression levels in WAT and in BAT between RT and cold exposed animals are indicated, '+' meaning an increase of expression level with the exposure to cold. See table 9 for more details about the homologies of the sequences to BLAST records. * These data are missing.

3.7 Expression of RAMP2 in adipose cells

Receptor activity modifying protein 2 (RAMP2) was one of the difference products sequenced. The signal intensity of the corresponding spot on the microarrays was very low, due to a low expression level or to a low amount of DNA on the arrays, so that no microarray expression data are available for it. But northern blot analysis revealed that RAMP2 shows an interesting expression pattern in adipose cells: in preadipocytes a 800 bp long transcript could be detected by northern blot, which is absent in adipocytes, where a 1100 bp long transcript was detected (figure 29 A). In the adipose tissues, both transcripts were found. For some cell cultures and tissue probes, the long transcript was found only at a very lower level in B10 and in BAT than in W10 and in WAT. A similar pattern of expression could be found in vivo: expression of the short transcript in stromal vascular fraction and of both short and long forms in the isolated adipocytes (figure 29 B).

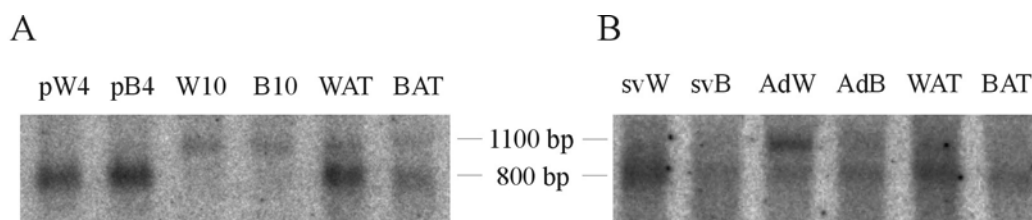


Figure 29. Northern blot analysis of the RAMP2 expression in primary cell culture and in hamster tissue. A. 10 μ g of pW4, pB4, W10, B10, WAT and BAT total RNA and B. 10 μ g of WAT stromal vascular fraction (svW), BAT stromal vascular fraction (svB), WAT isolated adipocytes (AdW), BAT isolated adipocytes (AdB), WAT and BAT were blotted and hybridised to the DP RAMP2 radiolabelled probe. The blots were exposed over night.

The RAMP2 difference product, long of 340 bp, matches to the mouse RAMP2 (mRAMP2) sequence (figure 30). It covers the region between bp 65 to 437, with some discordance between bp 65 and 208 (bp 1 to 111 of the hamster RAMP2). Thus, it is included in the coding sequence of the mRAMP2 mRNA. 3' RACE-PCR was applied to amplify and clone the hamster RAMP2 (pRAMP2) sequence till its polyadenylation site. As northern blot showed a transcript size close to 800 bp in hamster, about 100 bp sequence information in the 5' hamster RAMP2 is missing. By PCR amplification of genomic DNA with the pRA2-3f and pRA2-2r primers (table 1), introns were found at the positions corresponding to 174 bp, 242 bp and 345 bp of the mRAMP2 mRNA, confirming the published structure of the mouse RAMP2 gene (Derst et al., 2000).

```

3'- GATCGCGGCT  TGCTATGACC  CGCGCCGGGC  GGCCAGCCCC  GCTCCGCCCC  CCTCCGCTGC
    TGCTGGTGCT  GGTGCNGTGC  TGCTGCTGGG  CGCCGCTCTCA  ACCTCCCCGA  ATCAATCTCT
    TCCCACTGAG  GACAGCTTGC  TGTCAAAAGG  GAATATGGAG  GAGAGCTATG  AAGACAATGT
    CCTACCTTGC  TGGTATTATT  ACAAGAGTCA  TATGGACTCT  GTCAAGGACT  GGTGCAACTG
    GACTTTGATT  AGCAGGCATT  ACAGCGACCT  GCAGCATTGC  TTGGAGTACC  ATGCCGAGAG
    GTTTGGCCTG  GGTTTCCCAA  ATCCTTTGGC  GGAAAGGATC  ATCTTTGAGA  CTCACTTGAT
    ACACTTTACC  AACTGCTCCC  TGGTGCAGCC  CACATTCTCC  GATCCCCCAG  AGGACGTGCT
    ACTAGCCATG  ATCATCGCCC  CCATCTGCCT  CATTCTTTTC  CTGGNCACTC  TTGTGGTGTG
    GAGGAGTAAA  GACAGCGATG  CCCAGGCCTA  GAGGCAGCCA  TTCCTCTGCC  AGAACCAGGA
    ATCTCCCCTC  CCTACCCTCT  TTTTCTCACC  CTCATCTTTT  CCACGGGTTT  TTGGATTGGC
    GGAAAGGGAA  GCCAAGTGAT  GTAGTCTTTA  AAATAAATTT  TAAAAAATGC  GAAAAAAAAA
    AAAAAA -5'

```

Figure 30. 3' fragment of the Djungarian hamster RAMP2 sequence (667 bp). The DP cDNA fragment is indicated in grey. The stop codon (corresponding to the mouse stop codon) is underlined. The position of the 3 introns is indicated with arrows at the positions 98, 150 and 256. The beginning and the end of the 3'pRAMP2 fragment at bp 52 and 125 is indicated with a 3 above the sequence; the beginning and the end of the 5'pRAMP2 fragment at bp 215 and 319 is indicated with a 5.

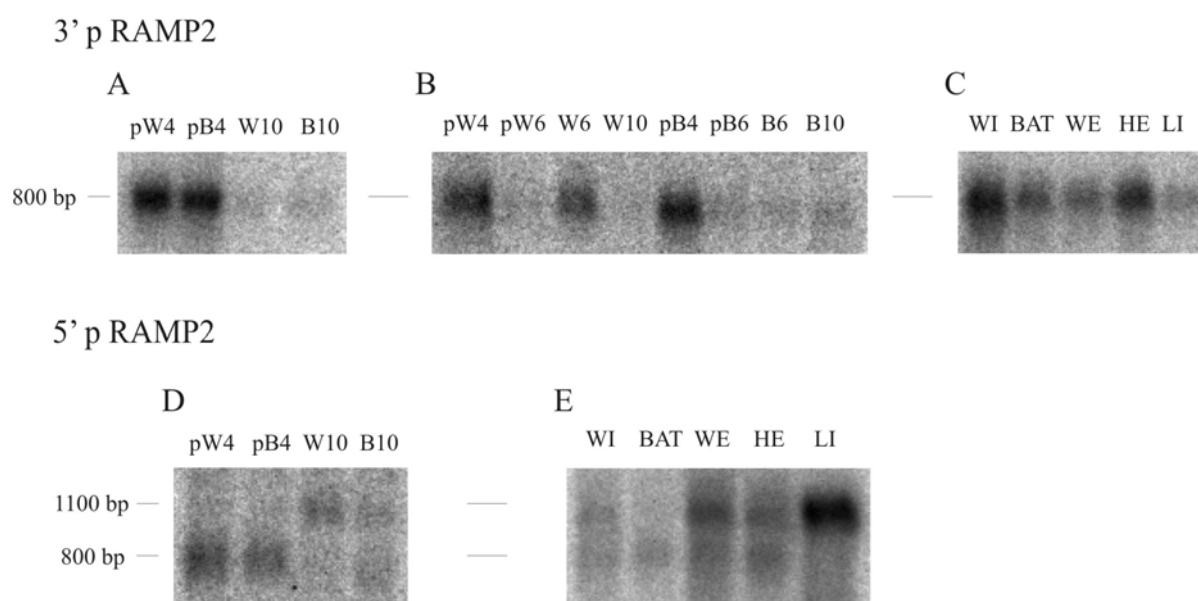


Figure 31. Northern blot analysis of transcripts including the 3'pRAMP2 and the 5'pRAMP2 fragments of the hamster RAMP2 mRNA in primary cell culture and in hamster tissue. 10 μ g of adipose cells or of inguinal WAT (WI), BAT, epididymal WAT (WE), heart (HE) or liver (LI) total RNA were blotted and hybridised to the 3'pRAMP2 (A, B and C) or to the 5'pRAMP2 (D and E) radiolabelled probes. The blots were exposed over night.

Two cDNA probes were constructed, covering the 3' and the 5' regions of the sequenced pRAMP2: 3'pRAMP2 amplified with the primers pRA2-4f and pRA2-2r (product size 73 bp) and 5'pRAMP2 amplified with pRA2-3f and pRA2-4r (104 bp). With the 3'pRAMP2 probe, only the 800 bp short transcript could be detected (figure 31 A, B and C). It is expressed in semi-confluent white and brown preadipocytes (pW4 and pB4) and in white adipocytes entering differentiation (W6) at higher levels. In all other cell types, only very low expression levels were found. Moreover, it was found in all tissues examined: inguinal and epididymal WAT, BAT, heart and liver. With the 5'pRAMP2 probe, both transcripts were detected. The expression pattern in cell culture was the same as with the DP pRAMP2 probe (figure 31 D). Both transcripts were found in WAT and heart, in BAT only the short transcript was detected and in liver only the long transcript at a high expression level (figure 31 E).

The primers mRA2-f and mRA2-r were used to amplify a mouse RAMP2 probe from a mouse WAT cDNA. In mouse WAT, two RAMP2 transcripts were found, corresponding to those found in hamster (figure 32 A). In BAT, only the short transcript was expressed. In lung, heart and muscle tissue probes, both transcripts were found, with a predominance of the short form in lung (figure 32 C). To compare the differentiation of preadipocytes to the differentiation of other cell types, RNA probes of myoblasts and of differentiated myocytes from the myogenic cell line C2C12 (Blau et al., 1983) were blotted and hybridised to the mRAMP2 probe (figure 32 B). In the differentiated cells, the two habitual transcripts were found at 800 and 1100 bp. In the myoblasts, none of them was detected, but a third transcript was found, larger than the 1100 bp one.

Primers listed in table 1 were used to amplify cDNA fragments of RAMP1, RAMP3, RCP, CRLR and ADM from mouse and hamster WAT cDNA. The mouse sequences were used to design the primers, choosing them preferentially in locations with a high inter-species conservation of the mRNA sequence. No RAMP3 cDNA could be amplified. Mouse RAMP1 and CRLR and hamster RCP and ADM were successfully amplified. The sequences of the cDNA fragments were checked. Northern blots with preadipocytes and adipocytes were hybridised with these probes. No RAMP1 and no CRLR could be detected. RCP was expressed in all cell types at a low level, ADM at a higher expression level (figure 33).

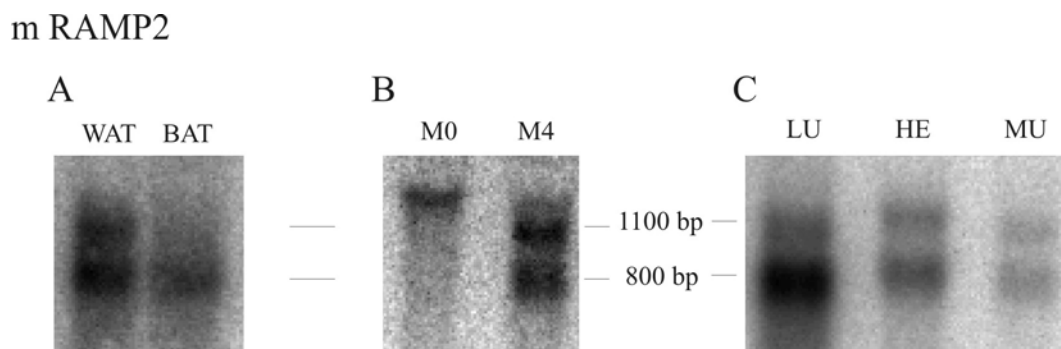


Figure 32. Northern blot analysis of the RAMP2 expression in mouse tissue and cells. 10 μ g of WAT and BAT (A), mouse myoblasts (M0) and differentiated myocytes (M4) from the C2C12 myogenic cell line (kindly provided by P. Van der Ven) (B), mouse lung (LU), heart (HE) and muscle (MU) total RNA were blotted and hybridised to a mouse RAMP2 radiolabelled probe. The blots were exposed over night.



Figure 33. Northern blot analysis of the RCP and ADM expression in cell culture. 10 μ g of pW4, pB4, W10 and B10 total RNA were blotted and hybridised to a hamster RCP (A, 1493 bp) and a hamster ADM (B, 1381 bp) radiolabelled probe. The estimated size of the detected transcripts was close to the size of the mouse transcripts indicated before. The blots were exposed over night.

4 DISCUSSION

4.1 Methodological aspects

4.1.1 Representational difference analysis

RDA was used to isolate genes expressed differentially in white and brown preadipocytes. We have chosen to compare cells obtained from parallel primary cell cultures of white and brown preadipocytes and cultivated until semi-confluence. There are two reasons for this choice:

- these cells originate from the white and brown fat pads of the same animals and were cultivated under identical conditions, so that no individual differences or cell line differences interfere with the differences between the two cell types.
- the cell culture leads to a high enrichment in preadipocytes and to a virtual elimination of other cell types present in the stromal vascular fraction of adipose tissues. As a matter of fact, adipose tissue contains a multitude of different cell types besides adipocytes and preadipocytes: epithelial cells, neuronal cells, fibroblasts, fibroblast-like interstitial cells, histiocytes, mast cells... (Cinti, 2001). These cells will all be found in the stromal-vascular fraction. Stromal-vascular fraction as starting material for RDA would represent a situation closer to *in vivo* conditions, but the high variety of cells present would strongly interfere with the study of the gene expression of preadipocytes. Preliminary experiments have shown that under our culture conditions almost 100% of adipose conversion was found when cells were plated at a high density (data not shown).

Thus, it can be expected that RDA will lead to the selection of genes related to the commitment of the preadipocytes to the white or brown adipocyte phenotype.

The quality of the cells was checked (figure 11), as well as the quality of the RNA and the efficiency of the removal of traces of genomic DNA (figure 3 and 4). The synthesized amplicon was of the expected size and aspect: a smear ranging from 200 to 1000 bp (figure 12). DP1 had a similar aspect for the pB4, but for pW4 some clear bands corresponding to individual cDNA fragments already appeared. These bands probably correspond to highly expressed genes with differences in expression, as the first cycle of RDA is not expected to lead to a very high enrichment in target sequences (Lisitsyn et al., 1993). It is mainly subtractive, leading to an enrichment “e” lower than the ratio driver:tester used. Because of the second order kinetic of self-reassociation (Britten et al., 1976), beginning in the second cycle of RDA, the enrichment in target will also have a kinetic compound. It should be in the range of “e³” after the second cycle and augment exponentially with further cycles.

DP2 and DP3 both consist of clearly discrete bands (figure 13). As their patterns were quite different, we decided to clone both.

23 % of the clones were considered as positive, i.e. showing a significant signal difference between white and brown preadipocytes. This is a rather high rate of false positives compared to published data (Frohme et al., 2000; Klingenspor et al., 1999; Welford et al., 1998; Lewis et al., 1997). But it should be noticed that all the genes showing no difference in gene expression in the microarray analysis are not necessarily false positives: RDA can also pick up differential splice variants which cannot be detected with microarrays. Furthermore, genes with very low expression levels may be missed as well by microarray hybridisations.

Meanwhile the analysis of the distribution of positive spots in the difference products revealed an apparent lower efficiency of the last cycle of subtractive hybridisation. In the hope to detect more genes with low differences of expression, we have chosen to use a low stringency for the last subtractive hybridisation, a tester:driver ratio of 1:16000, lower than most of the published data (Hubank et al., 1993; Klingenspor et al., 1999; Lewis et al., 1997; De Smet et al., 1997), which use as a standard the tester:driver ratio 1:80000. To which extent is it possible to lower stringency without loosing specificity ?

This question is very difficult to answer. Milner et al. (1995) established a statistical model of subtractive hybridisation based on the second order kinetics of self-reassociation. "Where several mRNAs are up-regulated, the model predicts a complex relationship between the abundance of each species in the (+) and in the (-) populations and their relative abundance after several rounds of subtraction". It can be seen from the southern hybridisations of the difference products (figure 14) that the kinetics of RDA are very complex. The target cDNA fragments are not continuously amplified from one cycle to the next. It should also be noticed that the selective PCR amplifications are not a "perfect" isolation of the tester:tester hybrids. Wieland et al. (1990) found out that independent PCRs of the same subtraction produced random representations. PCR is a "stochastic sampling of DNA molecules rather than a uniform amplification of molecules present in tester prior to PCR". For these reasons, it is not possible to make predictions on the results of RDA.

The method amplifies low abundant cDNA fragments with high differences in expression and abundant cDNA fragments with lower differences. By lowering the stringency of subtractive hybridisation, the latter are probably favoured. A too low stringency probably led the last subtractive hybridisation to have a lower efficiency.

4.1.2 Microarray hybridisations

Several sources of fluctuation affect data collected from microarray hybridisations, both locally, within one array, and globally, between different arrays (see 2.5.7.2 and Schuchhardt et al., 2000). We used a double labelling method to allow corrections for these fluctuations, and thus, to allow the comparison of multiple hybridisations (figure 5). But, as important as the correction of the data for these fluctuations, is the assessment of the uncertainty of the estimates thus calculated. Only with an

information about this uncertainty is it possible to draw conclusions from the data. For this reason, hybridisations were replicated.

We did not dispose of a good estimate of the background on the arrays: as shown in 2.5.7.3 (figure 6 and 7), it was not possible to use this estimate to correct the data for the background. Therefore, the raw signals were used and background estimates were used only as indicators to discard data points with too low signals compared to the background. Duplicate spots on the arrays and replicated hybridisations were then used to validate the local and global normalisation procedures and to assess their uncertainty.

Looking for significant differences in gene expression means looking for outliers in the comparison of hybridisations. By comparing replicate experiments it was possible to get an idea of the statistics of the fluctuations of the data, giving the possibility to identify true outliers when comparing afterwards the hybridisations with different probes. The comparison of duplicates and replicates led to the following conclusions:

- the method produced no bias in the comparison between arrays.
- not more than 2 % of the clones showed a more than two-fold difference in expression data of replicated hybridisations (see 2.5.7.5 and figure 9).
- fluctuations in the differences of expression data depend on the mean of the expression levels (Newton et al., 2001), but this dependency was found to be low after normalisation.

For these reasons, a comparison of arrays hybridised with different probes was possible. We used a two-fold and higher expression difference as cut-off for the identification of differentially expressed genes, as the reproducibility experiments showed an error of only 2 % at this threshold.

In addition to the internal controls of microarray hybridisations quality, the differences in gene expression found were validated with an alternative method: Northern blot hybridisations. For 5 genes the differential gene expression between brown and white preadipocytes was validated (figure 16). The changes estimated with Northern blots were lower or similar to those calculated from the microarray data. Even if the validation of microarray data with Northern blots is currently used, few of the published data sets give the possibility to such a comparison, as expression ratios are indicated only for one of the methods. Jelinsky et al. (1999) compared Northern blot to microarray data for 50 transcripts. They found a coefficient of correlation of the fold changes from microarray data to Northern of 0.79. For most of the transcripts there was a less than two-fold difference between the data originating from the two methods. They found this correlation to be weaker for the genes with the highest differences, indicating either an overestimation of the expression ratios by Northern blot analysis or an underestimation on the microarrays. These results are in agreement with our findings: for genes with rather low changes in gene expression, northern blot and microarray hybridisations lead to comparable results. In contradiction to this, another study using real-time PCR to validate microarray data found globally higher differences with real-time PCR than calculated from microarray data, even for genes with low differences in gene expression on the microarrays (Rajeevan et al.,

2001). Yet this discordance could be linked to the difference between the two methods used, real-time PCR and Northern blot.

4.2 Biological aspects

In order to better characterize the isolated genes, the microarrays were hybridised not only with white and brown preadipocyte probes as a screening of the cDNA libraries obtained by RDA, but also with probes from different kinds of cells and from tissue as listed in table 4. Insulin has been shown to be essential for lipid accumulation, i.e. adipogenesis of Djungarian hamster preadipocytes (Klaus et al., 1991 and 1995). We therefore compared not only preadipocytes and adipocytes, but also preadipocytes at confluence, treated with and without insulin (Ad 6 and pAd 6, respectively). Also included were cells treated chronically with isoproterenol, a general β -adrenergic agonist and with CL 316.243, a specific β 3-adrenergic agonist. The first treatment has been shown to induce proliferation of white and brown preadipocytes, to decrease lipid content by increasing lipolysis, and to increase UCP1 gene expression; the second has the same effects on lipolysis and thermogenetic function without inducing proliferation (Klaus et al., 2001c). Finally, the arrays were also hybridised to WAT and BAT probes from 6 animals kept at room temperature and from a pool of 3 animals exposed to 4 °C over night.

4.2.1 Biological controls

In the previous paragraph (4.1), we have shown how methodological controls (duplicate spots on the arrays and replication of the hybridisations) allowed us to assess the reproducibility of the expression data obtained, and how these data could be validated by the use of Northern blot hybridisations. A number of control genes with known expression profiles, e.g. differentiation markers, were spotted on the arrays. The expression profiles of these clones were used for a 'biological validation' of the whole data set.

4.2.1.1 Mitochondrial proteins

An obvious control when comparing white and brown adipose cells is UCP1 (figure 22 A). The expression profile corresponds quite well to previous findings. UCP1 expression is induced in the last steps of differentiation (Encke et al., 1997). The residual expression of UCP1 in WAT cultures is a commonly observed feature in primary cell cultures (figure 11). We have seen previously (see 1.2) that this is due to 10-15 % of adipocytes in WAT cultures expressing UCP1 and thus to the presence of brown preadipocytes within the WAT depots. The more than 10-fold increase of UCP1 expression by isoproterenol stimulation corresponds very well to previous results using Northern blot analysis

(Klaus et al., 1991 and 2001c). We found here that CL 316.243 led to more modest increases in UCP1 expression.

Another cDNA related to thermogenic capacity is the cytochrome c oxidase chain I subunit (COX), a mitochondrially encoded subunit of cytochrome c oxidase which can be used as a marker for mitochondrial transcription activity (figure 22 B). COX expression was very low in WAT compared to BAT and significantly higher in mature adipocytes than in preadipocytes, confirming previous findings (Klaus et al., 1995). However, isoproterenol, and in a more modest way CL 316.243, led to similar increases of COX expression in white and brown adipocyte cultures. In vivo, cold exposure had no effect on COX expression levels. This is in accordance with results showing that even after one week cold exposure of hamsters, there is no change in COX expression levels in BAT (Klingenspor et al., 1996). The raise in COX activity observed after cold exposure is explained by an increase in total RNA per BAT depot and a specific activation of the mitochondrial translation machinery. Liu et al. (1998) found that a chronic administration of CL 316.243 led to an increase of COX activity both in WAT and BAT, but at a higher level in the latter. Our results suggest that a chronic β -adrenergic stimulation leads to increases in COX mRNA in white and brown adipocytes in cell culture.

In vivo, UCP3 could not be linked to thermogenesis so far and its real function is not clear. We found similar expression levels in WAT and BAT (figure 23.A), whereas it has been reported to be higher expressed in BAT (Prunet-Marcassus et al., 1999; von Praun et al., 2001). Its expression does not vary during differentiation, but is strongly induced by isoproterenol, especially in brown adipocytes. This is in accordance with the finding that UCP3 expression is induced after 2 days cold exposure in hamster (von Praun et al., 2001).

4.2.1.2 Structure-related genes

During differentiation, preadipocytes undergo dramatic changes in morphology. These changes are programmed events and are accompanied by changes in the expression of several genes linked to structure or extra cellular matrix (ECM). Some of them can be used as markers for preadipose cells.

The expression of the α chain of type I collagen was found to be down-regulated at terminal differentiation (figure 28 D), which is in accordance with previous findings (Weiner et al., 1989). In vivo, we found higher expression levels in WAT than in BAT. The preadipocyte marker pOb24 is also a collagen: the $\alpha 2$ chain of type VI collagen. Its expression is also decreasing during differentiation (Ibrahimi et al., 1992). In our data set, the expression profile resembles that of type I collagen, with a lower difference between preadipocytes and adipocytes. We found also a higher expression level in WAT than in BAT.

This difference in the expression levels in vivo may be due to the presence of a higher amount of preadipose cells in WAT. Cousin et al. (1993) used expression levels of the $\alpha 2$ chain of type VI collagen in adipose tissues to assess the amount of preadipocytes in different depots. They found

higher amounts of preadipocytes in BAT than in inguinal WAT in rats, yet these characteristics can be very different from species to species. In mice, inguinal WAT was found to contain the highest amounts of preadipocytes compared to other WAT depots. In hamster, a higher amount of preadipocytes in WAT than in BAT would be in accordance with experimental observations when preparing primary cell cultures (unpublished observations).

Finally, β -actin displays an expression profile similar to that of collagen I and VI, which is also in accordance with published data (Spiegelman et al., 1982). It should be noticed that for all 3 genes, there is a slight tendency for higher expression levels in brown preadipocytes.

4.2.1.3 Cell cycle genes

A few cell cycle dependant genes were spotted as standards on the arrays. The expression of cyclin B is moderately decreasing during differentiation (table 10), the difference being higher in brown preadipocytes. Cyclin B is a protein from the G2/M phase (Morrison et al., 1999) and complexes with cdc2 (cell division cycle 2) to form the mitosis-promoting factor (MPF). A reduced expression with differentiation and the end of proliferation is thus expectable.

Cdc25A (cell division cycle 25A) is regulated in an opposed way (table 10): the expression is elevated in mature adipocytes. Cdc25A is a tyrosine kinase specific for the G1 phase. It plays a key role in the G1/S transition by activating diverse cell division kinases. No data are available regarding its expression in adipocytes, but the expression pattern we found is comparable to data available for cyclin D1, another G1 phase protein. Although Morrison et al. (1999) found cyclin D1 to be down-regulated during the differentiation of 3T3-L1 cells, two other groups found increasing expression levels during differentiation in 3T3-L1 cells and in pig preadipocytes primary cell cultures (Reichert et al., 1999; Kim et al., 2001). The latter hypothesise that cyclin D1 could have targets not linked to cell cycle in mature adipocytes. It seems that several G1 phase genes are expressed at higher levels in mature adipocytes, which are growth arrested cells. The role of these genes in these cells is unknown.

Ornithine decarboxylase (ODC) shows an expression pattern identical to that of cdc25A. ODC catalyses the conversion of ornithine to putrescine and is the rate-limiting step in the polyamine biosynthesis. Its expression is known to peak at the G1/S and G2/M phases (Pyronnet et al., 2000).

4.2.1.4 Other differentiation markers

A classical marker for adipocyte differentiation is the glyceraldehyde-3-phosphate-dehydrogenase (GAPDH), a key enzyme in lipid metabolism. As expected, we found its expression to increase during differentiation (figure 22 D), with no differences in the expression levels between the white and the brown adipocytes.

PPAR γ plays a key role in adipose conversion and is increased during adipocyte differentiation (Ntambi et al., 2000; Rosen et al., 2000), as confirmed by our findings (figure 22 C). Its expression in

both white and brown preadipocytes during proliferation was at the same low level and increased more than two fold in mature adipocytes. In tissue expression was higher in BAT than in WAT, also confirming previous findings (Jones et al., 1995).

4.2.1.5 Conclusions

The UCP1 expression data show that the cell cultures used were really cell cultures of white and brown preadipocytes. However they draw attention to the fact that they are not entirely pure: 10 to 15 % brown adipocytes are present in the white adipocytes cultures after differentiation, and vice versa, there are white adipocytes in the brown adipocytes cultures. A mixture in the same proportions of white and brown preadipocytes are presumably present in the semi-confluent cultures. Due to this heterogeneity, the expression ratios between white and brown preadipocytes of genes differentially expressed might be underestimated.

One confounder in the analysis of differential gene expression in preadipocytes could be that the cultured white and brown stromal vascular cells at semi-confluence represent different developmental stages. This would lead to the identification of genes regulated during preadipocyte differentiation rather than real differences between white and brown preadipocytes. The expression patterns of the α chain of type I collagen, and of PPAR γ and GAPDH, respectively down- and up-regulated during differentiation, were all found to be identical for white and brown preadipocytes in cell culture. This indicates that, at least at this degree of resolution of the differentiation process, the cell cultures can be considered as being in phase, so that cells at identical differentiation stages are compared.

4.2.2 General description of the expression data

12 genes were identified with different expression levels in white and brown preadipocytes (table 7). This may seem a low number of real difference products. As pointed out previously, there may be some methodological explanations for this, but white and brown preadipocytes in cell culture do not display any known morphological or metabolic differences and it seems reasonable that the number of differentially expressed genes is relatively low. The putative function of these genes will be discussed later (4.2.3). Before considering the function of interesting genes, let us focus on the overall analysis of the gene expression data based on a cluster analysis.

4.2.2.1 Typology of the expression data

The expression of all the genes in the different cell or tissue types was analysed. K-means clustering was used to identify typical expression profiles in the whole data set. 4 main expression profiles were thus identified:

(i) CW clusters: genes higher expressed in white preadipocytes

These clusters are relatively small and homogenous. They contain several highly redundant sequences, e.g. complement factor B (factB). Most genes have a significant higher expression level in white preadipocytes. They are characterised by an increasing expression during differentiation in brown preadipocytes, a more or less stable expression level in white preadipocytes and an inhibitory effect of isoproterenol (figure 19, table 10 and 11).

The genes from these clusters with significant differences between white and brown preadipocytes are 3 members of the complement system and the $\Delta 6$ FADS.

(ii) CB clusters: genes higher expressed in brown preadipocytes

A common feature of the clones of these clusters is a decreasing expression in brown preadipocytes during differentiation (table 10). Some of them have stable expression levels in white preadipocytes, so that there is a significant difference between the expression levels in preadipocytes (figure 20). Others have also decreasing expression levels in white preadipocytes, so that there is only a slightly higher expression in brown preadipocytes than in white, e.g. collagen (figure 28 D). β -agonist treatment has no effect on these genes. In vivo, most of them have similar expression levels in WAT and BAT, but some show higher expression levels in WAT: collagen, β -actin, HCAP, α -actinin4 and others (table 12).

The majority of the genes grouped in these clusters are functionally linked to structure or ECM (especially the genes with higher expression in WAT), code for proteins involved in the control of transcription at different regulation levels or have unknown functions.

(iii) CN1: genes down-regulated during differentiation

This is a small cluster. Clones from CN1 (and a few clones from CN3) have decreasing expression levels during differentiation (table 10 and figure 21). Only for a few of them the difference between preadipocyte and adipocyte is significant. Most of the genes are linked to structure or cell cycle.

(iv) CN2: genes up-regulated during differentiation

This is the largest of all clusters. It contains a majority of reference clones. The expression of these genes is increasing during differentiation and/or after isoproterenol treatment (table 10 and 11). A part of them shows higher expression levels in BAT than in WAT (table 12). These are the genes with the

highest differences in the comparison between tissue and cell culture. In vitro, no differences are found between white and brown adipocytes (except for UCP1), but in vivo there is a significantly higher expression in BAT (figure 22).

The genes from this cluster are mostly linked to signal transduction, transcriptional control, cell cycle regulation or metabolism. Only two of them are linked to structure or ECM.

4.2.2.2 A comparison of cell culture and tissue

Soukas et al. (2001) compared the differentiation in vitro of 3T3-L1 cells to the differentiation of adipocytes in vivo, using stromal-vascular fraction and isolated adipocytes. They conclude that “the gene expression changes associated with adipocyte development in vivo and in vitro, although overlapping, are in many respects quite different”. They found large groups of genes expressed in vivo but not or at very low levels in 3T3-L1 cells. We did not find tremendous differences between expression levels in vivo and in vitro. All genes expressed in cell culture were found to be also expressed in tissue, sometimes at a lower or higher level, but with differences that do not exceed ratios of 2 to 5. This should not be surprising, as we compared two closer related systems: primary cell culture represents a model closer to the situation in vivo than 3T3-L1 cells.

Adipose tissues contain a multitude of different cell types. The proportion of each cell type depends on the species and the depot considered. Different amounts of preadipocytes, for example, can result in different expression levels of collagen in total tissue (see 4.2.1.2). In mice brown adipose tissue, preadipocytes represent only about 10 % of all cells (Goglia et al., 1992). This makes a direct comparison of expression data in cell culture and in vivo very difficult. Supposing a gene is higher expressed in brown preadipocytes than in white and equally expressed in white and brown adipocytes, the low amount of preadipocytes in tissue samples and the differences in the composition of both kinds of tissue prevents any prediction about the expression levels in vivo. It should be noticed that the same difficulties are encountered when using stromal-vascular fractions, which contain all the non lipid-filled cells from adipose tissues.

We found several genes with moderately higher expression in WAT than in BAT (table 12). All these genes from cluster CN1 or from the CB clusters are down-regulated during differentiation, equally in white or brown cells or with moderately higher expression levels in brown preadipocytes. Thus, these differences could be due to a higher amount of preadipocytes in WAT.

Furthermore, several genes mostly from cluster CN2 are higher expressed in BAT. Except for UCP1, this difference is not linked to any difference between white and brown preadipocytes or adipocytes in vitro. These genes are up-regulated during adipogenesis, so that the differences found in vivo could be linked to different amounts of mature cells in the tissues. But, considering the case of COX (figure 22 B), this explanation seems unlikely. More probably, the equal expression levels in white and brown adipocytes in cell culture are due to differences between this artificial model and the situation in vivo,

for example the absence in cell culture of some specific signal inducing COX expression in brown preadipocytes or adipocytes in the tissue of hamster held at thermoneutrality.

4.2.2.3 Inter individual variability of gene expression in adipose tissues

Tissue samples from 6 animals were used for microarray hybridisations. The comparison of the expression levels in the BAT and in the WAT of the 3 male animals and the 3 female animals showed the absence of any sex-dependant difference (figure 24). Meanwhile, it could be observed that the inter-individual variation of gene expression was not uniform for all genes. Some genes, and particularly *factB* and *UCP1* in BAT, showed higher levels of inter-individual variation than the majority of the genes (figure 26).

Gene expression levels can vary a lot, even between identical inbred animals. These inter-individual variations can now be estimated on a large scale through microarray hybridisations. For certain types of applications, as for example the comparison of tissues from sane and from pathological individuals, this variation is an important factor to take into account. Miller et al. (2001) examined the expression of 153 genes in the liver of 4 mice and found variations of expression levels higher than 30 % for 80 % of them. Very high variations could be explained by bimodal distribution of the expression levels for certain genes. In our dataset, a higher number of animals would be necessary to establish this. Nevertheless, such high variability implicate the necessity to use different scales of measurement for different genes when comparing individual samples, as suggested by Wittes and Friedman (1999). With the growing amount of expression data available, catalogues of gene expression levels including indications on variability will be compiled. This kind of database is being set up for example at <http://www.hugeindex.org> (Hsiao et al., 2001). Yet the first conclusion to be drawn is the necessity of replication to establish if observed differences reflect real differences, or if they are due only to a high variability of the expression of the particular gene. The use of 6 animals allowed us to use a classical statistic test (Mann-Whitney test) for the identification of differentially expressed genes between WAT and BAT.

In the BAT, several genes showed relatively high inter-individual variations, particularly *factB* with a variation of 37 %, close to the variation of the *UCP1* expression. There was a significant negative correlation between the expression levels of these two genes (figure 27). The *UCP1* expression levels suggest different degrees of activation of the BAT of the animals, even if they were kept at exactly the same conditions. These differences did not correspond to differences in the COX expression, related to the respiratory capacity. More data would be necessary to investigate this question further. It would allow to define the distribution of the expression levels (normal or bimodal ?) and to establish the validity of the correlation found. Interestingly, von Praun et al. (2001) compared hamsters kept at 23 °C or at 4 °C for 2 or 7 days and found a significant positive correlation between the expression levels of *UCP1* in BAT and the serum free fatty acid levels. In cold induction, the higher serum FFA levels

are linked to an increased lipid catabolism. There may be no direct link between the expression of UCP1 and factB, but it is interesting to note that factB expression is negatively associated to catabolic states in adipocytes: higher UCP1 expression and β -adrenergic stimulation (figure 19).

4.2.3 Functions involved in adipocyte differentiation

Genes up-regulated during differentiation belong to many different functional groups (table 10): genes linked to metabolism, thermogenesis, lysosomal genes... , i.e. genes necessary in a functional white or brown adipocyte. Some of these genes as control genes were discussed above. Apart from them, genes linked to a few functional groups, mainly complement, structure and cell cycle, were particularly present among the genes regulated during differentiation.

4.2.3.1 Complement and fatty acid metabolism

Of the four genes with higher expression in white preadipocytes, three present homologies to members of the complement system. Complement component C3 and complement factor B (factB) belong to the alternative pathway of complement. This pathway is the base of an immunological response not based on an antibody / antigene recognition. The first link found between adipose tissue and complement was the discovery that factor D is identical to adipsin, a protein released by mature adipocytes (Rosen et al., 1989). Adipocytes were then found to express also C3 and factB and to activate the proximal portion of the alternative pathway (Choy et al., 1992). The expression of factor I, factor H, complement receptor 1 CR1 (Peake et al., 1997) and the absence of any C5 (Choy et al., 1992) explains why this activation of complement is not followed by cell lysis. Yet when the balance between the activators and the inhibitors of complement is perturbed, adipocyte lysis can occur. One example is the effect of C3 nephritic factor (C3NeF), an autoantibody inducing partial lipodystrophy. Through the catalytical action of adipsin, factB bound to the C3 fragment C3b is cleaved and the C3 convertase C3bBb is produced (figure 34). C3 NeF stabilises C3bBb, leading to the formation of more C3b and thus of more C3 convertase, to an induction of the alternative pathway of complement and finally to adipocyte lysis. A gradient in the amount of adipsin synthesised by adipocytes in the body is thought to be the cause of the partial lipodystrophy: a higher amount of adipsin in the upper part of the body leads to the loss of fat mass in these depots (Mathieson et al., 1997).

The C3 convertase C3bBb leads to the cleavage of C3 to C3b, which is important for the further activation of complement, and C3a, so to say a side product of this pathway (figure 34). Carboxypeptidase B can cleave the final arginin from C3a producing C3adesArg, which was found to be identical to the acylation stimulating protein (ASP, Cianflone et al., 1999). ASP stimulates triglyceride synthesis in adipocytes and glucose uptake through the translocation of the GLUT transporters to cell membrane. The main regulator of triglyceride synthesis in adipocytes is insulin.

Insulin increases glucose transport and acts on hormone sensitive lipase (HSL) to reduce lipolysis. ASP acts through different mechanisms. Its stimulation of triglyceride synthesis is achieved by direct stimulation of free fatty acid esterification and incorporation into triglycerides. It has been shown that its action on glucose transport is comparable and additive to that of insulin, suggesting also that different mechanisms are involved (Cianflone et al., 1999).

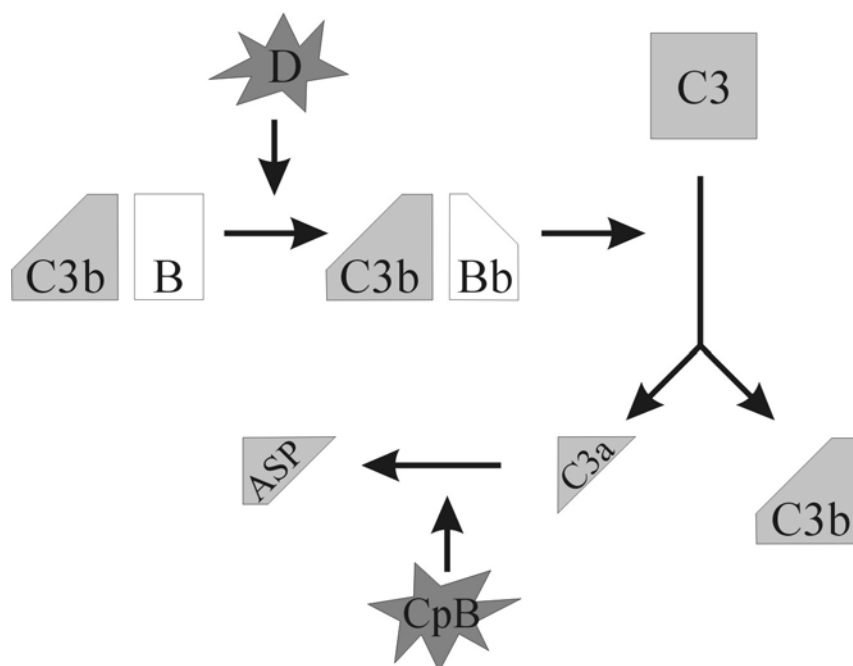


Figure 34. Schematic representation of the enzymatic conversion of C3 to ASP. Factor B (B) bound to C3b is cleaved by the action of factor D (or adipsin, D). The C3 convertase C3bBb cleaves C3 to generate C3a and C3b. By the action of the carboxypeptidase B (CpB) the carboxyl terminal arginin of C3a is cleaved to produce ASP.

We found a high expression level of factB both in white preadipocytes and adipocytes (figure 19 A), which is in accordance with the results of Peake et al (1997) in 3T3-L1 cells but contradictory to Cianflone et al. (1999) who found an induction of expression during differentiation in human adipocytes. Concerning C3, both groups found expression to be induced during differentiation of cells. There are no data available about expression levels of complement components in BAT.

What could be the role of complement components in preadipocytes ? Adipsin is expressed only in mature cells, so that no ASP synthesis is possible in preadipocytes. Do these components play an immunological role ? It has been found that preadipocytes can act as macrophage-like cells (Cousin et al., 1999). Furthermore, we found complement component C2 to be expressed also in adipose cells. C2 is the structural and functional homologue to factB in the classical pathway of complement. Cianflone et al. (1999) found no expression in adipose tissue, but other microarray experiments found also C2 expression in WAT (Gabrielsson et al., 2000; Nadler et al., 2000; Soukas et al., 2000). Possibly, complement components secreted by preadipocytes could also play a paracrine role, interacting with

the adiponectin released by adipocytes. This would be a new dimension in the “micro-environmental metabolic regulation in the adipose tissue space” through the ASP pathway (Cianflone et al., 1999).

The second question arising from these findings is: what could be the role of complement components in BAT? Some data indicate that it could play a different role than in WAT and be regulated differently. Male C3, and thus ASP, deficient mice were shown to display moderately smaller gonadal and perirenal WAT depots and almost 90 % larger BAT depots under a low fat diet (Murray et al., 1999). The authors of this study hypothesise that a lower non-esterified fatty acid (NEFA) uptake in WAT would lead to the repartition of NEFAs in BAT and in the muscle. Our data indicate that brown adipocytes could be able to synthesise ASP. This would mean that ASP plays a different role in BAT than in WAT. Furthermore, it was found that these animals show lower expression of UCP1, but higher expression of UCP3 in muscle and of UCP2 in WAT (personal communication from Digitale E, Nicolescu O, Stanhope KL, Cianflone K and Havel PJ). We found in BAT a negative correlation between the expression levels of UCP1 and factB, which is the rate limiting enzyme in ASP synthesis, and a down regulation of the expression of all complement components through β -adrenergic stimulation in cell culture, suggesting a sympathetic regulation in adipose tissue. More work needs to be done to elucidate the role of complement components and ASP in BAT. Our data indicate possible negative links to the thermogenic function.

The only other gene with significantly higher expression in white preadipocytes was the $\Delta 6$ fatty acid desaturase ($\Delta 6$ FADS, figure 19 B). This enzyme catalyses the rate limiting step in the conversion of linoleic acid and linolenic acid to respectively arachidonic acid and eicosapentaenoic acid, which are precursors for various hormones, prostaglandins etc., and thus involved in a large number of biological functions. Prostaglandins from the D₂ and J₂ series are natural ligands for PPAR γ and can thus act as regulators of adipocyte differentiation. Although $\Delta 6$ FADS activity is normally considered to be very low in non-hepatic tissues, the mRNA was recently reported to be similarly expressed in human liver, lung and heart and even higher in brain (Cho et al., 1999). The locus of the human homologue of $\Delta 6$ FADS is situated in the region of chromosome 11 (11q13) found to be coincident with several independently mapped quantitative trait loci for obesity.

4.2.3.2 Structure and extra cellular matrix (ECM)

3 genes linked to cellular structure and ECM were found to be expressed at a higher level in brown preadipocytes (table 7) and several others were found to be decreasingly expressed during differentiation (clusters CN1 and CB, table 10). This decrease in expression, in brown preadipocytes only or in both kinds of preadipocytes, is a common feature of all the structural genes identified here.

An important step in the functional differentiation of preadipocytes preceding lipid accumulation is the morphological rearrangement of the preadipocytes from a fibroblast-like appearance to a rounded shape. This remodelling is a programmed event: it can be triggered without subsequent triglyceride

accumulation (Kuri-Harcuch et al., 1978). A lot of genes are associated with this event and were found to be down-regulated during differentiation: ECM proteins such as fibronectin and β integrin as well as cytoskeleton proteins such as actin, tubulin, vinculin, α actinin and tropomyosin (Spiegelman et al., 1982; Antras et al., 1989; Rodriguez Fernandez et al., 1989). Some ECM components were shown to be able to block the differentiation of preadipocytes by increasing adhesion: fibronectin (Spiegelman et al., 1983, Guller et al., 1992) or polylysine and ECM extracts (Rodriguez Fernandez et al., 1989). Transforming growth factor β (TGF β) inhibits differentiation and morphological changes in preadipocytes through an induction of the synthesis of fibronectin and ECM components. It has been shown also that drugs targeting the cytoskeleton influence key events in gene expression and differentiation. The morphological rearrangement of preadipocytes is coupled to a rearrangement of ECM in the direction of decreasing adhesion. This event is a key step of adipogenesis and plays a regulatory role for the subsequent functional differentiation.

In accordance with Bouloumié et al. (2001) we found TIMP1 (tissue inhibitor of metalloproteinase 1) to be down-regulated during differentiation (figure 21 B). Matrix metalloproteinases (MMPs) degrade various compounds of the ECM. They play an important role in the degradation of the ECM of preadipocytes prior to morphological rearrangement: a treatment of the preadipocytes with MMP inhibitors blocks their differentiation. Thus, the down-regulation of TIMP1 can be supposed to be an important event in early differentiation. The MMP associated to TIMP1, MMP2, is up-regulated. In contrast to this, we found a membrane-type matrix metalloproteinase (MT-MMP) to be down-regulated in mature adipocytes. MT-MMPs, a new class of MMPs, are membrane bound and possess a cytoplasmic domain that may be important for cellular signalling (Fillmore et al., 2001).

Parallely to this, PAI-1 (plasminogen activator inhibitor), a serine protease inhibitor inhibiting tissue- and urokinase-type plasminogen activators and thus preventing fibrin degradation, was also found to be down-regulated during differentiation (figure 21 A). The attention of obesity researchers was drawn to PAI-1 when it was discovered to be over-expressed in the adipose tissue of obese patients. But the expression pattern of PAI-1 during differentiation of preadipocytes remains unclear. In mice, other microarray hybridisation experiments found higher expression levels in preadipocytes as well (Soukas et al., 2001; Zhou et al., 1999). Crandall et al. (2000b) found a decreasing release of PAI-1 with differentiation in human preadipocytes. But other groups found its expression to be increased during differentiation in mice (Seki et al., 2001) and in human preadipocytes (Birgel et al., 2000). In accordance to this, Ihara et al. (2001) found an induction of PAI-1 by thiazolidinediones, stimulators of differentiation. This, again, is in contrast with an induction of PAI-1 through tumor necrosis factor α (TNF α) and TGF β (Sethi et al., 1999; Birgel et al., 2000), factors known to inhibit differentiation. A lot of questions remain open regarding the role of PAI-1 in adipose tissue. Is the primary target of PAI-1 the adipose tissue itself or the vasculature? Does it play a role in preadipocytes migration, as suggested by Crandall et al. (2000a)? Is it of any importance for the preadipocytes ECM? The

heterogeneity of the compounds stimulating PAI-1 suggest that it may play different roles when expressed in different conditions.

Fibronectin was found to be almost 3 times higher expressed in brown preadipocytes than in white (figure 20 C). It is an adhesive ECM protein playing a role in the binding of collagen to cells. The inhibitory effect of fibronectin on preadipocytes differentiation can be reversed by insulin (Spiegelman et al., 1983; Rodriguez Fernandez et al., 1989). Mesenchymal cells were found to produce more fibronectin than 3T3 cell lines, and this fibronectin has been hypothesised to be a protection of the preadipocytes against differentiation (Antras et al., 1989). Is the fibronectin from brown preadipocytes protecting the cells from an induction of differentiation through insulin? In fact, fibronectin possesses not only an inhibitory but also a stimulatory domain for differentiation. The latter can be liberated through MMP digestion of fibronectin (Fukai et al., 1995). This could represent a mechanism by which the degradation of the preadipocytes ECM leads to a stimulation of differentiation.

Metargidin, a transmembrane glycoprotein from the metalloprotease disintegrins family was also found to be up-regulated in brown preadipocytes. Among others, metargidin contains a metalloprotease domain and an EGF-like domain (similarly to pref-1) and interacts with integrins (Krätzschmar et al., 1995).

A few immunohistochemical data support our observation of differences between the ECM of BAT and of WAT. Haraida et al. (1996) detected fibronectin in human BAT and BAT tumors (hibernomas) but not in the ECM of typical white fat cells. Accordingly, Pierleoni et al. (1998) found no fibronectin around differentiated white adipocytes in vivo. But apart from this, to our knowledge no data are available about the ECM composition of BAT. Our data suggest that the ECM remodelling and the linked regulatory events could play a role in the differential development of brown and white preadipocytes. A more systematic comparative study of the ECM composition of BAT and WAT and of the effect of ECM compounds on the differentiation of white and brown preadipocytes would be necessary.

4.2.3.3 Regulation of gene expression

Necdin is one of the genes found to be higher expressed in brown preadipocytes (figure 20 A). The nuclear factor necdin is a growth suppressor expressed in post-mitotic neurons in the central nervous system (Maruyama et al., 1991). It was later found to be also expressed in many other tissues in human, in opposition to mouse where its expression is restricted to neurons (MacDonald et al., 1997). It is functionally similar to the retinoblastoma (pRb) protein family and interacts also with viral oncoproteins and the E2F transcription factors (Yoshikawa, 2000). Members of the pRb family (p107, p130) were found to be expressed at different phases of differentiation. p107 is expressed specifically in undifferentiated cells and p130 transiently during differentiation. It seems to be linked

to cell cycle exit. pRb is expressed in differentiating cells and plays a role in the regulation of the expression of tissue specific genes (Yee et al., 1998; Classon et al., 2000; Puigserver et al., 1998). pRb was found to be important also for brown adipocyte differentiation. A pRb knockout in fibroblasts was reported to result in an up-regulation of UCP1, probably through the release of an inhibitory effect of pRb on PGC1 (K. Kristiansen, personal communication). We found necdin to be higher expressed specifically in brown preadipocytes.

Interestingly, necdin is associated to the Prader-Willi syndrome (PWS), a pathology caused by the loss of function of imprinted genes in the 15q11-13 human chromosomal region. Necdin is one of these genes and is thought to be responsible for at least a subset of the symptoms associated to PWS (Muscatelli et al., 2000). One of these symptoms is obesity. The cause for this obesity is unclear and several phenomena probably contribute to elevate body mass: hyperphagia due to decreased satiation, hypotonia, a dysregulation in the energy metabolism in adipocytes and hypothermia which was observed in the infancy of some patients. The extend of the role of necdin in PWS is unknown. Necdin knockout mice do not become obese, as far as assessed by the investigators (Tsai et al., 1999; Gerard et al., 1999; Muscatelli et al., 2000), which could be due to the differences in expression between human and mice. We think necdin remains an interesting candidate for genes involved in the determination of brown preadipocytes.

The function of hepatocellular carcinoma associated protein (HCAP, also named breast cancer associated gene 1), another gene showing higher expression levels in brown preadipocytes, is not known (figure 20 D). Its association with tumor cells might imply a role in cell proliferation. Thereby, it should be noticed that BAT was at several occasions found to have a high tumor potential (Zennaro et al., 1998). Cell lines of brown preadipocytes were established from BAT tumors induced by expression of the SV40 T-antigen in transgenic mice (Ross et al., 1992; Kozak et al., 1994b). SV40 T-antigen can interact with and alter the function of pRb, p107, p130 and necdin (Taniura et al., 1999). These observations support the hypothesis of another equilibrium between growth suppressors and oncogenes in brown preadipocytes.

Two other genes found to be higher expressed in brown preadipocytes are putatively linked to transcriptional regulation. Vigilin is also referred to as high density lipoprotein binding protein (HBP). It was first identified as a cholesterol responsive protein, possibly aiming to remove excess intracellular cholesterol, but its ability to bind HDL stays unclear and its structure does not comprehend any transmembrane domain (McKnight et al., 1992). The real function of vigilin may be completely different. It contains 14 RNA binding domains and a nuclear localisation sequence and was found to be present in cytoplasm and nucleus. For these reasons, vigilin could function as a RNA shuttle (Kügler et al., 1996). It was found to effectively bind mRNA (Dodson et al., 1997). Until now, no conclusive data allow to determine what the real function of vigilin is (Fidge et al., 1999).

The expression pattern of vigilin was very similar to that of the small nuclear ribonucleoprotein polypeptide A (snrpa) (Nelissen et al., 1991) belonging to the snRNPs (small nuclear

ribonucleoproteins) which are essential components of the mRNA splicing machinery. Vigilin, SnrpA and necdin are all nuclear proteins, which certainly warrants further investigation of their function in adipocyte proliferation and differentiation.

4.2.3.4 Signal transduction and cell trafficking

The Rab GDP dissociation inhibitor β (GDI β) was found to be up-regulated in WAT and BAT after 18 hours cold exposure (figure 28 B). Rab GTPases are small Ras-like GTPases which are active only in a GTP-bound state and are involved in the regulation of vesicle mediated cellular transport. The GDIs participate in the cycling between GDP and GTP-bound states for Rab proteins and in the translocation of Rab proteins between cytosol and cell membrane. GDI β interacts with several Rab proteins, including Rab4 and Rab6, and is expressed ubiquitously in rat and human, implicating a general role of this GDI subtype in vesicular trafficking in diverse cell types (Nishimura et al., 1994; Bachner et al., 1995; Janoueix-Lerosey et al., 1995).

Several groups found Rab4 and GDI β to be implicated in the response of adipocytes to insulin. Insulin triggers the translocation of the glucose transporters GLUT1 and GLUT4 to the cell membrane, increasing the glucose uptake of cells. The major regulatory mechanism for this process is thought to be translocation (Shisheva et al., 1994; Bortoluzzi et al., 1996; Kandror et al., 1996). Cold exposure increases glucose uptake in WAT and BAT of rats (Vallerand et al., 1990; Nikami et al., 1992) and uniquely in the BAT of mice (Olichon-Berthe et al., 1992), in both cases through a higher amount of GLUT4 on cell membranes. But besides glucose uptake, cold exposure also leads to many other responses implicating cellular trafficking. β -adrenergic receptors are recycled after endocytosis by a mechanism implicating Rab4 and Rab5 (Seachrist et al., 2000). These and other cellular events suppose higher cellular trafficking during cold exposure and thus higher requirements for the regulatory proteins of this mechanism, among others GDI β .

A gene not regulated by cold exposure but higher expressed in BAT is the α subunit of the stimulatory G protein (Gs α , figure 28 A). Gs α is coupled to β -adrenergic receptors in brown adipocytes. It is known for several years that BAT contains more Gs α mRNA than WAT (De Pergola et al., 1994). It has been observed that Gs α mRNA levels are not in a simple relationship to membrane Gs α concentration (Granneman et al., 1989), making it difficult to draw functional conclusions from these data. The higher expression of Gs α in isoproterenol treated cells probably reflects the higher differentiation state of these cells.

A gene with an interesting expression profile during preadipocyte differentiation is RAMP2. RAMPs are a family of proteins with a single transmembrane domain isolated in 1998 (McLatchie et al., 1998). They are associated to the calcitonin-receptor-like receptor (CRLR) on the cell membrane and define its pharmacology. CRLR associated to RAMP1 act as a CGRP (calcitonin gene-related peptide) receptor, associated to RAMP2 or RAMP3 as an adrenomedullin (ADM) receptor. Additionally,

RAMPs play a role in the transport of CLRL to the cell membrane and in the determination of the glycosylation state of the receptor (Foord et al., 1999).

Whereas a single human RAMP2 transcript of 0.8 kb was found (McLatchie et al., 1998), in mouse, an additional transcript of 1.2 kb was found in all tissues analysed (Husmann et al., 2000). This transcript could originate from alternative or incomplete splicing. We found RAMP2 to be expressed also in adipose tissue in mouse and hamster and in cultured preadipocytes from hamster. In vitro and in vivo, a shift was detected during differentiation from the 0.8 kb transcript expressed in preadipocytes to the 1.2 kb transcript expressed in mature cells (figure 29). This feature seems to be specific to the adipose lineage, as in undifferentiated and mature cells from the myogenic C2C12 cell line a different pattern was found (figure 32 B). It should be noted that these myoblasts can be trans-differentiated to adipoblasts (Teboul et al., 1995). The nature of the 1.2 kb transcript could not be determined so far. As the members of the RAMP family share only 30 to 35 % identity (Derst et al., 2000), this transcript is distinct from RAMP1 or 3. The 3' end of the transcript we isolated is specific to the known functional RAMP2 of 0.8 kb, whereas the 5' region is common to both transcripts. It could correspond to a splice variant or to a highly homologous different gene.

CRLR and RAMP1 cDNA could be amplified from mouse adipose tissue by RT-PCR. RCP (receptor component protein), an intracellular membrane-bound protein associated to CRLR and playing a role in signal transduction (Evans et al., 2000), is expressed in preadipocytes and adipocytes and could be detected by northern blot. Thus, all the members of this receptor machinery are found in adipose tissue.

Some findings indicate that the sensory innervation of adipose tissue could play a role as regulator of adipogenesis. Adipose tissues contain CGRP expressing nerves which could also play efferent roles. Capsaicin specific desensitisation of sensory nerves leads to a decrease in the number of brown adipocytes in rat periovarian WAT and to BAT atrophy in rats as well (Giordano et al., 1998; Cui et al., 1992). RAMP1 was found in total adipose tissue, so that preadipocytes or adipocytes might possess CGRP receptors, but our results point rather to a role of CRLR as ADM receptor in preadipocytes.

ADM is a vasodilator neuropeptide of the calcitonin family which was first isolated in pheochromocytomas, tumors of the adrenal medulla. It was soon found to be expressed also in a lot of other tissues and cells: in the brain and in vascular smooth muscle cells, cardiomyocytes, epithelial cells... We found it expressed also in preadipocytes and adipocytes (figure 33 B). Besides its vasodilatory effects, ADM displays also different functions (Takahashi, 2001). Depending on cell type, ADM can act as a paracrine and autocrine growth stimulator or inhibitor (Belloni et al., 2001). It is expressed in tumor cells, where it stimulates tumor growth. It was found to stimulate the proliferation of Swiss 3T3 cells and of osteoblasts but to inhibit the growth of smooth muscle cells (Isumi et al., 1998; Naot et al., 2001; Makino et al., 2001).

These findings open a lot of questions. Our results show that this paracrine and autocrine pathway might be important for adipogenesis. It might as well be an important link between adipogenesis and blood pressure regulation. The nature of the 1.2 kb transcript should be determined and the question of its binding to CRLR addressed. Is it also a protein modulating the activity of CRLR ? Additionally, the role of ADM in adipogenesis should be assessed.

4.3 Summary and conclusions

Based on the hypothesis that white and brown preadipocytes are distinct precursor cells for white and brown adipocytes, the aim of this project was to use a systematic approach to identify differentially expressed genes in white and brown preadipocytes and to compare gene expression during the differentiation of white and brown preadipocytes. RDA was used to isolate candidate genes which were spotted on microarrays for gene expression analysis. These allowed to compile a large-scale data set of gene expression levels during differentiation in cell culture and in vivo. This data set was validated by methodological controls, confirmation of expression data by northern blots and biological controls through the expression data of marker genes as UCP1, GAPDH or PPAR γ .

It could be shown that white and brown preadipocytes can be distinguished by the relative expression levels of several genes. This result is in favour of the hypothesis that two distinct types of preadipocytes determined to differentiate to white and brown adipocytes exist. Four genes with higher expression in white preadipocytes and 8 with higher expression in brown preadipocytes were identified. Cluster analysis helped to characterise the data set and led to the identification of 4 major typical expression profiles of genes during white and brown preadipocytes differentiation: genes higher expressed in white preadipocytes, higher expressed in brown preadipocytes, down-regulated during differentiation and up-regulated during differentiation.

This comparison of the differentiation in white and brown preadipocytes raised several points:

- the importance of complement in adipocytes biology and its possible negative link to the thermogenic function
- the importance of ECM in preadipocytes differentiation and its possible regulatory role in the specific functional differentiation of white and brown preadipocytes
- the expression of RAMP2 in preadipocytes and adipocytes and the potential importance of ADM in preadipocyte differentiation and in the interaction between adipose tissue and the vasculature

Furthermore, several interesting candidate genes for the determination of white and brown preadipocytes were identified: mainly necdin, vigilin, HCAP and the new sequence isolated.

This project did not lead to the identification of one master regulator of the determination of preadipocytes, but points to the possibility of several processes being involved in this. Specific

regulators of gene expression and ECM might play a role in the differentiation of white and brown preadipocytes. The functional analysis of these genes will allow elucidating the importance of these processes.

5 REFERENCES

- Ailhaud G, Grimaldi P, and Negrel R. Cellular and molecular aspects of adipose tissue development. *Ann Rev Nutr* 12: 207-233, 1992.
- Ailhaud G. Development of white adipose tissue and adipocyte differentiation. In: Adipose tissues edited by Klaus S. Landes Bioscience, Medical Intelligence Unit: Austin, Texas USA, 27-55, 2001.
- Antras J, Hilliou F, Redziniak G, Pairault J. Decreased biosynthesis of actin and cellular fibronectin during adipose conversion of 3T3-F442A cells. Reorganization of the cytoarchitecture and extracellular matrix fibronectin. *Biol Cell*. 66:247-54, 1989.
- Bachner D, Sedlacek Z, Korn B, Hameister H, Poustka A. Expression patterns of two human genes coding for different rab GDP-dissociation inhibitors (GDIs), extremely conserved proteins involved in cellular transport. *Hum Mol Genet*. 4:701-8, 1995.
- Bautz EK, Reilly E. Gene-specific messenger RNA: isolation by the deletion method. *Science* 151:328-30, 1966.
- Belloni AS, Albertin G, Forneris ML, Nussdorfer GG. Proadrenomedullin-derived peptides as autocrine-paracrine regulators of cell growth. *Histol Histopathol*. 16:1263-74, 2001.
- Birgel M, Gottschling-Zeller H, Rohrig K, Hauner H. Role of cytokines in the regulation of plasminogen activator inhibitor-1 expression and secretion in newly differentiated subcutaneous human adipocytes. *Arterioscler Thromb Vasc Biol*. 20:1682-7, 2000.
- Blau HM, Chiu CP, Webster C. Cytoplasmic activation of human nuclear genes in stable heterocaryons. *Cell*. 32:1171-80, 1983.
- Bloom JD, Dutia MD, Johnson BD, Wissner A, Burns MG, Largis EE, Dolan JA, Claus TH. Disodium (R,R)-5-[2-[[2-(3-chlorophenyl)-2-hydroxyethyl]-amino]propyl]-1,3-benzodioxole-2,2-dicarboxylate (CL 316,243). A potent beta-adrenergic agonist virtually specific for beta 3 receptors. A promising antidiabetic and antiobesity agent. *J Med Chem* 35:3081-4, 1992
- Bortoluzzi MN, Cormont M, Gautier N, Van Obberghen E, Le Marchand-Brustel Y. GTPase activating protein activity for Rab4 is enriched in the plasma membrane of 3T3-L1 adipocytes. Possible involvement in the regulation of Rab4 subcellular localization. *Diabetologia*. 39:899-906, 1996.
- Bouloumié A, Sengenès C, Portolan G, Galitzky J, Lafontan M. Adipocyte produces matrix metalloproteinases 2 and 9: involvement in adipose differentiation. *Diabetes*. 50:2080-6, 2001.
- Britten RJ, Davidson EH. Studies on nucleic acid reassociation kinetics: empirical equations describing DNA reassociation. *Proc Natl Acad Sci U S A*. 73:415-9, 1976.
- Bukowiecki L, Collet AJ, Follea N, Guay G, Jahjah L. Brown adipose tissue hyperplasia: a fundamental mechanism of adaptation to cold and hyperphagia. *Am J Physiol*. 242:E353-9, 1982.
- Cambon B, Reyne Y, Nougues J. In vitro induction of UCP1 mRNA in preadipocytes from rabbit considered as a model of large mammals brown adipose tissue development: importance of

- PPARgamma agonists for cells isolated in the postnatal period. *Mol Cell Endocrinol.* 146:49-58, 1998.
- Cassard-Doulcier AM, Gelly C, Bouillaud F, Ricquier D. A 211-bp enhancer of the rat uncoupling protein-1 (UCP-1) gene controls specific and regulated expression in brown adipose tissue. *Biochem J.* 333:243-6, 1998.
- Casteilla L, Champigny O, Bouillaud F, Robelin J, Ricquier D. Sequential changes in the expression of mitochondrial protein mRNA during the development of brown adipose tissue in bovine and ovine species. Sudden occurrence of uncoupling protein mRNA during embryogenesis and its disappearance after birth. *Biochem J.* 257:665-71, 1989.
- Champigny O, Ricquier D, Blondel O, Mayers RM, Briscoe MG, Holloway BR. Beta 3-adrenergic receptor stimulation restores message and expression of brown-fat mitochondrial uncoupling protein in adult dogs. *Proc Natl Acad Sci U S A.* 88:10774-7, 1991.
- Champigny O, Ricquier D. Evidence from in vitro differentiating cells that adrenoceptor agonists can increase uncoupling protein mRNA level in adipocytes of adult humans: an RT-PCR study. *J Lipid Res.* 37:1907-14, 1996.
- Cheung VG, Morley M, Aguilar F, Massimi A, Kucherlapati R, Childs G. Making and reading microarrays. *Nat Genet.* 21(1 Suppl):15-9, 1999.
- Cho HP, Nakamura MT, and Clarke SD. Cloning, expression, and nutritional regulation of the mammalian Delta-6 desaturase. *Biol Chem* 274: 471-7, 1999.
- Choy LN, Rosen BS, and Spiegelman BM. Adipsin and an endogenous pathway of the complement from adipose tissue. *J Biol Chem* 267: 12736-41, 1992.
- Chomczynski P, and Sacchi N. Single-step method of RNA isolation by acid guanidinium thiocyanate-phenol-chloroform extraction. *Anal Biochem* 162:156-159, 1987.
- Cianflone K, Maslowska M, Sniderman AD. Acylation stimulating protein (ASP), an adipocyte autocrine: new directions. *Semin Cell Dev Biol.* 10:31-41, 1999.
- Cinti S. The adipose organ. Editrice Kurtis, Milano, Italy, 1999.
- Cinti S. Morphology of the adipose organ. In: Adipose Tissues, edited by Klaus S., Austin, TX: Landes Bioscience, Medical Intelligence Unit, 11-26, 2001
- Classon M, Kennedy BK, Mulloy R, Harlow E. Opposing roles of pRB and p107 in adipocyte differentiation. *Proc Natl Acad Sci U S A.* 97:10826-31, 2000.
- Cousin B, Cinti S, Morroni M, Raimbault S, Ricquier D, Penicaud L, Casteilla L. Occurrence of brown adipocytes in rat white adipose tissue: molecular and morphological characterization. *J Cell Sci.* 103: 931-42, 1992.
- Cousin B, Casteilla L, Dani C, Muzzin P, Revelli JP, Penicaud L. Adipose tissues from various anatomical sites are characterized by different patterns of gene expression and regulation. *Biochem J.* 292:873-6, 1993.
- Cousin B, Bascands-Viguerie N, Kassis N, Nibelink M, Ambid L, Casteilla L, Penicaud L. Cellular changes during cold acclimatation in adipose tissues. *J Cell Physiol.* 167:285-9, 1996.

- Cousin B, Munoz O, Andre M, Fontanilles AM, Dani C, Cousin JL, Laharrague P, Casteilla L, Penicaud L. A role for preadipocytes as macrophage-like cells. *FASEB J*. 13:305-12, 1999.
- Crandall DL, Busler DE, McHendry-Rinde B, Groeling TM, Kral JG. Autocrine regulation of human preadipocyte migration by plasminogen activator inhibitor-1. *J Clin Endocrinol Metab*. 85:2609-14, 2000a.
- Crandall DL, Groeling TM, Busler DE, Antrilli TM. Release of PAI-1 by human preadipocytes and adipocytes independent of insulin and IGF-1. *Biochem Biophys Res Commun*. 279:984-8, 2000b.
- Cui J, Himms-Hagen J. Rapid but transient atrophy of brown adipose tissue in capsaicin-desensitized rats. *Am J Physiol*. 262:R562-7, 1992.
- Derst C, Engel H, Grzeschik K, Daut J. Genomic structure and chromosome mapping of human and mouse RAMP genes. *Cytogenet Cell Genet*. 90:115-8, 2000.
- De Pergola G, Xu X, Carlsson B, Eriksson P, Giorgino R, Bjorntorp P. Messenger RNA of G-proteins alpha-subunit in rat brown adipose tissue. *Int J Obes Relat Metab Disord*. 18:269-72, 1994.
- De Smet C, Martelange V, Lucas S, Brasseur F, Lurquin C, Boon T. Identification of human testis-specific transcripts and analysis of their expression in tumor cells. *Biochem Biophys Res Commun*. 241:653-7, 1997.
- Digby JE, Montague CT, Sewter CP, Sanders L, Wilkison WO, O'Rahilly S, Prins JB. Thiazolidinedione exposure increases the expression of uncoupling protein 1 in cultured human preadipocytes. *Diabetes*. 47:138-41, 1998.
- Dodson RE, Shapiro DJ. Vigilin, a ubiquitous protein with 14 K homology domains, is the estrogen-inducible vitellogenin mRNA 3'-untranslated region-binding protein. *J Biol Chem*. 272:12249-52, 1997.
- Duggan DJ, Bittner M, Chen Y, Meltzer P, Trent JM. Expression profiling using cDNA microarrays. *Nat Genet*. 21(1 Suppl):10-4, 1999.
- Eisen MB, Spellman PT, Brown PO, Botstein D. Cluster analysis and display of genome-wide expression patterns. *Proc Natl Acad Sci* 95: 14863-14868, 1998.
- Encke D, Ely M, Heldmaier G, Klaus S. Physiological approach to maturation of brown adipocytes in primary cell culture. *Biochim Biophys Acta*. 1357:339-47, 1997.
- Entenmann G, Hauner H. Relationship between replication and differentiation in cultured human adipocyte precursor cells. *Am J Physiol*. 270:C1011-6, 1996.
- Evans BN, Rosenblatt MI, Mnayer LO, Oliver KR, Dickerson IM. CGRP-RCP, a novel protein required for signal transduction at calcitonin gene-related peptide and adrenomedullin receptors. *J Biol Chem* 275:31438-43, 2000.
- Fidge NH. High density lipoprotein receptors, binding proteins, and ligands. *J Lipid Res*. 40:187-201, 1999.
- Fillmore HL, VanMeter TE, Broaddus WC. Membrane-type matrix metalloproteinases (MT-MMPs): expression and function during glioma invasion. *J Neurooncol*. 53:187-202, 2001.

- Foord SM, Marshall FH. RAMPs: accessory proteins for seven transmembrane domain receptors. *Trends Pharmacol Sci.* 20:184-7, 1999.
- Franssen-van Hal NLW, Vorst O, Kramer E, Hall RD, and Keijzer J. Factors influencing cDNA microarray hybridisation on silylated glass slides. Accepted in *Analytical Biochemistry*, 2002
- Frohme M, Scharm B, Delius H, Knecht R, Hoheisel JD. Use of representational difference analysis and cDNA arrays for transcriptional profiling of tumor tissue. *Ann N Y Acad Sci.* 910:85-104, 2000.
- Fukai F, Ohtaki M, Fujii N, Yajima H, Ishii T, Nishizawa Y, Miyazaki K, Katayama T. Release of biological activities from quiescent fibronectin by a conformational change and limited proteolysis by matrix metalloproteinases. *Biochemistry.* 34:11453-9, 1995.
- Gabrielsson BL, Carlsson B, and Carlsson LM. Partial genome scale analysis of gene expression in human adipose tissue using DNA array. *Obes Res.* 8: 374-384, 2000.
- Gerard M, Hernandez L, Wevrick R, Stewart CL. Disruption of the mouse necdin gene results in early post-natal lethality. *Nat Genet.* 23:199-202, 1999.
- Geschwind DH, Ou J, Easterday MC, Dougherty JD, Jackson RL, Chen Z, Antoine H, Terskikh A, Weissman IL, Nelson SF, Kornblum HI. A genetic analysis of neural progenitor differentiation. *Neuron.* 29:325-39, 2001.
- Ghorbani M, Himms-Hagen J. Appearance of brown adipocytes in white adipose tissue during CL 316,243-induced reversal of obesity and diabetes in Zucker fa/fa rats. *Int J Obes Relat Metab Disord.* 21:465-75, 1997.
- Giordano A, Morroni M, Carle F, Gesuita R, Marchesi GF, Cinti S. Sensory nerves affect the recruitment and differentiation of rat periovarian brown adipocytes during cold acclimation. *J Cell Sci.* 111:2587-94, 1998.
- Goglia F, Geloan A, Lanni A, Minaire Y, Bukowiecki LJ. Morphometric-stereologic analysis of brown adipocyte differentiation in adult mice. *Am J Physiol.* 262:C1018-23, 1992.
- Granneman JG, Bannon MJ. Neural control of the alpha-subunit of Gs messenger ribonucleic acid in rat brown adipose tissue. *Endocrinology.* 125:2328-34, 1989.
- Guerra C, Koza RA, Yamashita H, Walsh K, Kozak LP. Emergence of brown adipocytes in white fat in mice is under genetic control. Effects on body weight and adiposity. *J Clin Invest.* 102:412-20, 1998.
- Guller S, Allen DL, Corin RE, Lockwood CJ, Sonenberg M. Growth hormone and fibronectin expression in 3T3 preadipose cells. *Endocrinology.* 130:2609-16, 1992.
- Guo X, and Liao K. Analysis of gene expression profile during 3T3-L1 preadipocyte differentiation. *Gene* 251: 45-53, 2000.
- Haraida S, Nerlich AG, Wiest I, Schleicher E, Lohrs U. Distribution of basement membrane components in normal adipose tissue and in benign and malignant tumors of lipomatous origin. *Mod Pathol.* 9:137-44, 1996.
- Hida K, Wada J, Zhang H, Hiragushi K, Tsuchiyama Y, Shikata K, and Makino H. Identification of genes specifically expressed in the accumulated visceral adipose tissue of OLETF rats. *J Lipid Res* 41: 1615-1622, 2000.

- Himms-Hagen J, Cui J, Danforth E Jr, Taatjes DJ, Lang SS, Waters BL, Claus TH. Effect of CL-316,243, a thermogenic beta 3-agonist, on energy balance and brown and white adipose tissues in rats. *Am J Physiol*. 266:R1371-82, 1994.
- Himms-Hagen J, Ricquier D. Brown adipose tissue. In: Handbook of obesity, edited by Bray GA, Bouchard C and James WPT, published by Marcel Dekker, New York, 415-441, 1998.
- Himms-Hagen J, Melnyk A, Zingaretti MC, Ceresi E, Barbatelli G, Cinti S. Multilocular fat cells in WAT of CL-316243-treated rats derive directly from white adipocytes. *Am J Physiol Cell Physiol*. 279:C670-81, 2000.
- Hsiao LL, Dangond F, Yoshida T, Hong R, Jensen RV, Misra J, Dillon W, Lee KF, Clark KE, Haverty P, Weng Z, Mutter GL, Frosch MP, Macdonald ME, Milford EL, Crum CP, Bueno R, Pratt RE, Mahadevappa M, Warrington JA, Stephanopoulos G, Stephanopoulos G, Gullans SR. A compendium of gene expression in normal human tissues. *Physiol Genomics*. 7:97-104, 2001.
- Hubank M, and Schatz DG. Identifying differences in mRNA expression by representational difference analysis of cDNA. *Nucleic Acids Research* 22: 5640-5648, 1994.
- Husmann K, Sexton PM, Fischer JA, Born W. Mouse receptor-activity-modifying proteins 1, -2 and -3: amino acid sequence, expression and function. *Mol Cell Endocrinol*. 162:35-43, 2000.
- Ibrahimi A, Bonino F, Bardon S, Ailhaud G, Dani C. Essential role of collagens for terminal differentiation of preadipocytes. *Biochem Biophys Res Commun*. 187:1314-22, 1992.
- Ihara H, Urano T, Takada A, Loskutoff DJ. Induction of plasminogen activator inhibitor 1 gene expression in adipocytes by thiazolidinediones. *FASEB J*. 15:1233-5, 2001.
- Ismail RS, Baldwin RL, Fang J, Browning D, Karlan BY, Gasson JC, Chang DD. Differential gene expression between normal and tumor-derived ovarian epithelial cells. *Cancer Res*. 60:6744-9, 2000.
- Isumi Y, Minamino N, Katafuchi T, Yoshioka M, Tsuji T, Kangawa K, Matsuo H. Adrenomedullin production in fibroblasts: its possible function as a growth regulator of Swiss 3T3 cells. *Endocrinology*. 139:2552-63, 1998.
- Janoueix-Lerosey I, Jollivet F, Camonis J, Marche PN, Goud B. Two-hybrid system screen with the small GTP-binding protein Rab6. Identification of a novel mouse GDP dissociation inhibitor isoform and two other potential partners of Rab6. *J Biol Chem*. 270:14801-8, 1995.
- Jelinsky SA, Samson LD. Global response of *Saccharomyces cerevisiae* to an alkylating agent. *Proc Natl Acad Sci U S A*. 96:1486-91, 1999.
- Jones PS, Savory R, Barratt P, Bell AR, Gray TJ, Jenkins NA, Gilbert DJ, Copeland NG, Bell DR. Chromosomal localisation, inducibility, tissue-specific expression and strain differences in three murine peroxisome-proliferator-activated-receptor genes. *Eur J Biochem*. 233:219-26, 1995.
- Kandror KV, Pilch PF. Compartmentalization of protein traffic in insulin-sensitive cells. *Am J Physiol*. 271:E1-14, 1996.
- Kim HS, Hausman GJ, Hausman DB, Martin RJ, Dean RG. The expression of cyclin D1 during adipogenesis in pig primary stromal-vascular cultures. *Obes Res*. 9:572-8, 2001.

- Kirkland JL, Hollenberg CH, Gillon WS. Age, anatomic site, and the replication and differentiation of adipocyte precursors. *Am J Physiol.* 258:C206-10, 1990.
- Klaus S, Cassard-Doulcier A-M, and Ricquier D. Development of Phodopus sungorus brown preadipocytes in primary cell culture: effect of an atypical beta-adrenergic agonist, insulin, and triiodothyronin on differentiation, mitochondrial development, and expression of the uncoupling protein UCP. *J Cell Biol* 15: 1783-1790, 1991.
- Klaus S, Ely M, Encke D, and Heldmaier G. Functional assessment of white and brown adipocyte development and energy metabolism in cell culture. Dissociation of terminal differentiation and thermogenesis in brown adipocytes. *J Cell Sci* 108, 3171-3180, 1995.
- Klaus S. Brown adipose tissue: thermogenic function and its physiological regulation. In: *Adipose tissues*, edited by Klaus S. Landes Bioscience, Medical Intelligence Unit, Austin, Texas USA, 56-81, 2001a.
- Klaus S. Brown adipocyte differentiation and function in energy metabolism. In: *Adipose tissues*, edited by Klaus S. Landes Bioscience, Medical Intelligence Unit, Austin, Texas USA, 82-96, 2001b.
- Klaus S, Seivert A, and Boeuf S. Effect of the beta-3-adrenergic agonist CI316,243 on functional differentiation of white and brown adipocytes in primary cell culture. *Biochim. Biophys. Acta (Mol Cell Res)* 1539: 85-92, 2001c.
- Klingenspor M, Ivemeyer M, Wiesinger H, Haas K, Heldmaier G, Wiesner RJ. Biogenesis of thermogenic mitochondria in brown adipose tissue of Djungarian hamsters during cold adaptation. *Biochem J.* 316: 607-13, 1996.
- Klingenspor M, Xu P, Cohen RD, Welch C, and Reue K. Altered gene expression pattern in the fatty liver dystrophy mouse reveals impaired insulin-mediated cytoskeleton dynamics. *J Biol Chem* 274: 23078-23084, 1999.
- Kozak UC, Kopecky J, Teisinger J, Enerback S, Boyer B, Kozak LP. An upstream enhancer regulating brown-fat-specific expression of the mitochondrial uncoupling protein gene. *Mol Cell Biol.* 14:59-67, 1994a.
- Kozak UC, Kozak LP. Norepinephrine-dependent selection of brown adipocyte cell lines. *Endocrinology.* 134:906-13, 1994b.
- Kratzschmar J, Lum L, and Blobel CP. Metargidin, a membrane-anchored metalloprotease-disintegrin protein with an RGD integrin binding sequence. *J Biol Chem* 271: 4593-4596, 1996.
- Kugler S, Grunweller A, Probst C, Klinger M, Muller PK, Kruse C. Vigilin contains a functional nuclear localisation sequence and is present in both the cytoplasm and the nucleus. *FEBS Lett.* 382:330-4, 1996.
- Kuri-Harcuch W, Wise LS, Green H. Interruption of the adipose conversion of 3T3 cells by biotin deficiency: differentiation without triglyceride accumulation. *Cell.* 14:53-9, 1978.
- Lash AE, Tolstoshev CM, Wagner L, Schuler GD, Strausberg RL, Riggins GJ, Altschul SF. SAGEmap: a public gene expression resource. *Genome Res.* 10:1051-60, 2000.
- Lennon GG, Lehrach H. Hybridization analyses of arrayed cDNA libraries. *Trends Genet.* 7:314-7, 1991.

- Lewis BC, Shim H, Li Q, Wu CS, Lee LA, Maity A, Dang CV. Identification of putative c-Myc-responsive genes: characterization of rcl, a novel growth-related gene. *Mol Cell Biol.* 17:4967-78, 1997.
- Liang P, Pardee AB. Differential display of eukaryotic messenger RNA by means of the polymerase chain reaction. *Science* 257:967-71, 1992.
- Lisitsyn N, Lisitsyn N, and Wigler M. Cloning the difference between two complex genomes. *Science* 256: 946-951, 1993.
- Lisitsyn N. Representational difference analysis: finding the differences between genomes. *Trends Genet.* 11:303-7, 1995
- Liu X, Perusse F, Bukowiecki LJ. Mechanisms of the antidiabetic effects of the beta 3-adrenergic agonist CL-316243 in obese Zucker-ZDF rats. *Am J Physiol.* 274:R1212-9, 1998.
- Loncar D. Convertible adipose tissue in mice. *Cell Tissue Res.* 266:149-61, 1991.
- Lowell BB, Spiegelman BM. Towards a molecular understanding of adaptive thermogenesis. *Nature.* 404:652-60, 2000.
- MacDonald HR, Wevrick R. The necdin gene is deleted in Prader-Willi syndrome and is imprinted in human and mouse. *Hum Mol Genet.* 6:1873-8, 1997.
- McKnight GL, Reasoner J, Gilbert T, Sundquist KO, Hokland B, McKernan PA, Champagne J, Johnson CJ, Bailey MC, Holly R, et al. Cloning and expression of a cellular high density lipoprotein-binding protein that is up-regulated by cholesterol loading of cells. *J Biol Chem.* 267:12131-41, 1992.
- McLatchie LM, Fraser NJ, Main MJ, Wise A, Brown J, Thompson N, Solari R, Lee MG, Foord SM. RAMPs regulate the transport and ligand specificity of the calcitonin-receptor-like receptor. *Nature.* 393:333-9, 1998.
- Makino I, Honda K, Makino Y, Okano I, Kangawa K, Kamiya Ho HO, Shibata K, Kawarabayashi T. Phenotypic Changes of Adrenomedullin Receptor Components, RAMP2, and CRLR mRNA Expression in Cultured Rat Vascular Smooth Muscle Cells. *Biochem Biophys Res Commun.* 288:515-20, 2001.
- Maruyama K, Usami M, Aizawa T, Yoshikawa K. A novel brain-specific mRNA encoding nuclear protein (necdin) expressed in neurally differentiated embryonal carcinoma cells. *Biochem Biophys Res Commun.* 178:291-6, 1991.
- Mathieson PW, Peters DK. Lipodystrophy in MCGN type II: the clue to links between the adipocyte and the complement system. *Nephrol Dial Transplant.* 12:1804-6, 1997.
- Miller WH Jr, Faust IM, Hirsch J. Demonstration of de novo production of adipocytes in adult rats by biochemical and radioautographic techniques. *J Lipid Res.* 25:336-47, 1984.
- Miller RA, Galecki A, Shmookler-Reis RJ. Interpretation, design, and analysis of gene array expression experiments. *J Gerontol A Biol Sci Med Sci.* 56:B52-7, 2001.
- Milner JJ, Cecchini E, Dominy PJ. A kinetic model for subtractive hybridization. *Nucleic Acids Res* 11;23(1):176-87, 1995.

- Moitra J, Mason MM, Olive M, Krylov D, Gavrilova O, Marcus-Samuels B, Feigenbaum L, Lee E, Aoyama T, Eckhaus M, Reitman ML, Vinson C. Life without white fat: a transgenic mouse. *Genes Dev.* 12:3168-81, 1998.
- Morrison RF, Farmer SR. Role of PPARgamma in regulating a cascade expression of cyclin-dependent kinase inhibitors, p18(INK4c) and p21(Waf1/Cip1), during adipogenesis. *J Biol Chem.* 274:17088-97, 1999.
- Morroni M, Barbatelli G, Zingaretti MC, Cinti S. Immunohistochemical, ultrastructural and morphometric evidence for brown adipose tissue recruitment due to cold acclimation in old rats. *Int J Obes Relat Metab Disord.* 19:126-31, 1995.
- Moulin K, Truel N, Andre M, Arnaud E, Nibelink M, Cousin B, Dani C, Penicaud L, Casteilla L. Emergence during development of the white-adipocyte cell phenotype is independent of the brown-adipocyte cell phenotype. *Biochem J.* 356:659-64, 2001a.
- Moulin K, Arnaud E, Nibelink M, Viguerie-Bascands N, Penicaud L, Casteilla L. Cloning of BUG demonstrates the existence of a brown preadipocyte distinct from a white one. *Int J Obes Relat Metab Disord.* 25:1431-41, 2001b.
- Murray I, Sniderman AD, Havel PJ, Cianflone K. Acylation stimulating protein (ASP) deficiency alters postprandial and adipose tissue metabolism in male mice. *J Biol Chem.* 274:36219-25, 1999.
- Muscattelli F, Abrous DN, Massacrier A, Boccaccio I, Le Moal M, Cau P, Cremer H. Disruption of the mouse Necdin gene results in hypothalamic and behavioral alterations reminiscent of the human Prader-Willi syndrome. *Hum Mol Genet.* 9:3101-10, 2000.
- Nadler ST, Stoehr JP, Schueler KL, Tanimoto G, Yandell BS, and Attie AD. The expression of adipogenic genes is decreased in obesity and diabetes mellitus. *Proc Natl Acad Sci U S A* 97:11371-11376, 2000.
- Naot D, Callon KE, Grey A, Cooper GJ, Reid IR, Cornish J. A potential role for adrenomedullin as a local regulator of bone growth. *Endocrinology.* 142:1849-57, 2001.
- Nedergaard J, Herron D, Jacobsson A, Rehnmark S, Cannon B. Norepinephrine as a morphogen?: its unique interaction with brown adipose tissue. *Int J Dev Biol.* 39:827-37, 1995.
- Nelissen RL, Sillekens PT, Beijer RP, Geurts van Kessel AH, van Venrooij WJ. Structure, chromosomal localization and evolutionary conservation of the gene encoding human U1 snRNP-specific A protein. *Gene.* 102:189-96, 1991.
- Newton MA, Kendzioriski CM, Richmond CS, Blattner FR, Tsui KW. On Differential Variability of Expression Ratios: Improving Statistical Inference about Gene Expression Changes from Microarrays Data. *Journal of Computational Biology* 8: 37-52, 2001.
- Nikami H, Shimizu Y, Endoh D, Yano H, Saito M. Cold exposure increases glucose utilization and glucose transporter expression in brown adipose tissue. *Biochem Biophys Res Commun.* 185:1078-82, 1992.
- Nishimura N, Nakamura H, Takai Y, Sano K. Molecular cloning and characterization of two rab GDI species from rat brain: brain-specific and ubiquitous types. *J Biol Chem.* 269:14191-8, 1994.
- Ntambi JM, Young-Cheul K. Adipocyte differentiation and gene expression. *J Nutr.* 130:3122S-3126S, 2000.

- Olichon-Berthe C, Van Obberghen E, Le Marchand-Brustel Y. Effect of cold acclimation on the expression of glucose transporter Glut 4. *Mol Cell Endocrinol.* 89:11-8, 1992.
- Palou A, Serra F, Bonet ML, Pico C. Obesity: molecular bases of a multifactorial problem. *Eur J Nutr.* 39:127-44, 2000.
- Pastorian K, Hawel L 3rd, Byus CV. Optimization of cDNA representational difference analysis for the identification of differentially expressed mRNAs. *Anal Biochem* 283:89-98, 2000.
- Peake PW, O'Grady S, Pussell BA, Charlesworth JA. Detection and quantification of the control proteins of the alternative pathway of complement in 3T3-L1 adipocytes. *Eur J Clin Invest.* 27:922-7, 1997.
- Pierleoni C, Verdenelli F, Castellucci M, Cinti S. Fibronectins and basal lamina molecules expression in human subcutaneous white adipose tissue. *Eur J Histochem.* 42:183-8, 1998.
- Prins JB, O'Rahilly S. Regulation of adipose cell number in man. *Clin Sci (Lond).* 92:3-11, 1997.
- Prunet-Marcassus B, Moulin K, Carmona MC, Villarroya F, Penicaud L, Casteilla L. Inverse distribution of uncoupling proteins expression and oxidative capacity in mature adipocytes and stromal-vascular fractions of rat white and brown adipose tissues. *FEBS Lett.* 464:184-8, 1999.
- Puigserver P, Ribot J, Serra F, Gianotti M, Bonet ML, Nadal-Ginard B, Palou A. Involvement of functional and physical association with the adipogenic transcription factor C/EBPalpha. *Eur J Cell Biol.* 77:117-23, 1998.
- Pyronnet S, Pradayrol L, Sonenberg N. A cell cycle-dependent internal ribosome entry site. *Mol Cell.* 5:607-16, 2000.
- Qiu Z, Wei Y, Chen N, Jiang M, Wu J, Liao K. DNA synthesis and mitotic clonal expansion is not a required step for 3T3-L1 preadipocyte differentiation into adipocytes. *J Biol Chem.* 276:11988-95, 2001.
- Rabelo R, Camirand A, Silva JE. 3',5'-cyclic adenosine monophosphate-response sequences of the uncoupling protein gene are sequentially recruited during darglitazone-induced brown adipocyte differentiation. *Endocrinology.* 138:5325-32, 1997.
- Rajeevan MS, Vernon SD, Taysavang N, Unger ER. Validation of array-based gene expression profiles by real-time (kinetic) RT-PCR. *J Mol Diagn.* 3:26-31, 2001.
- Reichert M, Eick D. Analysis of cell cycle arrest in adipocyte differentiation. *Oncogene.* 18:459-66, 1999.
- Rodriguez Fernandez JL, Ben-Ze'ev A. Regulation of fibronectin, integrin and cytoskeleton expression in differentiating adipocytes: inhibition by extracellular matrix and polylysine. *Differentiation.* 42:65-74, 1989.
- Rosen BS, Cook KS, Yaglom J, Groves DL, Volanakis JE, Damm D, White T, Spiegelman BM. Adipsin and complement factor D activity: an immune-related defect in obesity. *Science.* 244:1483-7, 1989.
- Rosen ED, Spiegelman BM. Molecular regulation of adipogenesis. *Annu Rev Cell Dev Biol.* 16:145-71, 2000.

- Ross SR, Choy L, Graves RA, Fox N, Soleyjeva V, Klaus S, Ricquier D, Spiegelman BM. Hibernoma formation in transgenic mice and isolation of a brown adipocyte cell line expressing the uncoupling protein gene. *Proc Natl Acad Sci U S A.* 89:7561-5, 1992.
- Schena M, Shalon D, Davis RW, Brown PO. Quantitative monitoring of gene expression patterns with a complementary DNA microarray. *Science* 270:467-70, 1995.
- Schena M, Shalon D, Heller R, Chai A, Brown PO, and Davis RW. Parallel human genome analysis: microarray-based expression monitoring of 1000 genes. *Proc Natl Acad Sci U S A.* 93: 10614-10619, 1996.
- Schuchhardt J, Beule D, Malik A, Wolski E, Eickhoff H, Lehrach H, and Herzog H Normalization strategies for cDNA microarrays. *Nucleic Acids Res* 28: E47, 2000.
- Seachrist JL, Anborgh PH, Ferguson SS. beta 2-adrenergic receptor internalization, endosomal sorting, and plasma membrane recycling are regulated by rab GTPases. *J Biol Chem.* 275:27221-8, 2000.
- Seki T, Miyasu T, Noguchi T, Hamasaki A, Sasaki R, Ozawa Y, Okukita K, Declerck PJ, Ariga T. Reciprocal regulation of tissue-type and urokinase-type plasminogen activators in the differentiation of murine preadipocyte line 3T3-L1 and the hormonal regulation of fibrinolytic factors in the mature adipocytes. *J Cell Physiol.* 189:72-8, 2001.
- Sell H, Deshaies Y, Plamondon J. Effect of the PPAR gamma agonist L-805645 on the expression of UCP1 in adipose tissue. Abstract from the NAASO 2001 annual meeting in *Obesity research* 9, Suppl. 3: 148S, 2001.
- Sethi JK, Hotamisligil GS. The role of TNF alpha in adipocyte metabolism. *Semin Cell Dev Biol.* 10:19-29, 1999.
- Shimomura I, Hammer RE, Richardson JA, Ikemoto S, Bashmakov Y, Goldstein JL, Brown MS. Insulin resistance and diabetes mellitus in transgenic mice expressing nuclear SREBP-1c in adipose tissue: model for congenital generalized lipodystrophy. *Genes Dev.* 12:3182-94, 1998.
- Shisheva A, Buxton J, Czech MP. Differential intracellular localizations of GDP dissociation inhibitor isoforms. Insulin-dependent redistribution of GDP dissociation inhibitor-2 in 3T3-L1 adipocytes. *J Biol Chem.* 269:23865-8, 1994.
- Soukas A, Cohen P, Socci ND, Friedman JM. Leptin-specific patterns of gene expression in white adipose tissue. *Genes Dev.* 14:963-80, 2000.
- Soukas A, Socci ND, Saatkamp BD, Novelli S, Friedman JM. Distinct transcriptional profiles of adipogenesis in vivo and in vitro. *J Biol Chem.* 276:34167-74, 2001.
- Spiegelman BM, Farmer SR. Decreases in tubulin and actin gene expression prior to morphological differentiation of 3T3 adipocytes. *Cell.* 29:53-60, 1982.
- Spiegelman BM, Ginty CA. Fibronectin modulation of cell shape and lipogenic gene expression in 3T3-adipocytes. *Cell.* 35:657-66, 1983.
- Tai TA, Jennermann C, Brown KK, Oliver BB, MacGinnitie MA, Wilkison WO, Brown HR, Lehmann JM, Kliewer SA, Morris DC, Graves RA. Activation of the nuclear receptor peroxisome proliferator-activated receptor gamma promotes brown adipocyte differentiation. *J Biol Chem.* 271:29909-14, 1996.

- Takahashi K. Adrenomedullin from a pheochromocytoma to the eye: implications of the adrenomedullin research for endocrinology in the 21st century. *Tohoku J Exp Med.* 193:79-114, 2001.
- Taniura H, Matsumoto K, Yoshikawa K. Physical and functional interactions of neuronal growth suppressor necdin with p53. *J Biol Chem.* 274:16242-8, 1999.
- Tsai TF, Armstrong D, Beaudet AL. Necdin-deficient mice do not show lethality or the obesity and infertility of Prader-Willi syndrome. *Nat Genet.* 22:15-6, 1999.
- Vallerand AL, Perusse F, Bukowiecki LJ. Stimulatory effects of cold exposure and cold acclimation on glucose uptake in rat peripheral tissues. *Am J Physiol.* 259:R1043-9, 1990.
- Van Hal NLW, Vorst O, van Houwelingen AMML, Kok EJ, Peijnenburg A, Aharoni A, Van Tunen AJ, and Keijer J. The application of DNA microarrays in gene expression analysis. *J Biotechnol* 78, 271-280, 2000.
- Villena JA, Vinas O, Mampel T, Iglesias R, Giralt M, Villarroya F. Regulation of mitochondrial biogenesis in brown adipose tissue: nuclear respiratory factor-2/GA-binding protein is responsible for the transcriptional regulation of the gene for the mitochondrial ATP synthase beta subunit. *Biochem J.* 331:121-7, 1998.
- von Praun C, Burkert M, Gessner M, Klingenspor M. Tissue-specific expression and cold-induced mRNA levels of uncoupling proteins in the Djungarian hamster. *Physiol Biochem Zool* 74:203-11, 2001.
- Weiner FR, Shah A, Smith PJ, Rubin CS, Zern MA. Regulation of collagen gene expression in 3T3-L1 cells. Effects of adipocyte differentiation and tumor necrosis factor alpha. *Biochemistry.* 28:4094-9, 1989.
- Welford SM, Gregg J, Chen E, Garrison D, Sorensen PH, Denny CT, Nelson SF. Detection of differentially expressed genes in primary tumor tissues using representational differences analysis coupled to microarray hybridization. *Nucleic Acids Res.* 26:3059-65, 1998.
- Welsh J, Chada K, Dalal SS, Cheng R, Ralph D, McClelland M. Arbitrarily primed PCR fingerprinting of RNA. *Nucleic Acids Res.* 20:4965-70, 1992.
- Wieland I, Bolger G, Asouline G, Wigler M. A method for difference cloning: gene amplification following subtractive hybridization. *Proc Natl Acad Sci U S A.* 87:2720-4, 1990
- Wittes J, Friedman HP. Searching for evidence of altered gene expression: a comment on statistical analysis of microarray data. *J Natl Cancer Inst.* 91:400-1, 1999.
- Wu Z, Puigserver P, Andersson U, Zhang C, Adelmant G, Mootha V, Troy A, Cinti S, Lowell B, Scarpulla RC, Spiegelman BM. Mechanisms controlling mitochondrial biogenesis and respiration through the thermogenic coactivator PGC-1. *Cell.* 98:115-24, 1999.
- Yang MC, Ruan QG, Yang JJ, Eckenrode S, Wu S, McIndoe RA, She JX. A statistical method for flagging weak spots improves normalization and ratio estimates in microarrays. *Physiol Genomics.* 7:45-53, 2001.
- Yee AS, Shih HH, Tevosian SG. New perspectives on retinoblastoma family functions in differentiation. *Front Biosci.* 3:D532-47, 1998.

- Yoshikawa K. Cell cycle regulators in neural stem cells and postmitotic neurons. *Neurosci Res.* 37:1-14, 2000.
- Young P, Arch JR, Ashwell M. Brown adipose tissue in the parametrial fat pad of the mouse. *FEBS Lett.* 167:10-4, 1984.
- Zennaro MC, Le Menuet D, Viengchareun S, Walker F, Ricquier D, Lombes M. Hibernoma development in transgenic mice identifies brown adipose tissue as a novel target of aldosterone action. *J Clin Invest.* 101:1254-60, 1998.
- Zhou L, Halvorsen YD, Cryan EV, Pelton PD, Burris TP, Demarest KT. Analysis of the pattern of gene expression during human adipogenesis by DNA microarray. *Biotechnology Techniques* 13: 513-7, 1999.

DANKSAGUNG

Diese Arbeit wäre ohne die Hilfe, den Rat und die Geduld vieler Personen nicht zustande gekommen. Hiermit möchte ich mich bei ihnen bedanken.

Mein besonderer Dank gilt Susanne Klaus für die Überlassung des Themas und die Unterstützung zur Durchführung dieser Arbeit. Durch ihre internationalen Kontakte ermöglichte sie mir die fruchtbaren Arbeitsaufenthalte.

Martin Klingenspor danke ich für seine Gastfreundlichkeit und für die Unterstützung zur Durchführung der RDA.

Ich danke Jaap Keijer für den mehrmaligen Empfang im RIKILT in Wageningen. Nicole Franssen-van Hal gilt mein besonderer Dank für die arbeitsintensive Betreuung, die vielen Datenanalysen und die vielen „online“ Diskussionen über Normalisierungsverfahren. Bei Evelien Kramer bedanke ich mich für die Zusammenstellung der Kontrollklone.

Weiterhin danke ich Herrn Prof. W. Meyerhof dafür, daß er mich in der Abteilung molekulare Genetik, in der ein großer Teil dieser Arbeit angefertigt wurde, freundlich aufgenommen hat. Ich danke allen seinen Mitarbeitern für die tatkräftige Unterstützung.

Brigitte Geue und Antje Sylvester danke ich für die viele Zeit, die sie für Zellkulturen und RNA Isolierungen geopfert haben. Sie haben sich schnell zu Expertinnen auf dem Gebiet entwickelt. Bei Frau Thomas bedanke ich mich für die Betreuung der Hamster.

Weiterhin danke ich allen Mitarbeitern der Abteilung BPE für die angenehme gemeinsame Zeit.

LEBENS LAUF

Stéphane Bœuf
Gethsemanestraße 6
10437 Berlin

Persönliche Daten

Geburtsdatum 16.11.1972
Geburtsort Grenoble (Frankreich)
Nationalität deutsch und französisch
Familienstand ledig

Schule

1978 – 1983 Ecole primaire Sidi-Brahim, Grenoble
1983 – 1987 Collège des Eaux-Clares, Grenoble
1987 – 1990 Lycée International Stendhal, Grenoble, Abschluß: Abitur

Ausbildung

1990 – 1992 Classes préparatoire de mathématique supérieure et spéciale (allgemeine Ausbildung in Mathematik, Physik und Chemie) im Lycée Champollion, Grenoble
1992 – 1995 Studium in der Ecole Polytechnique, Paris
Spezialisierung: Biologie
Abschließendes Praktikum in der biologischen Fakultät der Mac Gill Universität, Montreal, Kanada, in einem Labor für Evolutionsgenetik
Abschlußdiplom als Ingenieur
1995 – 1997 Studium im Institut National Agronomique Paris-Grignon (INA P-G)
Spezialisierung: Nutztierkunde und Ernährung
Arbeit zum Erlangen des Diploms des INA P-G, im Deutschen Institut für Ernährungsforschung, Potsdam-Rehbrücke, AG Energiestoffwechsel
Thema: hormonelle Regulierung der Differenzierung von weißen und braunen Präadipocyten
Abschlußdiplom als Ingenieur des Institut National Agronomique Paris-Grignon, Diplome d'Agronomie Approfondie (DAA).
1998 – 2002 Wissenschaftlicher Mitarbeiter am Deutschen Institut für Ernährungsforschung, Abteilung Biochemie und Physiologie der Ernährung, AG Energiestoffwechsel, Potsdam-Rehbrücke
Anfertigung der Dissertation zum Thema: *Comparative study of gene expression during the differentiation of white and brown preadipocytes*